



HAL
open science

Morphogenesis without central control - case studies in social insect nest construction

Christian Jost

► **To cite this version:**

Christian Jost. Morphogenesis without central control - case studies in social insect nest construction. Quantitative Methods [q-bio.QM]. Université Toulouse 3, Paul Sabatier, 2015. tel-03078918

HAL Id: tel-03078918

<https://hal.science/tel-03078918>

Submitted on 16 Dec 2020

HAL is a multi-disciplinary open access archive for the deposit and dissemination of scientific research documents, whether they are published or not. The documents may come from teaching and research institutions in France or abroad, or from public or private research centers.

L'archive ouverte pluridisciplinaire **HAL**, est destinée au dépôt et à la diffusion de documents scientifiques de niveau recherche, publiés ou non, émanant des établissements d'enseignement et de recherche français ou étrangers, des laboratoires publics ou privés.



UNIVERSITÉ
TOULOUSE III
PAUL SABATIER



MÉMOIRE

en vue de l'obtention de

L'HABILITATION À DIRIGER DES RECHERCHES (HDR)

Ecole Doctorale Sciences Ecologiques, Vétérinaires, Agronomies, Bioingénieries de l'Université
de Toulouse

Spécialité: Ecologie, Biodiversité et Evolution

présenté par

Christian JOST

sous la direction de Guy THERAULAZ

**Morphogenesis without central control - case studies in social insect nest
construction**

(written in english/rédigé en anglais)

MANUSCRIT VERSION FINALE, DÉCEMBRE 2015

Soutenue le 11/12/2015 devant le jury composé de:

| | |
|------------|--|
| Rapporteur | M. Flavio ROCES, University of Würzburg, Germany |
| Rapporteur | M. Johan VAN DE KOPPEL, NIOZ Yerseke, Netherlands |
| Rapporteur | M. François GRANER, Université Paris 7, France |
| Examineur | M. Jean-Baptiste FERDY, U. Fédérale de Toulouse — Midi-Pyrénées |
| Directeur | M. Guy THERAULAZ U. Fédérale de Toulouse — Midi-Pyrénées. |

Contents

| | | |
|----------|---|-----------|
| 1 | Preface | 5 |
| 2 | Introduction | 7 |
| 2.1 | Mechanisms of morphogenesis | 7 |
| 2.2 | Why do we need modeling? | 10 |
| 2.3 | A methodology to study SO | 10 |
| 2.4 | What does it take to understand social insect nest construction? | 13 |
| 3 | Self-clustering of animals (or robots) | 14 |
| 3.1 | Apply the SO methodology to study cockroach aggregation behavior | 15 |
| 3.2 | A first scheme for quantitatively based model selection | 17 |
| 3.3 | Cockroach clustering and collective robotics | 18 |
| 3.3.1 | Clustering and collective decision making | 19 |
| 3.3.2 | Trail formation in robots: light as a substitute to pheromones | 20 |
| 4 | Object-clustering: corpse clustering in ants | 25 |
| 4.1 | The influence of temperature on corpse clustering behavior | 30 |
| 4.2 | Thigmotactic behavior and its role in corpse clustering | 32 |
| 4.2.1 | A new model for ant thigmotactic behavior | 34 |
| 4.3 | Corpse clustering in 2D and its interactions with a dynamic template | 37 |
| 4.3.1 | Clustering dynamics with and without a laminar air flow | 38 |
| 4.3.2 | Modulation of corpse picking-up and depositing by a laminar air flow | 38 |
| 4.3.3 | Clusters as a dynamic template that modulate positive feedback and thus their own growth | 40 |
| 4.3.4 | Modeling corpse clustering in 2D without a laminar air flow | 40 |
| 4.3.5 | Modeling corpse clustering in 2D with a laminar air flow | 43 |
| 4.3.6 | Towards a macroscopic model of corpse clustering in 2D? | 44 |
| 5 | Nest construction in social insects: state of the art | 46 |
| 5.1 | Ant nest construction: the case of the black garden ant <i>Lasius niger</i> | 48 |
| 5.2 | Termite nest construction: on architecture and underlying individual behaviors | 53 |
| 5.2.1 | The network approach to understand Termitinae nests | 54 |
| 5.2.2 | The virtual nest museum | 60 |
| 5.2.3 | Tunnel networks in termites | 61 |
| 5.2.4 | Comparative study of <i>Procornitermes araujoii</i> and <i>Cornitermes cumulans</i> nests | 63 |

| | | |
|----------|--|-----------|
| 6 | Where to go now? | 69 |
| 6.1 | The role of individual movement in the emergence of the nest architecture in <i>Procornitermes araujoï</i> | 69 |
| 6.2 | The interplay between nest architecture, environmental parameters and individual behavior | 70 |
| 6.3 | Are there alternatives to our methodology to study self-organization? | 70 |
| | Bibliography | 73 |

Chapter 1

Preface

The present document was written with a simple goal in mind: allow me to defend my habilitation at the [University of Toulouse](#), France. For those not familiar with the concept of “habilitation”: according to the guidelines of the aforementioned University, a habilitation (or “HDR: Habilitation à Diriger des Recherches”) « sanctionne la reconnaissance d’un haut niveau scientifique, le caractère original d’une démarche, la maîtrise d’une stratégie de recherche dans un domaine large et la capacité à encadrer de jeunes chercheurs (arrêté du 23 novembre 1988, modifié par les arrêtés des 13 février 1992 et 13 juillet 1995, interprété par les circulaires des 5 janvier 1989 et 16 novembre 1992) ». As you probably guess, it is quite an important document in the french academic system, not least because it will allow me to supervise a PhD student on my own. With this document, I have to convince three referees and a jury that I

- can work at a high scientific level,
- develop my own ideas,
- master a scientific strategy in an extended domain, and
- that I am capable to supervise young scientists.

This document is therefore often written in the first person. But please keep in mind that I worked in a team and that the presented work is mostly teamwork, with influences from everybody with whom I discussed or worked during the last 20 years. I apologize in advance if the value of these influences has been diluted by this emphasis on the first person, please also take a look at the co-author list in the cited papers to get a more complete picture.

Besides this official and target oriented character, I nevertheless hope that the present document will be of some interest to everybody who is interested in the study of complex biological systems. I will present case studies that combine experimental with theoretical approaches in order to understand the underlying mechanisms of morphogenetic processes in a large sense: from the aggregation of individuals over the aggregation of objects to the collaborative construction of a social insect nest. I also hope that it will appeal to a wide interdisciplinary audience, covering biologists, physicists and mathematicians. I have myself started my career with a Masters in Applied Mathematics ([Jost, 1993](#)) at the [University of Zürich](#), Switzerland, while doing in parallel a Bachelors degree in Biology. Both interests merged during my PhD in ecology ([Jost, 1998](#)) at the [Institut national agronomique Paris-Grignon](#) (supervised by [Roger Arditi](#)), where I explored what time series data of prey and predator abundances can tell us about the underlying predator-prey interaction (and, without having ever had any formal course on statistical inference, had to learn on the fly the statistical approaches to model selection). This PhD taught me, amongst other things, that if we only have data of the final result in a

biological process (here predator-prey abundances, measured several times to catch the dynamics), we have only limited statistical power to infer something on the underlying processes (here prey growth, predation, predator growth). I was therefore lucky to get my job here in Toulouse, where the goal was exactly to identify the underlying processes on the individual level that let emerge some intriguing behavior on the collective level. Lucky in two ways, actually: I got the occasion to design and perform my own experiments (easier said than done, the biologists in the lab often sadly shook their heads), and I found colleagues in statistical physics that taught me a modeling approach to understand collective behavior as emerging from the underlying individual behavior. They also taught me that parameter estimation from experimental data is not only a statistical/numerical problem, but that thoughtful modeling combined with simulation (Monte Carlo) can often work wonders. This habilitation is therefore also the story of my scientific journey here in Toulouse, combining mathematics, physics, computer science and biology in order to advance our understanding of pattern formation in social insects.

This document would not have been possible without the enthusiastic participation of many students. I would not want to miss the freshness and (sometimes naive) scientific curiosity of Bachelor level students: I usually set them to work on very precise questions for which I more or less already know the result, but they often surprised me by developing their report beyond my expectations or by insisting on questions that I considered initially to be of less importance but that turned out to shed new light on the studied topic (B-R Bengoudifa, A Gu  r  cheau, N Hurard, B Piccinini, M Schwalm, A Solacroup, V Rossi). Master students in their first year (M1) played an important role because the evaluation of their internship focusses on the research approach and how they develop it, not on the results themselves: it is therefore possible to let them work on speculative questions, their supervision just requires frequent discussions with them and a close look at what they are actually doing in order to refine the methods and identify the results that merit to be further pursued (G Talbot, J Champeau, S de Mendon  a, V Loisel, S Causse, D Fouquet, T Robert, L Chauvet, S Faber, C Bonnand, N Boulic, A Uhart, A Pessato, R Runghen). Master students in their 2nd year (formerly called DEA, now simply M2) require a similar supervision, but I try to set them on questions for which I expect publishable results (M Challet, J Verret, S Garnier, E Casellas, J Olivera, M Keromest, V Loisel, D Fouquet, C P  chabadens). Finally, supervising all these students, in particular teaching them the necessary methods and techniques to become operational, was largely facilitated by the active help of the PhD students I co-supervised (M Challet, C Sbai). Working with PhD students is more like a scientific cooperation than student supervision. The hard work is to find a promising subject and how to attack it, the day to day supervision then mostly consists in discussing intermediate results, explore alternative explanations and refine the methods and techniques in order to best anticipate all possible critics and objections of future anonymous referees. The goal is to advance our understanding of the subject and to accompany the PhD student how to achieve that – this type of cooperation is largely based on trust.

Having said all this I just hope that you will enjoy reading part or all of this document. Thanks in advance for your interest.

Christian Jost, Toulouse, 2015.

Chapter 2

Introduction

| |
|--|
| “All models are wrong - but some models are useful” Box (1976) |
|--|

In the title I use the word **morphogenesis** rather than the more general [pattern formation](#): what do I mean by this? Wikipedia defines [morphogenesis](#) as “the biological process that causes an organism to develop its shape”. This definition seems to restrict this term to the growth of a single organism (and many authors use this restricted view). However, in biology we also have the concept of [extended phenotype](#) (popularized by [Dawkins 1982](#)) where an organism develops other things than shape, in particular behavior. By this behavior it also changes its environment and can create patterns in this environment (a bird building its nest, a beaver constructing a dam, ...). Morphogenesis can therefore also be the process how an organism creates patterns in its environment, this is still a biological process. [Turner \(2002\)](#) in his book *The extended organism* took this concept a step further by treating the resulting pattern as an organism in itself and emphasizing the physiology of such animal built structures (thus resembling even more the wikipedia definition of morphogenesis). The book cover shows a termite mound, illustrating Turner’s preferred model organism. But other social insects such as ants, wasps or bees also construct nests that don’t shy a comparison with termite mounds. With social insects we have arrived in the field of collective animal behaviors ([Sumpter, 2010](#)) or, more general, in group living animals ([Krause and Ruxton, 2002](#)). My research during the last 14 years has been about understanding how animals collectively create patterns, be it a simple aggregation of individuals (as in cockroaches, [Jeanson et al. 2005](#)), the aggregation of objects (as corpse clustering in ants, [Theraulaz et al. 2002](#)), or the aggregation of soil pellets to construct a shelter (as in ants, [Franks et al. 1992](#), or in termites, [Bruinsma 1979](#)). I consider all such pattern formation processes as morphogenetic processes, and my goal was and is to understand the underlying behavioral mechanisms that coordinate the animal’s behavior in their group.

2.1 Mechanisms of morphogenesis

How are these patterns created? There might be somewhere in the animal a map or a plan of the pattern to be built, the animal just following this plan in order to converge towards the final pattern. This plan might be a genetic program that triggers a sequential order of behaviors that lead to the pattern. The problem with this concept alone is the amount of information that would have to be encoded for such a plan. Even if this were feasible, many animal structures are built collectively: in this case the animal not only needs the sequential program how to build, it also needs the cognitive capacities to assess the state of the structure in order to continue its construction after some coworker has worked on it. In short, the notion

of a map or plan seems rather complicated to get to work, it is therefore rarely invoked as an explanation for the observed morphogenesis (but see also nest construction in the solitary paper wasp *Paralastor* sp – [Smith 1978](#); [Downing and Jeanne 1988](#)). A second explanation might be that the pattern already exists as a template, though not visible to our eyes. You surely remember the physics experiment in college where iron filings are spread randomly on a sheet of paper above a magnet: when vibrating the paper gently the iron filings become ordered and reveal the form of the magnetic field created by the magnet and that has been there all the time, even if we did not see it. Such patterns can also exist in biological systems as spatial heterogeneities: a humid spot in the soil which will be excavated by ants and form the nest cavity, a temperature or humidity gradient along which the nest is excavated and that serves to raise eggs, pupae or larvae at the right conditions ([Brian, 1983](#); [Thomé, 1972](#)). Sometimes the template is created by a single individual as in the case of the *Macrotermes subhyalinus* queen which emanates constantly a pheromone whose concentration decreases with increasing distance from the queen: it is this concentration that lets workers construct a shelter chamber adapted to the queen’s size ([Bruinsma, 1979](#); [Ladley and Bullock, 2005](#)). This template mechanism also solves the coordination problem between different workers, they are all guided by the template independently of the other worker’s activity. However, a template alone is a limited solution because it must pre-exist somehow. It is also only a partial solution in the case of the termite queen and nuptial chamber construction: as the shelter walls rise, the pheromone concentrations inside will change, thus changing the template. How do the workers maintain the right distance from the queen? This is where an additional concept, self-organization ([Camazine et al., 2001](#)) or stigmergy ([Grassé, 1959, 1967](#); [Theraulaz and Bonabeau, 1999](#)), becomes handy. Much has already been said about stigmergy: here I will consider it simply as a predecessor of self-organization (SO) and concentrate on the latter. [Camazine et al. \(2001\)](#) define SO as:

Self-organization is a process in which pattern at the global level of a system emerges solely from numerous interactions among the lower-level components of the system. Moreover, the rules specifying interactions among the system’s components are executed using only local information, without reference to the global pattern.

This is a rather wide definition, its key components are only

- dynamical system: a pattern emerges as the result of a dynamic process,
- two or more scales of interest: there are at least two levels in the system (global and lower in the definition, or collective and individual in the examples treated here),
- no global information available to lower level components: the rules guiding the interactions between the lower level components (and their environment) only depend on local information (each individual has a limited perception, not extending to the global level, and its behavior is driven by this local information).

Several ingredients of SO are implicitly following from this definition ([Bonabeau et al., 1997](#)):

- there must be some positive feedback that amplifies small fluctuations (the origin of these fluctuations can be the result of a random or non-random process) in an out-of-equilibrium system,
- there must also be some negative feedback that finally controls this amplification and helps to stabilize the emerging pattern (forcing it to a stationary state or new equilibrium)

The fact that both ingredients exist implies that the dynamical system cannot be linear (if a reader wants a technical definition of a linear or non-linear dynamical system I warmly recommend to read the introduction in the habilitation of [Gautrais 2015](#)). Other ingredients are less obvious but have been found in all such non-linear dynamical systems:

- several stable states can co-exist, that is the system can converge to different stationary states as a function of initial conditions and random fluctuations,
- there is always some so-called bifurcation parameter, that is a variable in the system that, if changed, let the pattern on the global level emerge or not.

The last few lines have become rather technical, let's illustrate them with the termite queen chamber construction. The emerging pattern is the queen chamber, while the local interaction is termite construction activity based on local queen pheromone concentration (template) and, in addition, current theory postulates also mixing of the pellets with some construction pheromone that stimulates further pellet deposits. Actually, when [Bruinsma \(1979\)](#) put an unprotected queen in an arena with soil and termite workers, these workers didn't build directly a wall around the queen as the template mechanism would suggest, but started by building evenly spaced pillars at the right distance around the queen. These pillars are assumed to be the result of a **positive feedback**: termites mix pellets with saliva and probably with some pheromone (different from the queen pheromone) before depositing the pellet¹. Another pellet transporting termite can sense this local pheromone and its rate to deposit its pellet increases with the sensed construction pheromone concentration. This is the positive feedback. The rising pillars still let the queen pheromone diffuse quite freely around them, thus maintaining the required concentration template. This first phase therefore replaces the pheromone template by a pillar template. Once the pillars are sufficiently high the termites start to fill the space between them from the bottom up, thus building the wall. The **negative feedback** is simply the completeness of the shelter: once the shelter is finished there are no more pillars with empty space between them (except the entrance hole, see [Ladley and Bullock 2005](#) for a possible explanation): with no place where to put new pellets the termite construction activity ebbs out. There are no **multiple stable states** in this system since there is only one queen, but we will see them in later examples. However, there is a **bifurcation parameter**: worker density. If the worker density is too low the positive feedback weakens because pheromone evaporates more quickly than new transporting termites arriving at the construction site: no pillars will rise.

As this example shows, morphogenesis is rarely the result of a single mechanism. Here, a template mechanism works hand in hand with SO to let the queen chamber emerge. However, when SO was suggested as an important mechanism in biological pattern formation, the first experimental validations did their best to eliminate explanations other than SO simply to make sure SO was the only possible explanation for the observed patterns (eg. [Franks et al. 1992](#); [Theraulaz et al. 2002](#); [Jeanson et al. 2005](#)). This emphasis on "its only SO" led to some "accusations" that protagonists of SO were too narrow minded and didn't see beyond SO. I think this debate has now ebbed out: SO does not exclude inter individual variability or even leadership. Inter individual variability can even play a crucial role in a SO process (see review in [Jeanson and Weidenmüller 2014](#)), such as thermoregulation in honey bees ([Jones et al., 2004](#)) where polyandric colonies have a more stable temperature than monoandric colonies. Leadership in itself is a debated concept ([King, 2010](#); [Bourjade et al., 2015](#)), but recent research has shown that its mechanistic origins are diverse and include SO ([Petit and Bon, 2010](#)) combined with evolutionary processes ([Conradt and Roper, 2010](#)). [Gautrais \(2010\)](#) showed that leadership can result from a combination of inter individual variability and SO, with a continuum from distributed leadership to "despotic" leadership according to certain individual behavioral parameters. Coming back to morphogenesis, SO not only interacts with templates, SO can even generate dynamic templates that play a crucial role in the emerging structure ([Jost et al., 2007](#);

¹Note that the described mechanism hasn't been experimentally verified in all detail and is currently again under discussion ([Petersen et al., 2015](#)). This means that the story told above may have to be refined in the future

Weitz, 2012). A current challenge in morphogenesis is therefore to mount experimental systems where several mechanisms are at work in order to understand their interplay (eg. Jost et al. 2007), preferably concerning processes with a sound biological meaning/function. The role of inter individual variability or leadership are still completely unknown in such morphogenetic processes, but the reviews cited above suggest that they play one, the question is to identify it experimentally.

2.2 Why do we need modeling?

You may have wondered why I started this chapter with a (negative) citation on modeling. Well, first, that might be due to my teaching activity. Students frequently assume that in an experimental approach one tries to describe reality. While, in reality, we try to understand one aspect of the real system, an aspect of which we have a caricature in mind. Furthermore, when we want to understand underlying mechanism, we have a caricature of these mechanisms in mind, neglecting some details while favoring others. In sum, we see the real biological system as a caricature, and “caricature” is just another word for “model”. Just as a caricature is not reality, thus wrong, any model we have in mind is wrong: but sometimes this caricature helps us see connections and helps us understand the principal mechanisms underlying some emergent pattern. Then the model is useful, and for a biologist this usefulness is the only “raison d’être”² to formulate a model. Second, when we try to understand emerging behavior, a qualitative model is often insufficient to help us see what emerges from a particular choice of mechanisms and behaviors on the individual level (remember, we have non-linearity in a system, and predicting non-linear systems is all but trivial, just see the latest Jurassic Park sequel). Or, on the other side, several different qualitative models predict the same emerging qualitative pattern (Weitz et al., 2012), how do we compare between the models and identify the most likely one? In both cases we can go towards a quantitative model in the form of mathematical equations that can be studied either analytically or by numerical simulation, and that can be confronted statistically with the biological data. However, most biology students want to do science, but have chosen biology because they detest mathematics. My task is therefore to explain that when we do modeling, we do biology, not mathematics. We may need some mathematical techniques to understand model predictions, but this is not for fun, just a necessary nuisance. These techniques rarely exceed what they have already learned in their “baccalauréat” (bachelor in the anglo-saxon system?). The citation helps me to remind them of this, that our interests are biological questions, and that modeling is just one tool to answer them. Last not least, modeling comes more and more down to computer simulations, and many biology students are open to this tool and can use it actually fairly well.

The question asked in the section heading is therefore the wrong question: we always do modeling when we think about how biological systems work. The real question would be why we should resolve to a mathematical model to answer our biological questions. Students can accept that we do not do this for fun, but because we see no other way to answer the question.³

2.3 A methodology to study SO

The method we use to study SO in collective animal behaviors is the one well described in Camazine et al. (2001) and illustrated in Fig 2.1.

²The most important reason or purpose for something or someone’s existence

³Last not least, this citation also tells us that there is more behind Box than the box plot.

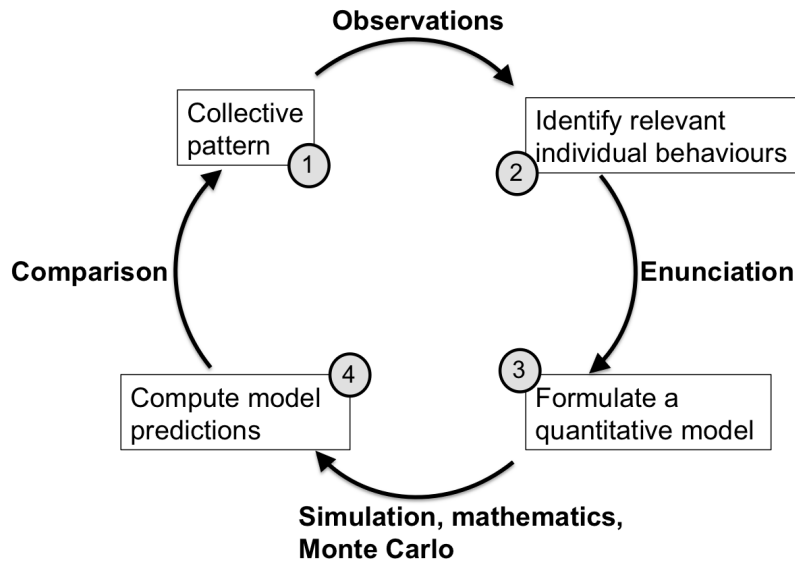


Figure 2.1 – The methodology we use to study collective animal behaviors. It starts (1) with some intriguing collective behavior we want to understand, and continues (based on observation of the system) with a first choice of relevant individual behaviors (2). These behaviors are then precisely translated into a quantitative model (enunciation) from which we predict the emerging collective patterns (3+4). Finally, the predicted pattern is compared to the actually observed pattern (4+1). If this comparison is not satisfactory, we go back to the choice of individual behaviors (maybe an important behavior was missed) or to the model enunciation (have we correctly translated the behavior into quantitative terms? are there statistical biases in the parameter estimation methods?) and redo the cycle until we find a satisfactory prediction of the collective pattern.

The main goal of this methodology is to identify the individual behaviors that can explain some collective behavior we are interested in. It therefore starts with the identification and description of some intriguing collective behavior we want to understand (step 1). In the example cited above this pattern was the construction of a shelter of the right size to protect the queen. The next step is to identify, by direct observation of the biological system, candidate individual behaviors that can explain this collective pattern (step 2). In the case of queen shelter construction this had been done in the early work of P.-P. Grassé (summarized in [Grassé 1984](#)) and by controlled experimental approaches by [Bruinsma \(1979\)](#) in his PhD work. All subsequent modeling work on this shelter construction found their biological inspiration in Bruinsma’s PhD work ([Deneubourg, 1977](#); [Courtois and Heymans, 1991](#); [Bonabeau et al., 1998a](#); [Ladley and Bullock, 2005](#); [Hill and Bullock, 2015](#)). We will illustrate the methodology with the work by [Ladley and Bullock \(2005\)](#) who selected the following elements from Bruinsma’s work:

- the termites move around randomly on the ongoing construction with a tendency to deposit pellets where previous pellets have been deposited or to move towards such places,
- the pellets themselves are impregnated by the termites with some volatile marking (cement pheromone),
- the queen emits queen pheromone at a constant rate and which diffuses in the air,
- termites only deposit pellets at a certain queen pheromone concentration.

The next step in the methodology is to formulate precisely how these behaviors are translated into a model (step 3), which is in their case a computer simulation model. My physics colleagues

call this step **model enunciation** to emphasize that a clear and precise description of this translation of individual behavior into the model is required in this step. By this emphasis there is a clear separation between step 2 (selection of individual behaviors) and step 3 (writing the model), and subsequent critical examination of the work can separately question the decisions made in both steps. [Ladley and Bullock \(2005\)](#) choose to implement construction in a 3D lattice model, where each soil pellet corresponds to a cube. Their pellet carrying termites move around randomly in the empty cells adjacent to the built cubes (according to some precise rules that the authors call logistic constraints) with a bias towards cells with a higher cement pheromone concentration. They have a fixed probability to deposit their pellet. The cement pheromone in the deposited cube decreases/evaporates exponentially. There is a fixed number of pellet carrying termites, and when one deposits pellet it disappears and a new pellet carrying termite is generated at a random location. The queen is modeled as a fixed template that emits queen pheromone at a constant rate. This pheromone spreads in the empty cells according to a standard diffusion implementation in lattices. Pellets can only be deposited within a fixed range of queen pheromone. This implementation leads indeed to the formation of a dome shaped shelter around the queen (Fig 2.2) that compares well with the observed queen shelters in [Bruinsma \(1979\)](#) or [Grassé \(1984\)](#) (step 4).

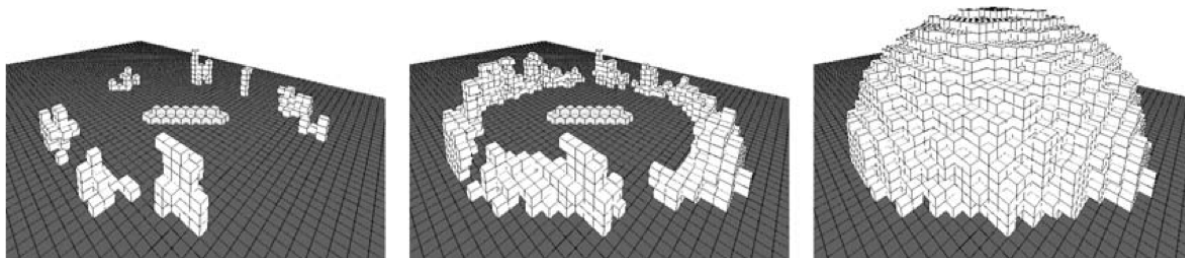


Figure 2.2 – Termite queen shelter construction according to [Ladley and Bullock \(2005\)](#): the pheromone emanating queen is the straight object in the center or the arena, rather evenly spaced pillars are formed at a constant distance around the queen and rise continually, then the space between pillars is filled up to form walls, and the queen is finally covered by a regular dome (Fig from [Ladley and Bullock 2005](#)).

Though this model relies on precise quantitative descriptions I would rather call it a **qualitative model** because none of the parameters used in the model has been estimated directly from experimental data, nor is the queen shelter described in any quantitatively precise form. Step 4 is therefore limited to a qualitative comparison, and if one is not satisfied with this comparison it is possible to “play around” with the parameter values (or, in more scientific terms, tune them) until the comparison is satisfying. While this proof of concept is useful to show that the proposed mechanisms are capable to explain the observed collective behavior, [Weitz et al. \(2012\)](#) has shown in another experimental system that many different mechanisms can produce the same collective outcome, even if the latter is precisely quantified. This illustrates that with a qualitative model we have only limited statistical power to identify/select the underlying individual behaviors. For this reason [Camazine et al. \(2001\)](#) postulates a strict **quantitative approach** for their methodology:

- the resulting collective structure must be precisely quantified to permit a quantitative (statistical) comparison between observed pattern and model predicted pattern,
- the enunciated individual behavioral rules must be parameterized as good as possible from experimental data on the individual level that are independent of the data/experiments on the collective level.

With this additional requirement the methodology resembles the well known statistical ‘in-sample out-of-sample’ model validation concept: the model is fit to part of the data (in-sample), and model validation is based on how well this fitted model predicts the out-of-sample data. The in-sample data are the one on the individual level on which the parameters of the individual behavioral rules are calibrated, while the out-of-sample data are the one on the collective level. This strict quantitative approach should increase our statistical power to detect and reject “wrong” individual behaviors (in the sense that they are not relevant to the emerging collective pattern) or “wrong” enunciations of these behaviors (in terms of model formulation and parameter estimation). Since the publication of [Camazine et al. \(2001\)](#) this full quantitative methodology has been successfully applied in several case studies: cockroach aggregation ([Jeanson et al., 2005](#); [Amé et al., 2005](#)), cockroach collective decision making ([Halloy et al., 2007](#); [Canonge et al., 2009](#)), corpse-clustering in ants ([Theraulaz et al., 2002](#)), collective motion in fish ([Gautrais et al., 2012](#)), ...

2.4 What does it take to understand social insect nest construction?

Let’s come back to morphogenesis in social insect nest construction as announced in the title. The concepts and examples described in the previous sections make it clear that several mechanisms are at work: there is self-organization as in pillar construction in termites, there are templates as in termite queen shelter construction, and these templates can even be dynamic either by external changes (day-night, winter-summer) or by internal changes (queen size, the ongoing construction itself). My research goal in the next few years will be to understand the emergence of some termite nest architectures in this framework, with the mathematical and computational tools that are needed for this goal. The rest of this text will retrace my work over the last 14 years to check whether I have the skills to pursue this goal, both conceptually as well as technically. In chapter 3 I will retrace the work on cockroach aggregation. This work started in 2001, when I came to Toulouse in Guy Theraulaz’s research group, and it was my initiation to the groups theme “collective animal behavior”. Chapter 4 will review our work on the clustering of objects, in particular corpse-clustering in the harvester ant *Messor sanctus*. During this work I started to supervise my own students both on the Masters and PhD level. Chapter 5 will summarize what we know about the mechanisms underlying nest construction in both ants and termites. During this work we also received our first ANR grant that permitted us to create a large data-base of 3D nest-architectures and the presentation of some of these nests in a public virtual museum (<http://www.mesomorph.fr>). Finally, in chapter 6 I will develop my research program for the next couple of years that involves in particular two PhD students that started their work in fall 2014 or will start it in fall 2015, the jury’s assessment of these perspectives will therefore be highly valuable.

Chapter 3

Self-clustering of animals (or robots)

The clustering of animals of the same species is a widespread phenomenon in nature ([Krause and Ruxton, 2002](#)). Such clustering can have an adaptive purpose (create a locally favorable micro climate, better defense against predators, more efficient predation, mate finding, . . .), but it also includes costs (competition for resources, more visible to predators, . . .). Independently of the adaptive nature of this clustering, one can also investigate the behavioral mechanisms that permit the animals to group together. When I arrived in the CRCA in Toulouse in 2001 Raphaël Jeanson had just started his PhD and was working on these individual behavioral mechanisms in the case of the aggregation of german cockroach larvae (*Blattella germanica*, Fig 3.1). These cockroaches frequently aggregate together during the resting phase, Fig 3.1, purportedly to create a favorable microclimate ([Dambach and Goehlen, 1999](#)). Clustering has also been shown to increase individual growth ([Prokopy and Roitberg, 2001](#)).

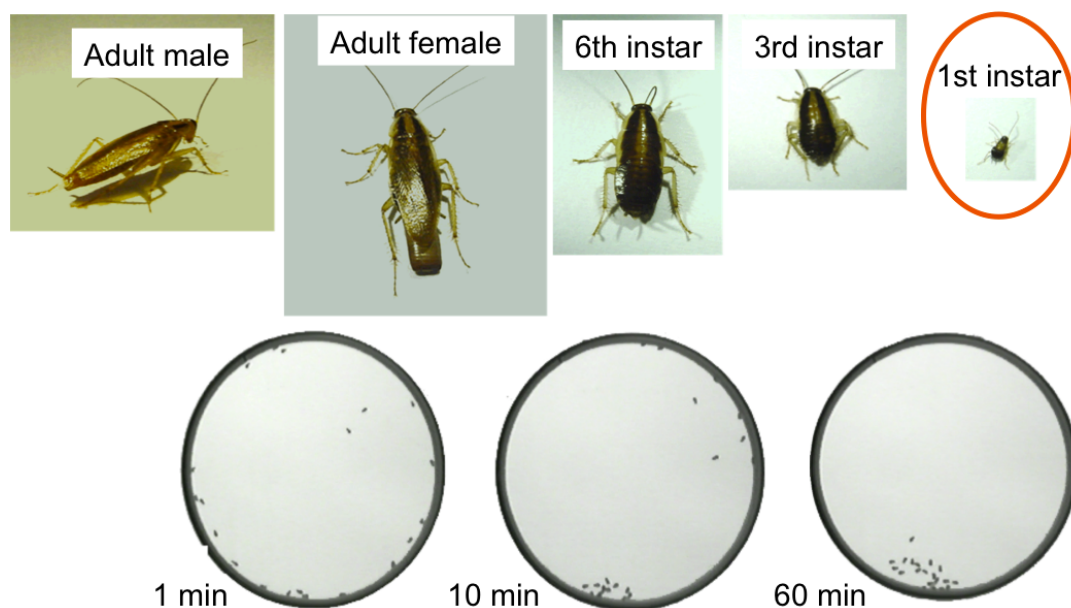


Figure 3.1 – The german cockroach (*Blattella germanica*): adult male and female (the latter carries an ootheca) and three instars during their development. The bottom row shows the experimental aggregation pattern: 20 cockroach 1st instar larvae are released in a Petri Dish (diameter 11 cm), they first move around to explore the arena, then start aggregating until in the end there is a single or two aggregates.

3.1 Apply the SO methodology to study cockroach aggregation behavior

Raphaël's work required to program cockroach aggregation as an individual based model (IBM) in order to predict the emerging aggregation pattern from his experimentally determined individual behaviors¹. His PhD supervisors Guy Theraulaz and Jean-Louis Deneubourg decided that I could work with him for several reasons: (a) Raphaël was new to programming, an independent implementation by another programmer in a different language would therefore ensure that no major bug distorted his results, (b) my background in model selection could be useful to decide which behaviors are essential to be included in his IBM, and (c) for me this was the ideal opportunity to dive into the world of collective animal behaviors.

Cockroach aggregation behavior has three components: (1) cockroach movement, (2) cockroach stopping and (3) cockroach departure. Cockroach movement in the experimental arena (Petri Dish with diameter 11 cm) has itself two components, a standard diffusive random walk in 2 dimensions when far (>5 mm) from the Petri Dish wall, and a strong tendency to follow the wall (often called [thigmotactic behavior](#)) for a long time, sometimes making a U-turn (thus a 1-dimensional random walk), before returning to the arena center. This switching between 2-D and 1-D random walk had already been worked out by Raphaël and our physics colleagues Richard Fournier and Stéphane Blanco ([Jeanson et al., 2003](#)), in particular how to estimate model parameters from the experimental data. Several key ingredients of their model are worth mentioning. The size of the arena permitted to model the 2-D random walk in the arena center with an isotropic phase function (rather than the correlated random walk that describes an animal's trajectory more precisely, [Codling et al. 2008](#)): the longer ballistic phase in the correlated random walk had no importance for the emerging cockroach distribution in the arena and parameter estimation for a random walk with isotropic phase function is much simpler than for a correlated random walk, it only required to estimate mean cockroach speed and the mean free transport path from the slope of the net squared displacement (if you are completely lost with this terminology I suggest to read [Challet et al. \(2005b\)](#) for an introduction to correlated random walks and the appendix in [Casellas et al. \(2008\)](#) for the formal link between correlated random walks, isotropic random walks and net squared displacement that actually goes back to [Einstein \(1905\)](#)). The rate to do a U-turn when following the arena wall was much smaller than the rate to leave the arena wall, it could therefore be neglected. Sometimes a cockroach stopped and rested for a certain time before moving again. The inclusion of this behavior proved to be essential to correctly predict cockroach density in the arena center as well as along the arena wall. We will come back to the details of this stopping behavior in the next paragraph.

Cockroach stopping behavior was then studied as a function of how many stopped neighbors a moving cockroach can detect. This neighbor detection happens by tactile contact with either antenna or cerci, the number of neighbors can therefore be considered as the number of individuals within reach of antenna and cerci (fixed perception radius). Raphaël needed in particular to estimate the **rate** of stopping as a function of the number of stopped neighbors. For spontaneous stops this was rather easy, it was sufficient to measure the time of movement before a spontaneous stop and estimate this rate as the inverse of the mean movement time. Furthermore, the survival curve of the moving times resembled an exponential distribution, the rate can therefore also be estimated as the slope of this survival curve on log-linear scale (technically this means that spontaneous stopping can be modeled as a memory-less or Markovian process with a constant stopping rate - the underlying mathematics can be found in any textbook on statistical physics). Estimating the stopping rates when the cockroach senses N

¹A cluster or aggregation can be defined as any assemblage of individuals that results in a higher density than in the surrounding environment ([Camazine et al., 2001](#)).

stopped neighbors required a different technique: Raphaël observed all encounters between a moving cockroach and an aggregate of size N and computed the fraction of cockroaches that actually stopped in the aggregate. Assuming a constant speed and a fixed encounter duration between the moving cockroach and an aggregate of size N one can estimate the stopping rate of each N (see Appendix in Jeanson et al. 2003). It turned out that the stopping rate increases monotonically with size N - this is a positive feedback, the cockroach has an increased tendency to stop the more stopped neighbors are around it.

Finally, stop duration turned out to be the most tricky part in Raphaël's model. Fig 3.2(a) shows the survival curves of the times an aggregate remained of fixed size N before changing its size (departure or arrival of a cockroach). Contrary to the spontaneous stop survival curve, these curves do not resemble an exponential distribution (that would be a straight line on log-linear scale), at best they resemble the combination of two straight lines. Indeed, when observing the stopped cockroaches more closely, Raphaël saw that some of them remained rather nervous (moving the antenna and cerci), while others appeared to be very calm. The first had on average shorter stop durations than the latter. Raphaël and coworkers therefore suggested that a stopped cockroach can be in two states: a nervous state with a (fixed) high departure rate, and a calm state with a (fixed) low departure rate. The resulting survival curve of such a process would be the superposition of two exponential curves, resulting in such a bilinear pattern. When estimating the associated parameters from his survival curves he found that the fraction of nervous cockroaches decreased with aggregate size N , while the departure rates for both states also decreased with N . In short, the larger the aggregate, the longer the cockroaches tend to stay - this is again a positive feedback.

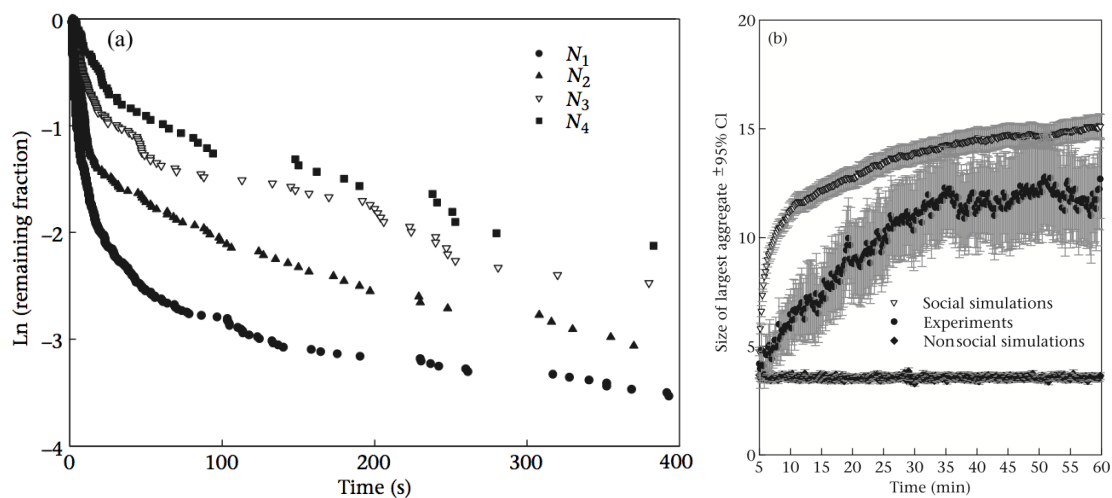


Figure 3.2 – (a) Survival curves (on log-linear scale) of the stop durations of aggregates of size $N = 1, 2, 3$ and 4, (b) comparison between the dynamics of the largest aggregate size (with 20 cockroaches in the arena) between experiments, the IBM's predictions (Social simulations) and the predictions when the two positive feedbacks had been removed from the simulations (Nonsocial simulations). These are Figs 2 and 3 from Jeanson et al. 2003.

The combination of the two positive feedbacks, stop when there are many stopped neighbors and leave when there are few stopped neighbors, results in a strong overall positive feedback that promotes cockroach aggregation. Raphaël identified this positive feedback as the core social behavior that promotes cockroach aggregation. Putting all these behaviors together in his simulation code (Fig 3.2(b)) the experimental dynamics of the largest aggregate size were close to the model predictions, but when he removed the positive feedback from this model there was simply no aggregation at all (Nonsocial experiments in Fig 3.2(b)).

3.2 A first scheme for quantitatively based model selection

Raphaël decided to include (or not include) a behavior in his model by comparing the experimental data visually to the model predicted values (for example the fit of the “double exponential” curves in Fig 3.2(a), or the closeness between experimental dynamics and Social simulation dynamics in Fig 3.2(b)). However, while the “double exponential” seemed to fit the survival curves much better than a simple exponential distribution, this criterion does not tell whether the “double exponential” is important with respect to the global aggregation dynamics. To test this question one could fit exponential distributions to the survival curves, redo the simulations and compare visually whether the model with “double exponential” distributions improves model predictions. As my modest original contribution to Raphaël’s work I tried to develop a quantitative model assessment criterion to decide whether the “double exponential” is indeed necessary (Jost et al., 2002).

We keep the in-sample and out-of-sample framework outlined in section 2.3: estimate all model parameters with data on the individual level (in-sample), then predict the emerging collective level and compare it to the actually observed pattern on the collective level (out-of-sample). On the individual level the stop durations will either be fit to a simple exponential curve or to the double exponential curve, predicting then in both cases the out-of-sample prediction by Monte Carlo simulation. The only difference to Raphaël’s will be, following the ideas of model selection theory in Linhard and Zucchini (1986), to define a so-called “discrepancy”, which is simply a quantitative measure of proximity between predicted and observed pattern. Since the predicted pattern is a whole dynamic system (as in Fig 3.2(b) I will use the dynamics of the largest aggregate) this discrepancy has to properly weigh the different phases in the dynamics (increasing phase, stationary state). Since Raphaël had performed 22 experiments with 20 cockroaches in the arena, we have at each time step 22 largest aggregates from which we compute the cumulative distribution (CDLA, Fig 3.3). Since the cockroaches had to be anesthetized (CO₂) when transferred to the Petri Dish, the beginning of the experiments may have been perturbed due to their waking up. We therefore sampled these dynamics at 20, 40 and 60 minutes only to catch the increasing and the stationary phase.

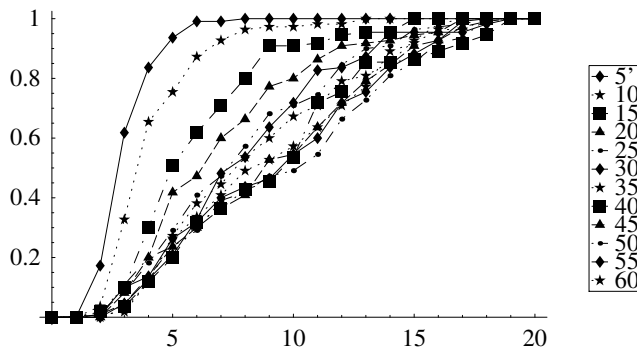


Figure 3.3 – The dynamics of the cumulative distribution of the largest aggregate (CDLA), sampled over the 22 original experiments every five minutes. The x -axis is aggregate size (figure taken from Jost et al. 2002).

To get the predicted pattern I computed the cumulative distribution of the size of the largest aggregate for 22 *in silico* experiments at 20, 40 and 60 minutes, estimating its expected form in a Monte Carlo setup by repeating the 22 experiments 20 times. The discrepancy between these predicted distributions and the observed distributions in Fig 3.3 is computed as the sum of weighted squared differences for all aggregate sizes (X_w^2), the weight being the variance of

the estimated distributions at each aggregate size (see Fig 3.4). The results are ambiguous: the exponential distribution actually produced a smaller overall X_w^2 , but the CDLA barely moved between the sampled times, that is it was at stationary state already at 20 min contrary to the observed CDLA. With the double-exponential distribution we recover the dynamics of the CDLA, but overall X_w^2 is much worse.

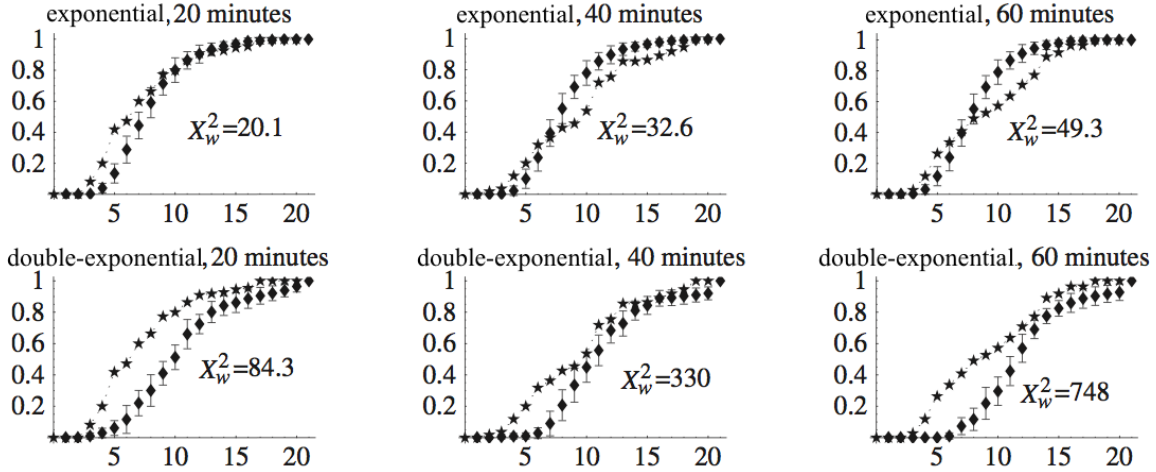


Figure 3.4 – Comparison between the observed CDLA at 20, 40 and 60 minutes and the model predicted CDLA, on the top row assuming exponential distributions of the stopping times, on the bottom row assuming double-exponential distributions (figure modified after Jost et al. 2002).

In sum, this first shot at a quantitative model selection approach in the context of collective animal behaviors was not conclusive. We could choose other or more sampled times to give more weight to the dynamics of the CDLA. We could also replace the X_w^2 by a Kolmogorov-Smirnov type maximal distance between observed and predicted CDLA. Note also that my discrepancy measure did not account for model complexity (the exponential distributions require one parameter, the double exponential three parameters). The approaching dead-line for the Monte Verità workshop put a stop to these first trials, as unsatisfying as they were, but I will come back to this problem of model selection and controlling model complexity in chapter 6.

3.3 Cockroach clustering and collective robotics

When I arrived in Toulouse in 2001 our workgroup had also just started as a partner in the European LEURRE project² under the coordination of Jean-Louis Deneubourg (ULB, Bruxelles, Belgium). The goal of the LEURRE project was to create mixed animal-robot societies and to apply self-organization theory in order to let the robots control the collective animal behavior (Halloy et al., 2007). The robots themselves should merge with the animal group and be accepted by them as one of their own. The principal model organism were cockroaches (*Periplaneta americana*, with Colette Rivault from the University of Rennes as the expert partner on cockroach chemical communication, the experiments themselves being done in Bruxelles), the robot partners were Roland Siegwart and Gilles Caprari from the Ecole polytechnique fédérale Lausanne (EPFL), and Toulouse explored how the results achieved with cockroaches could be transferred to a more complex organism, sheep. Gilles had actually already developed an autonomous mini-robot, the “sugar cube” robot Alice (Fig 3.5). For the LEURRE project he would develop with his partners a new insbot (insect like robot) tailor made for the interaction with

²Future and Emerging Technologies – Information Society Technologies, grant FET-OPEN-IST-2001-35506

cockroaches. But while waiting for this robot to be engineered (it was actually ready in the 3rd LEURRE year) we decided to start collective robotics experiments with the Alice robots in Toulouse (where we already had a couple of these robots, Gilles delivered 20 more to make a nice little robot herd).

Raphaël’s model of German cockroach (*Blattella germanica*) aggregation served as the starting point to implement the same aggregation behavior in the Alice robots. The standard Alice has 4 infrared (IR) sensors to detect objects around them (Fig 3.5), two independent motors to move around freely, they can recognize other Alice by radio contact, and they have about 5h autonomy. A diode on the Alice’s top can also signal its state to an observer. Gilles had developed a library to program Alice in the C-language. I started the work by implementing the single cockroach behavior in a circular arena (Jeanson et al., 2003). We were lucky that at this moment a gifted Master student, Simon Garnier, arrived in the workgroup. He was interested in exactly what we did: study collective animal behavior with the help of experiments, modeling, simulation and robotics. During his Master internship we implemented together the whole cockroach aggregation behavior (Fig 3.5) and tuned the robots minutely to do quantitatively exactly the same as the cockroaches (Garnier, 2004; Jost et al., 2004; Garnier et al., 2008). This was the proof of concept that mini-robot technology could reproduce a simple collective insect behavior at the same scale as the insects.³

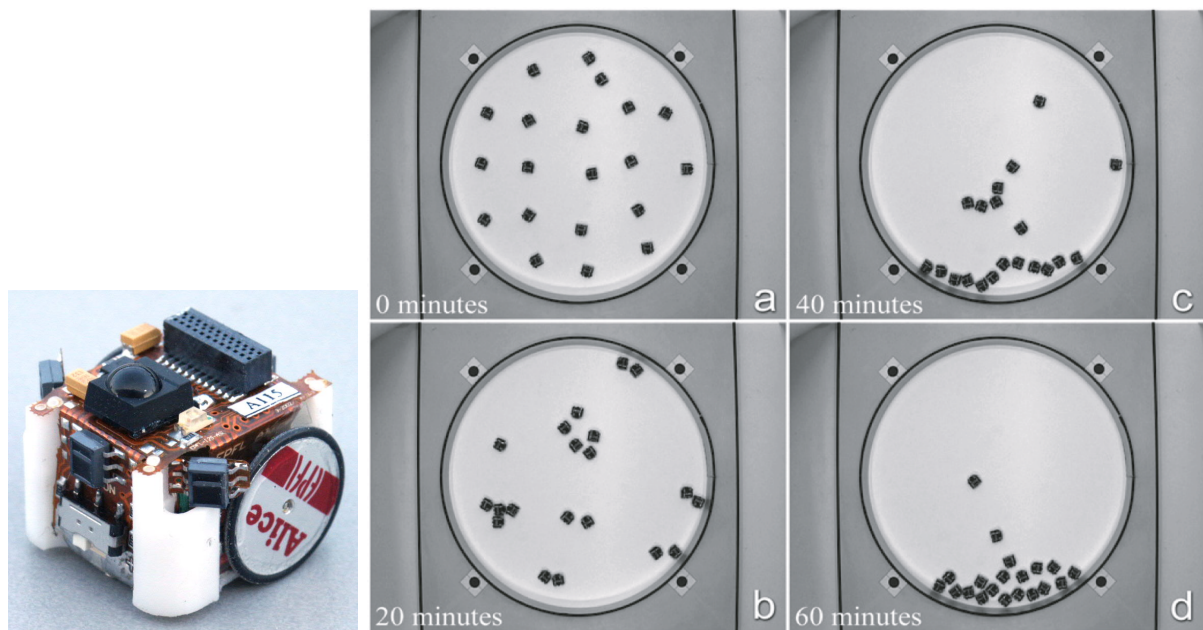


Figure 3.5 – An Alice robot with his three infrared sensors pointing forward (there is also one in the back). (a-d) Aggregation process of the Alice in a circular arena (diameter 50cm).

3.3.1 Clustering and collective decision making

Collective decision-making is a cornerstone for the functioning of animal groups: see Sumpter (2010, Ch 4) for a general review, Camazine et al. (2001, Ch 12) for bee foraging, Beckers et al. (1990) for ant foraging, Detrain and Deneubourg (2008) for the comparison between bee and ant foraging, Seeley et al. (2012) for bee nest site selection, to cite but a few. For a collective decision to happen there must be a strong positive feedback (Detrain and Deneubourg, 2008). Is

³In the final mixed societies the insbot had actually a much simpler behavioral program – key to the successful subtle interaction with cockroaches was to make it smell like a cockroach (Sempo et al., 2006; Halloy et al., 2007).

the positive feedback in cockroach aggregation (stop where there are many cockroaches, depart when there are few around the cockroach) sufficiently strong to trigger a collective decision? Indeed it is, [Amé et al. \(2006\)](#) could even show that the process leads to optimal mean benefit for group individuals. Note also that the final experimental setup chosen in the LEURRE project to show that the mixed societies worked and that the robots could influence collective behavior was a collective decision setup ([Halloy et al., 2007](#)).

After his Master, Simon started a PhD on collective decisions in general under the supervision of Guy Theraulaz. The robot setup developed during his Master ([Garnier, 2004](#)) continued to serve as a testbed (together with collective foraging in the Argentine ant *Linepithema humile*). Inside the arena there were two suspended disks of red acrylic glass to provide two shelters from light (very similar to the final setup used in the LEURRE project). The robots could move freely under these disks or in the rest of the arena, but they were programmed to stop only under the shelters. The positive feedback implemented previously could therefore only unfold beneath these shelters. Stopped robots light their diode to be detectable below the shelters. See [Fig 3.6](#) for the setup and a typical experiment.

In a first setup ([Garnier et al., 2005](#)) the robots had the choice between two disks of the same size (14 cm diameter). While a trinomial distribution (distribution of randomly moving animals without a positive feedback between shelter 1, shelter 2, and the rest of the arena) would predict an equal number of robots under each shelter ([Fig 3.6B.1](#)), the robot experiments as well as computer simulations show a U-shaped choice distribution, meaning that in each experiment robots cluster preferentially under one of the two disks, but either disk can be chosen with equal probability ([Fig 3.6B.2-B.3](#)). In a second series of experiments they had a choice between a 10 cm disk and a 14 cm disk: they preferentially chose the 14 cm disk ([Fig 3.6A.2-A.3](#)). In a final series of experiments they had a choice between an 18 cm disk and a 14 cm disk: they preferentially choose the 18 cm disk ([Fig 3.6C.2-C.3](#)). [Garnier et al. \(2005\)](#) concluded that robots, just as cockroaches, make a collective decision for the larger disk without robots explicitly comparing between the two sites. This could be explained by the higher probability for a randomly moving robot to encounter the larger disk, but robot densities under the larger disk tend to be lower, thus decreasing the strength of the positive feedback. To explore the interplay between these two mechanisms [Garnier et al. \(2009a\)](#) performed further simulation work where they varied the ratio between the two shelter sizes continuously from 0 to 7 (while keeping the arena size always proportional to the sum of the sizes of the two shelters): indeed, the preference for the larger disk had a maximum for a ratio around 2 and then decreased continuously, though still preferring the larger disk but with decreasing asymmetry.

3.3.2 Trail formation in robots: light as a substitute to pheromones

Insect communication relies to a large extent on pheromone communication. Robot technology is still far away from using pheromones in the same way as insects. In [Halloy et al. \(2007\)](#) the insbots were made to smell like cockroaches by glueing filter paper on them that was sprinkled with the pheromone cocktail identified by the group in Rennes ([Saïd et al., 2005](#)). However, the robot had neither control of pheromone emission, nor could it detect the pheromones. This shuts the door to the transfer of many social insect solutions to collective robotics. However, when discussing this problem with Fabien Tâche (one of the roboticists in Lausanne involved in the *Leurre* project) we thought that light is very easy to detect by a robot. We thus started fantasizing about a system where light trails are projected by a video-projector, the robot detects the light with two photosensors (to imitate the osmotropotaxic pheromone orientation in ants, [Fraenkel and Gunn 1961](#)), its position being tracked in real time and this information used to program what should be projected by the video-projector. Unfortunately, when time is ripe,

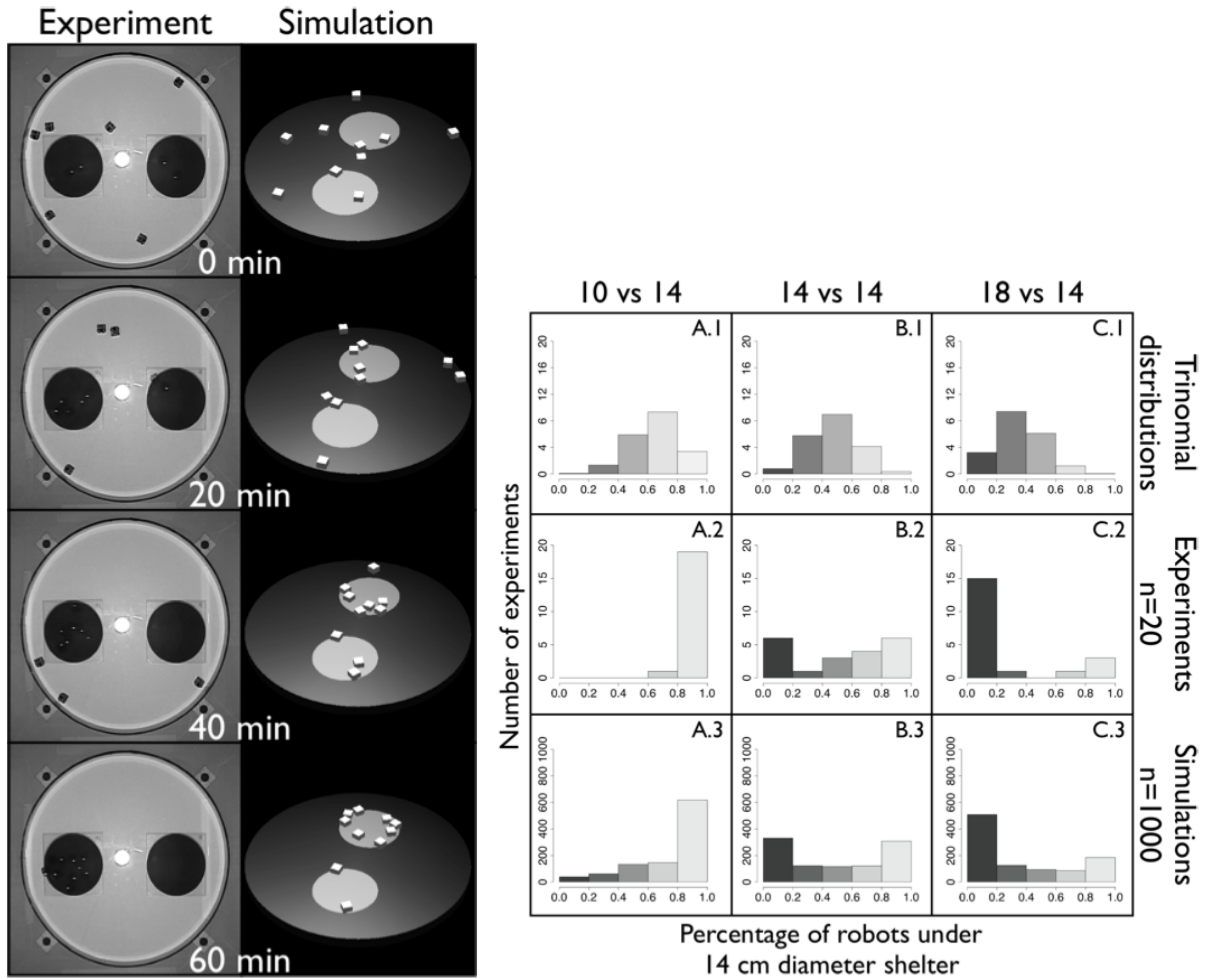


Figure 3.6 – Collective decisions by the Alice robot: (left) experimental setup with two shelters seen from the top or in a 3D visualization, (right) choice distributions (percentage of cockroaches under the 14 cm diameter disk on the x -axis, number of experiments that ended with this percentage on the y -axis: a dominant bar on the right means the 14 cm disk has been chosen in columns A and C) when the robots had a choice between two disks of sizes 10 cm and 14 cm (column A), between two equal sized disks of 14 cm (column B) and between two disks of sizes 18 cm and 14 cm (column C). The top row shows the expected choice distribution from a trinomial distribution (that has no positive feedback mechanism), the middle row the result of 20 robot experiments with 10 robots each, and the bottom row the result of spatially explicit Monte-Carlo simulations. Figs taken from [Garnier et al. \(2005\)](#).

great ideas tend to emerge in parallel in many places. By the time Fabien had developed the first prototype of this system we discovered that the Japanese had had exactly the same idea and were beyond prototypes (Kazama et al., 2004; Sugawara, 2005). Nevertheless, Simon took up Fabien’s prototype and adapted it (Fig 3.7) to study questions he had faced in the foraging decisions made by argentine ants *Linepithema humile* (Garnier et al., 2009b). If ants access a food source via a bridge with two equal length branches they make a collective decision and most traffic will circulate on only one of these branches (Beckers et al., 1992b; Dussutour et al., 2004). The underlying mechanism is the ant’s choice function when facing a Y junction with pheromone concentrations on the left and on the right: this choice function is highly non-linear, with small differences in pheromone concentrations amplifying the turning bias towards the higher pheromone side.⁴ Simon constructed the same setup for the Alice robot (Fig 3.7(b)):

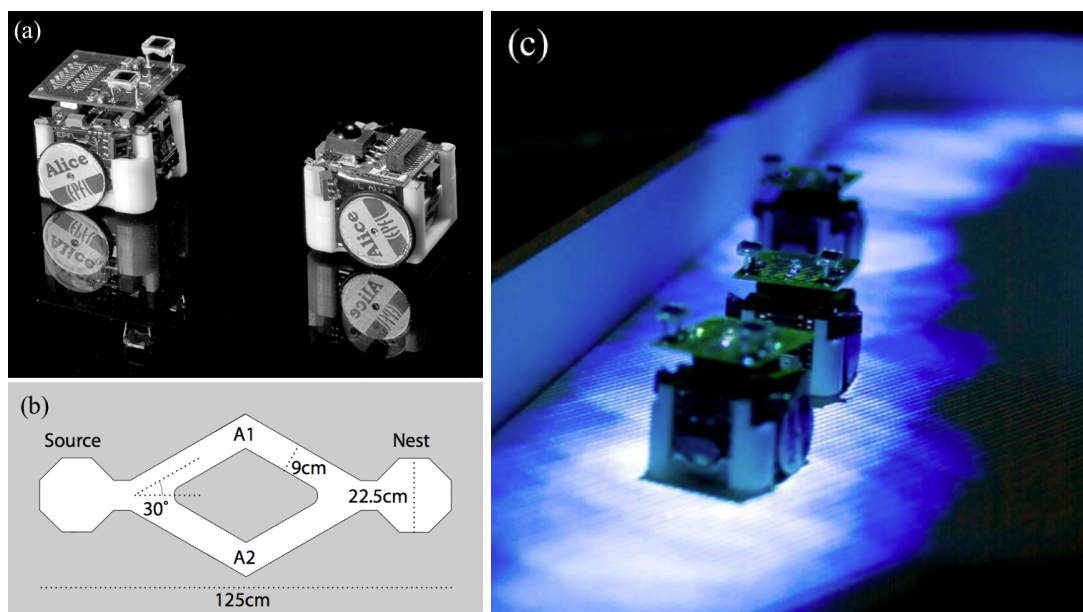


Figure 3.7 – The Alice light trail experiments: (a) An Alice equipped with two photosensors that can detect independently light intensity (similar to the two ant antennas that detect pheromone concentration), (b) the simple experimental setup used, with a diamond shaped channel system between the “nest” and the “food”, (c) three Alice robots following the projected light trail. Figs modified after Garnier et al. (2007).

as soon as the robot leaves the nest or the source it switches on its LED, is detected by the tracking system which projects on this position a light spot (pheromone) which decays slowly with an exponential type decay. The robots perform a standard correlated random walk unless they detect light, in which case they turn preferentially towards the higher light intensity (Fig 3.7(c)). With this “simple” setup the robot herd produced the same branch selection as the ants (Garnier et al., 2007).

The next step was to let the robots navigate in a more complex network with variable geometry. Fig 3.8 shows the used setups: they had 3 loops and the junctions were either symmetrical or asymmetrical. Argentine ants tend to choose the branch where they have to turn less, and they found the shortest path faster in the asymmetrical setup than in the symmetrical

⁴Note that ants do not compare the pheromone concentrations between the left and right branch, they simply detect the pheromone concentrations with their two antenna and the net difference influences the magnitude of turning behavior according to a Weber’s law. Perna et al. (2012) showed this experimentally and further showed analytically that this simple behavior combined with some directional noise can result in the Deneubourg type non-linear choice function (Beckers et al., 1992b) usually used in the literature.

one (Garnier et al., 2009b). Note that such asymmetries in trail bifurcations had been found in real ant trails (Jackson et al., 2004). Simulations in Garnier et al. (2009b) had shown that the ant’s preference for small deviations could explain this difference and that foraging efficiency (measured in the simulations as the number of ants going from S to T or from T to S) was three times higher in the asymmetrical setup. The implementation in the robotics system (Garnier et al., 2013) showed two things: (a) the light “pheromone” recruitment system combined with asymmetrical junctions resulted in the highest recruitment efficiency (Fig 3.8), (b) the robots did not need to know the turning angle to the next branch in order to bias their choice to the lesser angle, the “inertia” of their correlated random walk combined with obstacle avoidance behavior and the amplification power of pheromone trails was sufficient to reproduce this behavior.

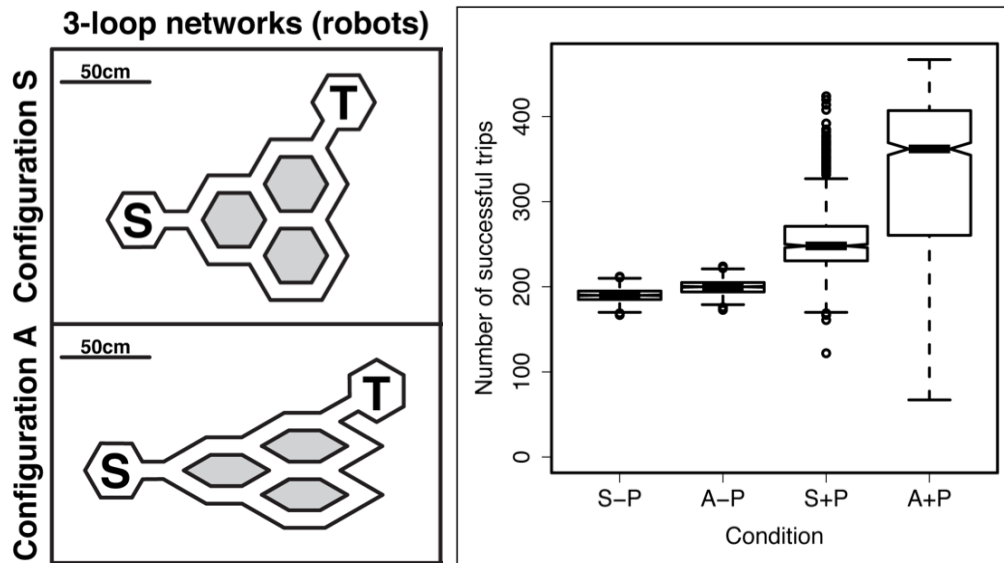


Figure 3.8 – (left) The 3 loop networks used in Garnier et al. (2013) with either symmetrical junctions (wherever the robot comes from, it has to turn the same angle) or asymmetrical junctions (the angle to turn depends where the robot comes from and where it goes). S marks the starting area, T the target area. (right) Foraging efficiency (measured by the number of successful trips) of the robots in the symmetrical (S) or asymmetrical (A) setup and with (+P) or without (-P) light “pheromones”. Figs taken from Garnier et al. (2013).

When we had started working with robots (Garnier, 2004) we had only in mind to use social insect behavior as a bio-inspiration for collective robotics, with the additional challenge to reproduce cockroach behavior on the right scale. However, when Jean-Louis Deneubourg remarked provocatively that this work had taught us nothing about biology we were nevertheless somewhat disappointed. Continuing to think about this problem we meanwhile nevertheless think that collective robotics experiments can also help us answer biological questions. Garnier (2011) mentions several reasons:

1. robots require a complete specification and implementation of the individual behavior in a given environment (similar to simple computer simulations),
2. robots are physical entities that move around in physical space with all its constraints (this is more difficult to include realistically in computer simulations). It was exactly this property that made robots the tool of choice in the mixed societies study (Halloy et al., 2007), and robots, as modern lures, are used in many other areas of behavioral research,
3. robots can be inadvertent sources for biological inspiration (as in Garnier et al. (2013))

that taught us that robots do not need to measure angles in order to favor low directional changes in a Y-maze – so why should ants need to know such angles to show their behavioral bias towards low angle directional changes?),

4. robots are simply very “cool” gadgets that help direct attention to our questions and that are of great use with students to illustrate biological ideas (more so than simulations which are less transparent for many biology students). The last point is well illustrated by the media coverage given to [Garnier et al. \(2013\)](#).

In sum, collective robotics will remain in the behavioral biologist’s toolbox, in particular because robot behavior is completely controlled by the programmer and their physical presence make interactions with real animals possible.

Chapter 4

Object-clustering: corpse clustering in ants

The first step towards nest construction is the clustering of objects. It was the clustering of soil pellets by termites that inspired [Grassé \(1959, 1967\)](#) to create his stigmergy concept ([Theraulaz and Bonabeau, 1999](#)). One of the first experimental demonstrations of self-organization in social insect nest construction was with *Leptothorax* ants that chose small cavities for nesting where they build additional walls by simply bulldozing sand pellets together ([Franks et al., 1992](#)). In the last century [Chrétien \(1996\)](#) invented another clustering paradigm to study the underlying mechanisms: the aggregation of dead nest mates by the black garden ant *Lasius niger*. When an ant dies within its colony the corpse is usually picked up by some nest mate and transported outside the nest ([Wilson et al., 1958](#); [Haskins and Haskins, 1974](#); [Howard and Tschinkel, 1976](#)) where it is aggregated in refuse piles (or middens) together with other waste from the nest (Fig 4.1).



Figure 4.1 – *Messor sanctus* is a harvester ant living around the Mediterranean. They harvest grains from plants and store them in their underground chambers as food reserve. Waste, such as the corpses of dead conspecifics, is expelled from the nest and accumulated by the ants in refuse piles or middens, purportedly for nest hygienics. They have often erroneously been called “cemeteries”, but corpses are treated just as any other garbage object.

This behavior is usually interpreted as serving nest hygienics. Dead corpses, as all other

waste, let pathogens grow on them: expelling them from the nest reduces the risk of infection and aggregating them reduces the risk for foraging ants to get in contact with contaminated material. Workers identify corpses by their production of fatty acids (eg. oleic acid, [Wilson et al. 1958](#); [Howard and Tschinkel 1976](#)) and they usually never bring the corpses back into the nest (but see also [Gordon 1983](#) who found that this behavior may depend on the social context). This last property was used by [Chrétien \(1996\)](#): she distributed ant corpses in a flat arena and let the ants arrive spontaneously in the arena. The ants quickly started assembling/aggregating the corpses into piles, and since the corpses are never brought back to the nest the dynamics of the complete clustering process and the fate of all corpses could be observed by simply filming the experimental setup. [Chrétien \(1996\)](#) found that any corpse found by the ant had the same probability to be picked up (she did not assess whether local corpse density changes this probability, she only varied their distance from the nest), that they are then transported a certain distance away from the nest entrance and preferentially deposited at the arena border or on other objects such as corpse piles (spontaneous depositing occurred, but with a low rate). A simple simulation model (1-dimensional cellular automaton with a cell line along the arena border, ants moving from cell to cell at constant velocity, with a constant probability to pick up an encountered corpse, while varying the deposition probability with local corpse density) permitted her to reproduce the observed aggregation patterns qualitatively.

To fully apply the methodology outlined in section 2.3 [Theraulaz et al. \(2002\)](#) started the same kind of experiments with the harvester ant *Messor sanctus*¹ (Fig 4.2). Since [Chrétien \(1996\)](#) had observed that corpses are mostly deposited along the arena border and, once there, remained there even if picked up again, they chose to distributed the corpses in the beginning homogeneously along the arena border. As can be seen in Fig 4.2 the aggregation dynamics took indeed place along the arena border.

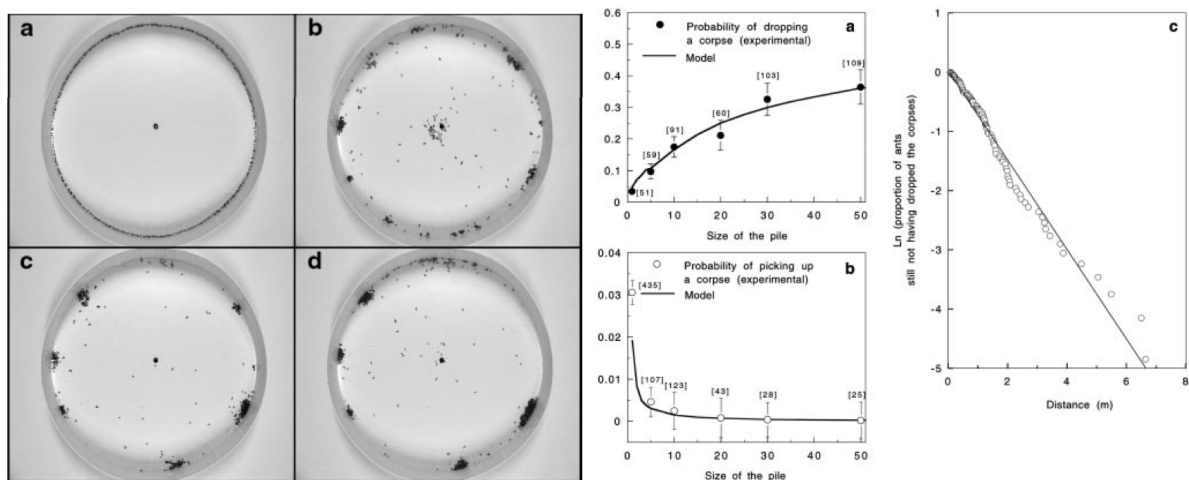


Figure 4.2 – (left) Corpse-clustering in *Messor sanctus* in a circular arena when the corpses are initially distributed homogeneously along the arena border. The nest is beneath the arena and exploring ants enter the arena along a wood stick through the hole in the centre of the arena. Corpses are distributed in the beginning regularly along the arena border and apparently remain there during the hole aggregation process. (right) Corpse depositing (top left) and picking up (bottom left) probability as a function of pile size, with the calibrated theoretical curve; survival curve of transport distance (right) that resembles an exponential distribution. (Figs 1 and 3 from [Theraulaz et al. 2002](#)).

In a first series of experiments they measured the probability for a corpse transporting ant

¹Note that this species is also called *Messor sancta*, but since the latin root of *Messor* is masculine L. Passera argues that the adjective should also be masculine – I go along with L. Passera in this text.

to deposit a corpse on a pile of size 1, 5, 10, 20, 30 or 50 corpses, for a free exploring ant to pick up a corpse on the same pile sizes, and the transport distance before depositing a corpse (Fig 4.2(right)). We can see a similar positive feedback as in cockroach aggregation: pick up corpses at low densities and deposit them preferentially at high corpse densities. The increasing scarcity of isolated corpses and the low picking up rates of corpses in piles act as a negative feedback that maintain the dynamical system finally in a stationary state.

How to model these observed behaviors? Since transport distance was distributed like an exponential distribution (memory less process) spontaneous corpse deposition can be modeled with a constant deposition rate k_d (estimated as the slope of the survival curve on log-linear scale). Depositing and picking up behavior are more complicated. Let Φ_c be perceived corpse density (up to 1 cm behind and in front of an ant), ρ a fixed free (non-transporting) ant density, a the density of transporting ants and c the corpse density. The picking-up rate can then be modeled as $\frac{\alpha_3 \rho}{\alpha_4 + \Phi_c}$, and the deposition rate as $\frac{\alpha_1 \Phi_c}{\alpha_2 + \Phi_c}$. Inversion techniques permitted to estimate the parameters α_i from the observed probabilities: the fitted functions are shown in Fig 4.2 (the full details of the inversion process can be found in Weitz 2012). Given the uncertainties in the measured probabilities the fitted functions well describe individual depositing and picking up behavior. Finally, they also measured average ant speed v and the mean distance following the border before making a U-turn, mean free transport path l .

Given all this information an individual based model (IBM) could be implemented on a computer in order to predict the emerging clustering dynamics and compare them to the observed dynamics. But one can also derive from these parameterized individual behaviors a mean field model in the form of partial differential equations (PDE):

$$\begin{aligned} \frac{\partial c}{\partial t} &= \Omega(c, a) \\ \frac{\partial a}{\partial t} &= -\Omega(c, a) + \underbrace{D \frac{\partial^2 a}{\partial x^2}}_I \\ \Omega(c, a) &= v \left[\underbrace{k_d a}_{II} + \underbrace{\frac{\alpha_1 \Phi_c}{\alpha_2 + \Phi_c} a}_{III} + \underbrace{\frac{\alpha_3 \rho}{\alpha_4 + \Phi_c} c}_{IV} \right] \end{aligned}$$

Part I represents the diffusive random walk of transporting ants along the arena border (follow the border and make a U-turn at rate $1/l$) with the diffusion coefficient $D = vl/2$. Note that ants usually deposited their corpse before making a U-turn, diffusion could therefore be neglected. Part II is the increase in corpse density through a spontaneous deposition (without any corpses within the ants perception area), part III the increase due to corpse induced deposition, and part IV corpse picking up. Numerical simulations of this set of equations showed that the model perfectly predicts the observed clustering dynamics, illustrated in Fig 4.3 for the case of the dynamics of the number of clusters.

Furthermore, the analysis of the equations showed that no aggregation should occur below a certain corpse density (this density is therefore a bifurcation parameter). This prediction was also experimentally verified. Overall, Theraulaz et al. (2002) is an example of the completely applied methodology (section 2.3) in order to identify the underlying behavioral mechanisms.

To show the importance of doing the whole methodology, in particular to predict the emerging pattern from experimentally observed and quantified individual behaviors, physics PhD student Sébastien Weitz (see also his other work below) choose in the methodological paper Weitz et al. (2012) 6 different behavioral models and fitted them only to the collective data in Fig 4.3 by choosing freely the functional forms of these behaviors and the associated parame-

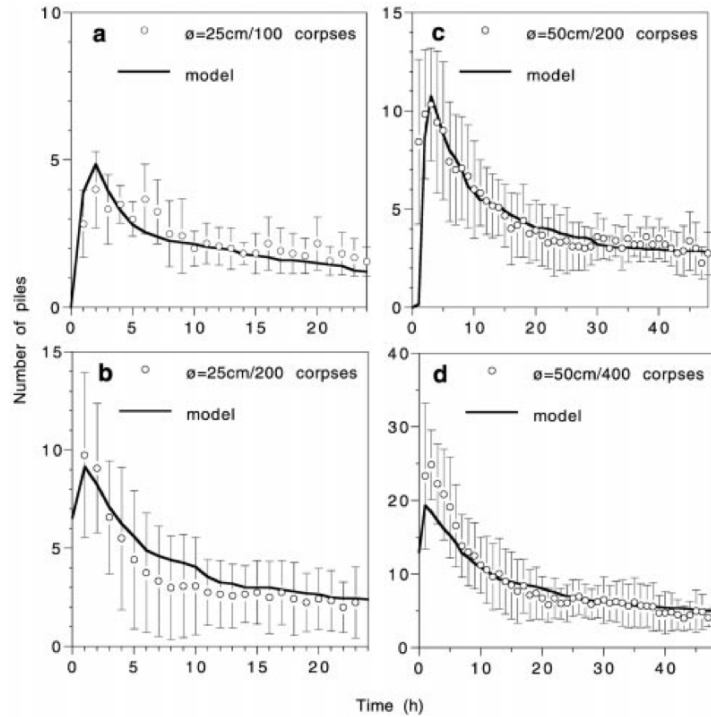


Figure 4.3 – Dynamics of the number of piles: comparison between model predictions (solid curves) and experimentally observed values (mean \pm sd) for arena $\varnothing=25$ cm with 100 and 200 corpses, and for arena $\varnothing=50$ cm with 200 and 400 corpses (Fig 5 from [Theraulaz et al. 2002](#)).

ters. The six models were various combinations of three behavioral traits: (a) inter individual variability: picking-up and deposition statistics depend on an activity level that is constant in time but varies from ant to ant, (b) temporal correlation (or memory effects): the propensity to pick-up or deposit a corpse decreases as the time since the last behavioral action (deposit or picking-up) has elapsed, (c) picking-up inhibition: the picking-up rate of an object decreases with increasing local corpse density. Note that deposition rate increased in all six models with perceived corpse density. Table 4.1 lists which behavioral traits were included in the six tested models.

Table 4.1 – The six different models calibrated by [Weitz et al. \(2012\)](#) to the emergent pile number statistics in [Theraulaz et al. \(2002\)](#).

| behavior: | inter-individual variability | temporal correlation | picking-up inhibition |
|-----------|------------------------------|----------------------|-----------------------|
| model 1 | no | no | no |
| model 2 | no | no | yes |
| model 3 | yes | no | no |
| model 4 | yes | no | yes |
| model 5 | no | yes | no |
| model 6 | no | yes | yes |

[Weitz et al. \(2012\)](#) first showed that all six models could be calibrated to fit perfectly well the collective pattern in Fig 4.3. He then showed analytically that even if the precision of the data on the collective level were arbitrarily good one could not select a best fitting model: hence the need to study the underlying individual behaviors directly in dedicated experiments. Redoing

then the whole methodology underlying [Theraulaz et al. \(2002\)](#), [Weitz et al. \(2012\)](#) discuss in detail the methodological issues while also emphasizing the “biological” decisions that had to be made during the process. Without surprise the finally selected model 2 corresponds to the one reported in [Theraulaz et al. \(2002\)](#), though they also showed that a slightly simpler functional version (the deposition rate increases linearly with perceived corpse density) gives an equally good fit.²

Where to go from here? Literature suggested that a template in the form of a laminar air flow could modify the emerging patterns ([Bruinsma, 1979](#); [Bonabeau et al., 1998b](#)), but the underlying behavioral mechanisms had never been identified experimentally in a rigorous manner (ie. applying methodology 2.3). Such a laminar air-flow cannot be created along the circular arena borders in the experimental setup in [Theraulaz et al. \(2002\)](#), one needs a morphogenetic process in 2 dimensions. Preliminary experiments with *Messor sanctus* showed that a slight change in initial conditions could lead to cluster formation in 2D space – one only had to disperse the corpses homogeneously on the whole surface in a sufficiently large arena (Fig 4.4).

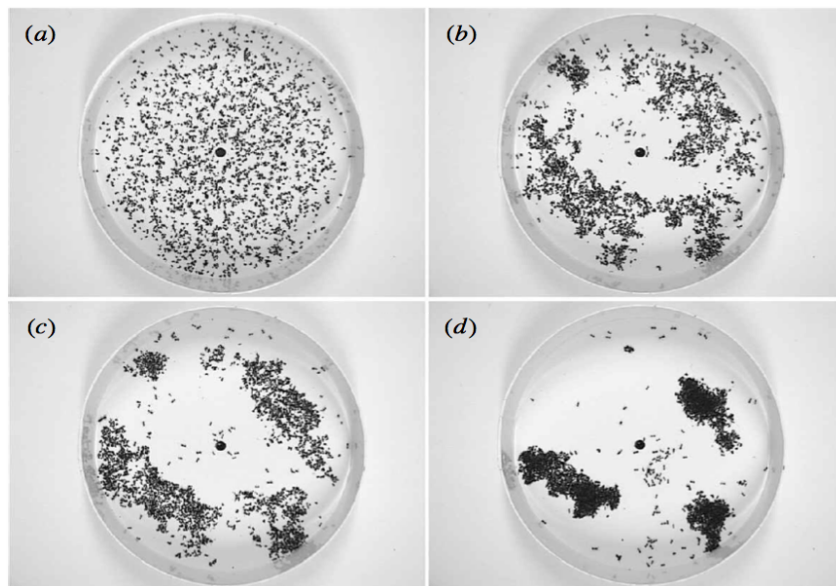


Figure 4.4 – Corpse-clustering in *Messor sanctus* in a circular arena when the corpses are initially distributed homogeneously on the whole surface (Fig 3 from [Theraulaz et al. 2003](#))

When I arrived in Toulouse in 2001 Guy and his collaborators had already found the funding to construct an experimental setup permitting the creation of a controlled laminar air-flow in a setup with 2D corpse clustering (Fig 4.5). After the cockroach work this was my second opportunity to introduce myself to the study of collective animal behaviors. We were lucky to find gifted students that I could co-supervise with Guy: Mélanie Challet during her DEA (Diplôme d’Etudes Approfondis, now Master 2) internship in 2002 and during her PhD on the same subject (2002-2005), Julie Verret during her DESUPS (Diplôme d’Etudes Supérieures Universitaires Paul Sabatier) in 2003/4, and Eric Casellas during his DEA in 2004/5 (and several Master students in their first year, of course). I was also involved as an advisor and collaborator in the work of Sebastian Weitz during his Master internship and PhD (2008-2012) where he formalized and modeled the 2D corpse clustering phenomenon with and without

²My role in all the cited work by Sebastian was minor, simply the one of a critical observer and reader who wanted to understand the methods in detail while redoing at the same time the same kinds of experiments and modeling in a 2-dimensional environment.

laminar air flows.

4.1 The influence of temperature on corpse clustering behavior

The experimental setup that had been developed to induce a controlled laminar air flow built on the principal of convection (Fig 4.5): it was a closed chamber with temperature controlled floor and walls. When setting one wall at 30°C and the opposite wall at 15° convection creates an airflow inside the chamber. At ant antenna height (≈ 3 mm) this wind speed is ≈ 1 cm/s in about 75% of the floor area, but reaches 3-5 cm/s in a zone close to the cold side (see Fig 4.5).

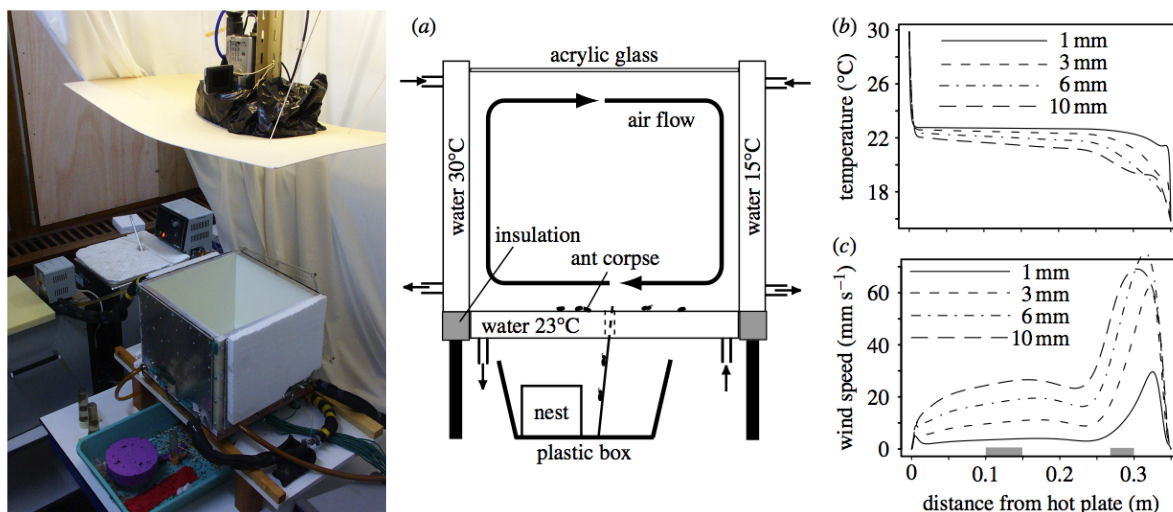


Figure 4.5 – (left) experimental setup to induce a laminar airflow in the area where the ants aggregate the corpses. The colony is placed beneath the setup and the ants access the arena by climbing spontaneously along a wood stick through a hole in the arena center. Temperature controlled water flows through the arena floor and the four walls in order to heat them to specific temperatures. The setup is covered by acrylic glass that can be placed at a chosen height above the arena floor and through which the clustering dynamics can be filmed. The parameters that define the created convective air current are the temperature difference between left and right wall and the height of the acrylic glass. (right) The finally retained setup to induce laminar air flows: one wall is set at 30°C, the opposite one at 15°C, while the floor and the lateral walls are set at 23°C. The acrylic glass is placed at height 27 cm. Inset (b) shows the temperature at various heights above the floor, and inset (c) shows the laminar wind speeds at the same heights. The grey bars show the zones where corpse piles were arranged for the individual corpse depositing and picking-up experiments. Right side Fig from [Jost et al. \(2007\)](#).

The temperature in the ant zone can vary from 23°C to 21°C in 75% of the arena, but can drop to 18°C close to the cold wall. Temperature is a driver of animal behavior, before starting the convection experiments we had therefore to test whether the clustering behaviors were sufficiently constant in these emerging temperatures.

Mélanie Challet attacked this question during her DEA internship in 2002 ([Challet, 2002](#); [Challet et al., 2005b](#)). She first measured experimentally the diffusion coefficient of exploring *Messor sanctus* ants at three temperatures: 16°C, 25°C and 30°. More specifically, she tracked exploring single ants, estimated their mean speed v , and then decomposed the trajectories by a makeshift algorithm into a sequence of straight free paths and turning angles. The idea of the algorithm was to group together consecutive positions into a single free path until the turning angle between this free path orientation and the direction of the next move (straight line between two consecutive positions) exceeded a given threshold of 0.175 rad (see Fig 1 in [Challet](#)

et al. 2005b)³. Mean free path length l and the mean cosine g of the turning angle distribution (called phase function in statistical physics) permitted to compute the ants associated diffusion coefficient $D = \frac{lv}{2(1-g)}$ as a measure of ant dispersion. D increased with increasing temperature, that is ants explore larger areas at higher temperatures. However, this effect was statistically not detectable for temperature differences below 5°C.

The next step was to assess the effect of temperature on corpse picking-up and depositing behavior. Mélanie measured the probability of a free (or loaded) ant to pick-up (or deposit) a corpse on a pile of size 1, 10, 50 or 200. The result is shown in Fig 4.6. For both temperatures,

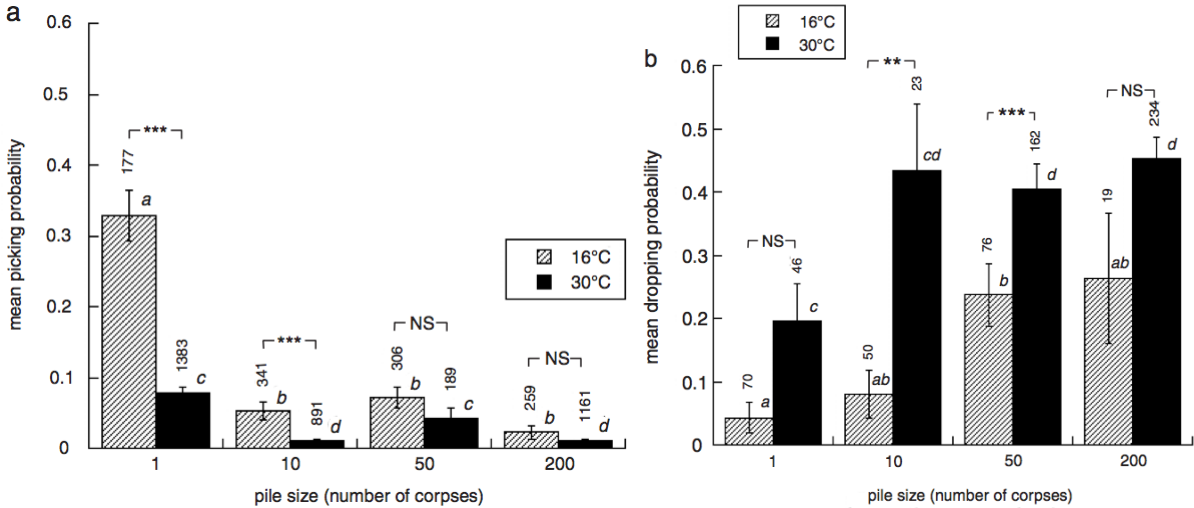


Figure 4.6 – (a) Mean picking-up probability ($\pm se$) on piles of size 1, 10, 50 and 200 corpses at 16°C and 30°C. (b) Mean depositing probability for the same pile sizes and temperatures. The number of observed contacts underlying each estimate is shown above the bars. Fig from Challet et al. (2005b).

picking-up probability decreases with pile size and depositing probability increases with pile size. This is again the positive feedback underlying corpse clustering as found in Theraulaz et al. (2002), but this time assessed in 2D clustering. The positive feedback is significantly stronger at 30°C compared to 16°C, that is the clustering process is faster at higher temperatures. But again, the detection of this effect requires high temperature differences (here 14°C), at low differences as in the setup (2°C) we expect a very small effect of temperature.

These results therefore reassured us that the small temperature differences in the experimental setup with convective laminar air flows (Fig 4.5) can be neglected, at least in a first time. Beyond this first result, Challet et al. (2005b) shows that the clustering phenomenon is faster at high temperatures (higher diffusion let ants encounter more corpses, higher positive feedback accelerates cluster formation). Preliminary computer simulations (IBM) showed that in a heterogeneous environment with two temperatures, 16°C and 30°C, corpses will finally all be clustered at the higher temperature. Environmental modulation of local positive feedback and dispersion can therefore be quite a general mechanism to explain the aggregation of diverse objects (eggs, larvae, fungus, harvested grains) at optimal conditions (temperature, humidity, air currents), see e.g. Bollazzi and Roces (2003) and Roces and Kleineidam (2000) for fungus culturing in leaf-cutting ants or Scholes et al. (2006) for egg clustering in ants.

³There are many algorithmic possibilities how to decompose a path into this sequence of straight free paths and turning angles, but each one requires ad-hoc decisions. Gautrais (2015) concluded that the problem itself is badly defined, thus preventing the development of a method providing unbiased estimates of mean free path and turning angle statistics (mean, variance, distribution). Nowadays we would directly estimate the diffusion coefficient from the slope of net squared displacement, a much less biased estimate.

4.2 Thigmotactic behavior and its role in corpse clustering

Another key issue when going from 1D corpse clustering (Theraulaz et al., 2002) to 2D clustering is ant movement. Already Chrétien (1996) had noted the ant’s tendency to move preferentially along the arena border (and thus a tendency of corpses to accumulate along the border). In the literature this tendency is well known for many animals and was termed thigmotaxis (Fraenkel and Gunn 1961, thigmo = ‘touch’), that is a tendency to align with a border and move along it for some time. We had already encountered it in Raphaël’s work on cockroaches (Jeanson et al., 2003), a classical model to study the underlying physiological base (Creed and Miller, 1990; Camhi and Johnson, 1999; Cowan et al., 2006). In the ecological literature this thigmotactic behavior has been recognized as important in heterogeneous, patchy or fragmented habitats with borders separating or connecting patches (Fagan et al., 1999; Ovaskainen and Cornell, 2003). The amplification mechanisms in social insects (eg. mass recruitment by pheromone trails) can further accentuate the impact of thigmotactic behavior (Dussutour et al., 2005). In sum, when passing to a 2D corpse-clustering paradigm we had to address the role of thigmotactic behavior in this process. We first thought that it is a simple question of knowing ant density modulations along arena borders (Casellas et al., 2008), but it soon turned out to be of far more importance because the emerging clusters’ borders elicit also thigmotactic behavior (Weitz et al., 2012; Weitz, 2012).

Casellas et al. (2008) started with the cockroach movement model of Jeanson et al. (2003) and applied it to the case of the temperature controlled setup in Fig 4.5. Single exploring ants were let into the arena and their wall-following times were measured. Since this setup has straight borders and corners, he first verified that the survival curves of these wall following times had the same slope (on log-linear scale) independently of whether the observed path included a corner or not (showing on the fly that these survival curves corresponded to exponential distributions as in cockroaches). He then introduced circular obstacles of diameter 6 cm, 4 cm and 2 cm (see Fig 4.7) and showed that wall following times along a border with a given curvature (inverse of obstacle radius, zero for straight borders) were also exponentially distributed. Furthermore, the mean wall following times increased with decreasing curvature. In other words, the individual rate to quite a border (inverse of mean following time) increased with increasing border curvature. In sum, Eric validated Raphaël’s cockroach model for *Messor sanctus* and discovered that border leaving rate is a simple function of border curvature. He further validated that ants move according to a diffusive correlated random walk outside border zones (border width 1 cm).

In a next step Eric applied mesoscopic techniques to derive mean field equations (see eg. Case and Zweifel 1967, the techniques actually going back to Ludwig Boltzmann in the 19th century). The idea is to look at ant densities moving in a given direction, write the individual behavior in terms of these densities (combined with the transport equation), and then pass to mean densities by integrating the equations over all directions. For a fully worked out example I refer to the Appendix in Casellas et al. (2008): however, the resulting model can be interpreted without knowing the details how it was derived. The crucial point is to distinguish between individuals moving along the arena border in a 1D random walk, or moving in the arena centre with a 2D random walk, and to identify the equation governing the flux between these two compartments. Let n_b be the (1D) border density of ants, n_c the (2D) centre density, \vec{j} the flux density, v_c and v_b ant speed in the arena centre or along the border respectively, λ_b the mean border following distance, D_c and D_b the diffusion coefficients in the arena centre or along the border (\vec{n} is the normal vector to the border pointing away from it). The resulting set of

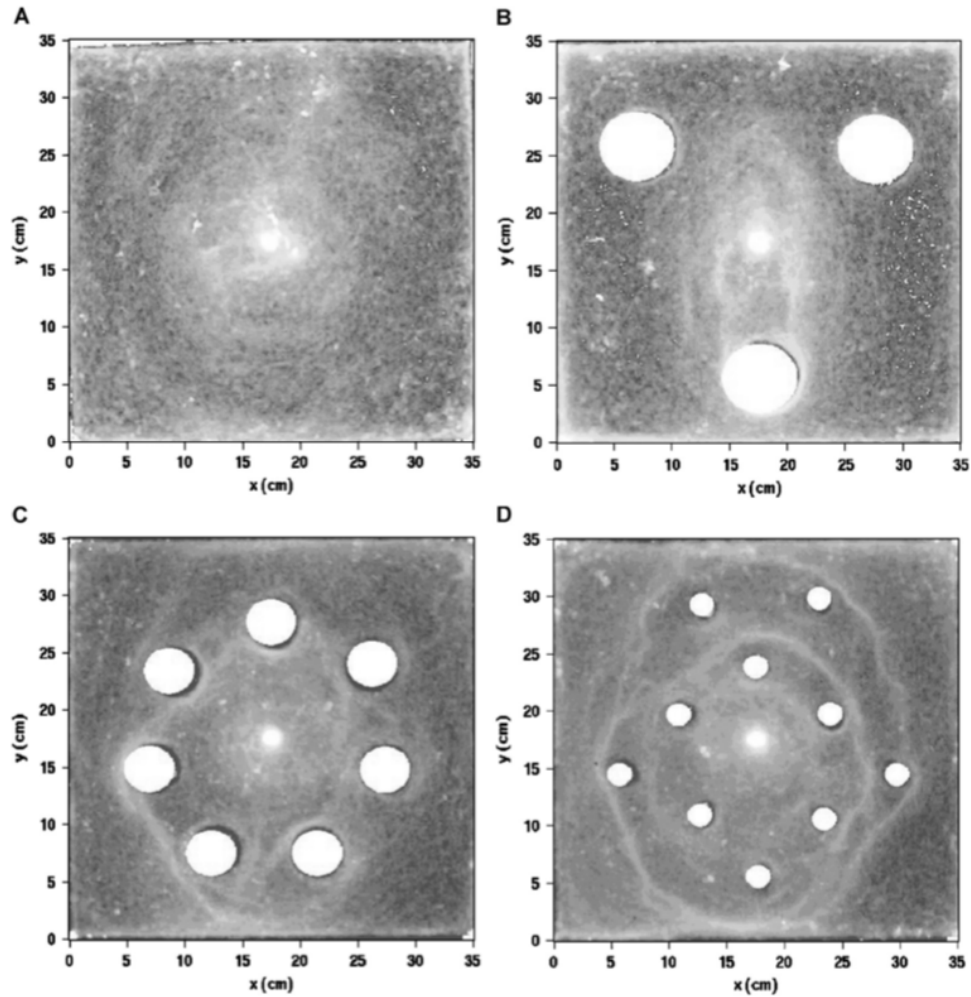


Figure 4.7 – Reconstructed mean ant densities (the darker the grey the lower the density) from 2h films where ants could freely access the arena (Fig 4.5) through the hole in the center. The figures show the averaged ant density over the last 90 min. The arena was either empty (A) or contained circular obstacles (shown in white) with diameters 6 cm (B), 4 cm (C) and 2 cm (D). Fig from [Casellas et al. \(2008\)](#).

coupled partial differential equations (PDE) is

$$\frac{\partial n_c}{\partial t} = D_c \Delta n_c \quad (4.1)$$

$$\frac{\partial n_b}{\partial t} = D_b \Delta n_b + 2 \left(\underbrace{n_c \frac{v_c}{\pi}}_I - \underbrace{n_b \frac{v_b}{\lambda_b}}_{II} \right) \quad (4.2)$$

$$\vec{j} \cdot \vec{n} = 2 \left(n_c \frac{v_c}{\pi} - n_b \frac{v_b}{\lambda_b} \right) \quad \text{boundary conditions} \quad (4.3)$$

where I represents the ants arriving in the border zone and II the ants leaving the border zone. Experimentally we found no difference in ant speed in the centre or along the border, $v_c = v_b$. At stationary state we therefore get the relations

$$n_c^s \frac{v_c}{\pi} = n_b^s \frac{v_b}{\lambda_b} \xrightarrow{v_b=v_c} \frac{n_c^s}{\pi} = \frac{n_b^s}{\lambda_b} \quad (4.4)$$

Note that we have in most experimental setups two types of border, the straight or convex arena border and the concave obstacle borders of various curvatures (see Fig 4.5). Let λ_w be the arena border following time, n_w the arena border density and n_b the object border density, equation (4.4) therefore makes two predictions

$$\lambda_b = \pi \frac{n_b^s}{n_c^s} \quad \text{and} \quad \lambda_w = \pi \frac{n_w^s}{n_c^s} \quad (4.5)$$

that we tested experimentally in Casellas et al. (2008). We used the temperature controlled setup in Fig 4.5 (without corpses) at 23°C and let ants spontaneously enter it through the hole in the arena centre. The arena was either empty or had 3 circular obstacles of diameter 6 cm, 8 obstacles of diameter 4 cm or 10 obstacles of diameter 2 cm. Once the ants had access we waited 30 min to let the system reach stationary state (the number of ants entering the arena was approximately the same as the number of ants exiting from the arena) and we filmed for 90 min. From this film we extracted one image per second, binarized these images by a simple threshold value, and then computed mean ant density in a border zone of width 1 cm and in the arena centre. These densities were plugged into prediction (4.5) and the predicted wall follow times were compared with the experimentally measured wall follow times (Fig 4.8). These predictions were quite good for the empty arena and for the arena with obstacles of diameter 6 cm. However, they were not very satisfactory for the smaller obstacles. Fig 4.7 gives a hint why: the model predicts that ant density should be constant along a border of a given curvature and in the rest of the arena. For the smaller obstacles this is clearly not the case, there are high density curved lines: pheromone trails (experimentally verified by removing after 2 h all ants and obstacles and let new ants enter the arena – the high density lines re-appeared at exactly the same places). This was actually a surprise, the current literature suggested that *Messor sanctus* does not lay pheromone trails during exploration, it supposedly only does so after having found food. This result also raises a more important question: do these pheromone trails play a role in the 2D corpse clustering dynamics? We will come back to this question in the next section.

4.2.1 A new model for ant thigmotactic behavior

The modeling and experimental analysis of thigmotactic movement with equations (4.1-4.3) or with the underlying individual based movement model is straightforward in an environment as

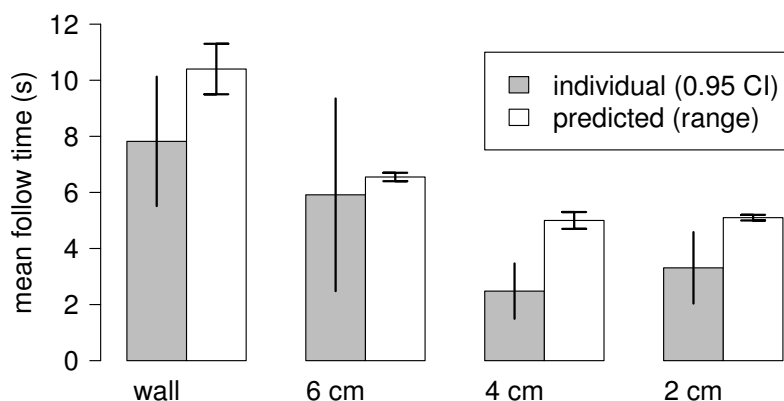


Figure 4.8 – Comparison between the observed individual mean border follow times (with 95% confidence interval) and the wall follow times predicted by the model from the mean border and center densities (border width 1cm, range obtained by varying the truncation of the highest pixel densities that corresponded to shaded parts of the arena). Fig from [Casellas et al. \(2008\)](#).

shown in Fig 4.7 with well defined borders that do not move during the experiment. However, what shall we do when these borders emerge in time and are dynamic objects as in the case of corpse clustering (Fig 4.4)? How do we distinguish in this case between border zone and central zone? Another problem in the way we modeled thigmotactic behavior is of cognitive nature: since there is a behavioral switch between 2D random walks in the arena centre and 1D random walks along the arena border ants are supposed to be able to detect a border and to move along it with a curvature dependent rate to leave it (that is, detect its orientation and its curvature). What are the required physiological mechanisms that enable such a cognitive ability, in particular in the case of a corpse cluster with irregular borders and highly varying corpse densities? The answers to both questions are not known and would require ad-hoc decisions when integrating this model with corpse clustering, or to do additional experiments to justify such decisions experimentally.

When Sebastian Weitz started his PhD he was soon aware of these difficulties. Rather than to start modeling corpse clustering in 2D with many uncertain hypotheses he chose to dig out the original films of ants moving around the artificially formed clusters ([Challet, 2005](#); [Casellas et al., 2008](#)) and to rethink completely how this behavior could be modeled. [Weitz et al. \(2014\)](#) measured in particular the angular distribution function of ants as a function of distance d to a corpse and found that the ants' distribution function corresponds to an isotropic distribution, contrary to the model in [Casellas et al. \(2008\)](#) or [Jeanson et al. \(2003\)](#) that assume alignment with the border (Fig 4.9(b)). He then defined that thigmotactism occurs if ant residence times in a small surface near the corpse is higher than ant residence time in a surface of the same size far away from a corpse (free field condition). Fig 4.9(c) shows the boundary following criterion (defined as the observed mean residence time in a grey band of width d around a corpse divided by the expected residence time for a diffusive random walk in the same band without a corpse) as a function of width d . If ant movement were not influenced by the corpse this criterion should give 1 (free-field condition): clearly this is not the case for *M. sanctus*, they show thigmotactism according to our criterion.

The next step was to develop a model of wall-following behavior that can explain these two

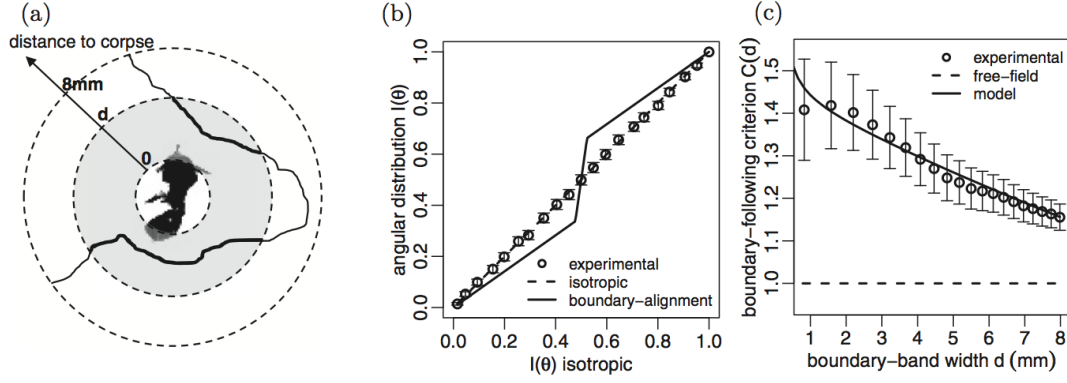


Figure 4.9 – Analysis of ant movement near a single corpse. (a) a typical ant trajectory around a single corpse. The grey zone is an 8 mm wide band around the corpse in order to compute the mean residence time (defined as the time until first return to the limit of the near-boundary region) of ants moving in this band (the shown example provides two residence times to the computation of the mean). (b) normalized cumulative angular distribution function computed at various distances d from the corpse and plotted against the expected distribution of isotropic ant orientation (θ is the absolute angle between the ant orientation and the radial vector departing from the corpse centre). If ants orient along the arena border (as in the model in Casellas et al. 2008) we expect a relationship such as depicted by the solid line. The observed relationship is, however, a straight diagonal line. (c) The boundary following criterion (defined as the observed mean residence time in the grey band of width d (shown in a) divided by the expected residence time for a diffusive random walk in the same band without a corpse, mean \pm se): these ants clearly show boundary following behavior according to our definition. Fig 1 from Weitz et al. (2014) where the technical details can be found.

observed features (isotropic orientation everywhere but increasing density towards the border). This is the occasion to introduce some mesoscopic thinking. Let $f \equiv f(\vec{r}, \vec{\omega}, t)$ be the ant distribution function at location \vec{r} and movement direction $\vec{\omega}$ at time t . The ants move at constant speed c with a direction change frequency $\nu \equiv \nu(\vec{r}, \vec{\omega})$, and $p(\vec{\omega}|\vec{\omega}') \equiv p(\vec{\omega}|\vec{\omega}', \vec{r})$ is the direction-change phase function. The constant speed Boltzmann walker satisfies the following equation:

$$\underbrace{\frac{\partial f}{\partial t} + c\vec{\omega} \cdot \nabla f}_I = \underbrace{-\nu f}_{II} + \underbrace{\int \nu' f' p(\vec{\omega}|\vec{\omega}') d\vec{\omega}'}_{III} \quad (4.6)$$

(I is the pure transport term, II the ants that change direction from $\vec{\omega}$ to something else, and III the sum of all ants that change their direction from some $\vec{\omega}'$ to direction $\vec{\omega}$; II and III are also called collision terms in reference to the particle physics origin of these equations, but in our context they represent the spontaneous decision of the animal to change direction). f' is a shorthand for $f(\vec{r}, \vec{\omega}')$ and the same for ν' . Part II implies that free paths (the distances between successive direction changes) are exponentially distributed as experimentally observed for *M. sanctus* in Challet et al. (2005b) and Casellas et al. (2008). The direction change frequency is supposed to be symmetrical around the current animal direction ω , it can therefore be written as $p(\vec{\omega}|\vec{\omega}') = p(\vec{\omega} \cdot \vec{\omega}')$ with a mean cosine $g = \int \vec{\omega} \cdot \vec{\omega}' p(\vec{\omega} \cdot \vec{\omega}') d\vec{\omega}$. Given all this notation we can now look at the model proposed by Weitz et al. (2014). He assumed that the phase function p (direction change distribution) is not modified when approaching a border (it has been experimentally determined for *M. sanctus* in free field conditions in Challet et al. (2005b) and Casellas et al. (2008), and was modeled in Weitz et al. (2014) by an elliptic function), but that this border affects direction change frequency ν :

$$\nu(\vec{r}, \vec{\omega}) = \frac{K(\vec{r})}{\Phi(\vec{r}, \vec{\omega})} - \frac{c}{1-g} \vec{\alpha}(\vec{r}) \cdot \vec{\omega} \quad (4.7)$$

Φ and $\vec{\omega}$ are adjustable functions with the only constraints that $\int \Phi(\vec{r}, \vec{\omega}) d\omega = 1$, $\int \Phi(\vec{r}, \vec{\omega}) \omega d\omega = 0$ and ν remains positive for all \vec{r} and $\vec{\omega}$. $K(\vec{r})$ is a free scalar field with the only constraint that ν remains positive – it does not modify the ants’ stationary distribution or their residence times in Fig 4.9(c) and is therefore not further specified in Weitz et al. (2014)⁴. For the fitted function in Fig 4.9 he chose $\hat{\alpha} = 46(1 - g)\vec{e}_r \text{ m}^{-1}$ (where \vec{e}_r is the radial vector departing from the corpse center towards position \vec{r}), $\Phi(\vec{r}, \vec{\omega}) = 10$ if $\|\vec{\omega} \cdot \vec{e}_r\| < 0.3$ and $\Phi(\vec{r}, \vec{\omega}) = 1$ else. The choice for $\hat{\alpha}$ is specific for the case one corpse cluster/boundary treated in Weitz et al. (2014), in more complex environments it has to be adapted in order to have greater direction change frequency the greater the difference between the ant orientation and the direction towards the boundary. I refer to Weitz et al. (2014) and its section “Inversion properties” for further ideas and details how to parameterize equation (4.7). The curvature dependence of wall following times observed in Casellas et al. (2008) emerges from this model without an explicit curvature detection on the individual level (Weitz et al., 2014, ref 52). Note that this type of model is not completely new, the underlying idea is the same as in the “run-and-tumble” models for bacterial chemotaxis where the direction change frequency depends on the movement direction with respect to some chemical gradient (Erban and Othmer, 2004, 2007).

The invariance property used above to define thigmotactism applies to any Boltzmann random walk where the walkers have no orientation information and where the boundary conditions at the limit of some domain \mathcal{D} are compatible with a locally isotropic stationary state (Weitz et al., 2014; Blanco and Fournier, 2003, 2006). It states that an isotropic homogeneous equilibrium is reached with mean residence time $\langle T \rangle = \frac{\pi S}{P}$ in any domain with surface S and periphery length P . This invariance property can actually be used as an alternative to net squared displacement to test whether the movement of some organism can be modeled as a diffusive random walk. In a methodological paper (Challet et al., 2005a) we showed by simulation that this criterion can help detect border or trail following behavior with a typical sample size of 50-100 trajectories. Applying it in particular to the case of *Messor sanctus* we showed that indeed, near the corpse clusters, ants no longer move according to a diffusive random walk (Challet et al., 2005a).

4.3 Corpse clustering in 2D and its interactions with a dynamic template

After this excursion to thigmotactism and its modeling lets come back to corpse clustering in 2D. We now want to understand how the laminar air flow of 1-5 cm/s in the experimental setup 4.5 modifies the corpse clustering dynamics. The experimental work in this section was performed by Mélanie Challet (Challet, 2002, 2005) during her DEA and PhD, Julie Verret (Verret, 2004) during her DESUPS and Eric Casellas (Casellas, 2005) during his DEA. They have been published together in Jost et al. (2007).

⁴If $K(r)$ is needed it can be chosen in order to satisfy some physically or biologically motivated constraints. This was Sebastian’s choice in the corpse clustering model in the next section: a first (physical) constraint was that $\nu(\vec{r}, \vec{\omega})$ must be positive for all \vec{r} and all ω (a negative direction-change frequency would be physical nonsense): this constrains the minimal value for $K(\vec{r})$. Then $K(\vec{r})$ is fully fixed by the two following choices: (a) $K(\vec{r})$ is constant (motivated by parsimony) and (b) the direction-change frequency for an ant walking exactly in the direction towards the pile is the same as in the free-field. This last choice means that an ant coming from the free field does not modify its propensity to turn when walking towards the pile whereas it will turn more often when walking in any other direction

4.3.1 Clustering dynamics with and without a laminar air flow

In all the experiments reported below 3260 corpses were randomly distributed in the experimental arena of size 35 cm \times 35 cm (that is, 2.66 corpses/cm²). Ants were given access to the arena for 24 h and the experiments were filmed from the top for 2 s every 10 min. Fig 4.10 shows an example of the observed dynamics without (9 replications in total) or with an air current (14 replications in total). In a control experiment we used the same temperature setup as for the experiments with a laminar air flow (Fig 4.5), but lowering the acrylic glass plate to a height of 3 cm, thus preventing the formation of convective air currents (4 replications).

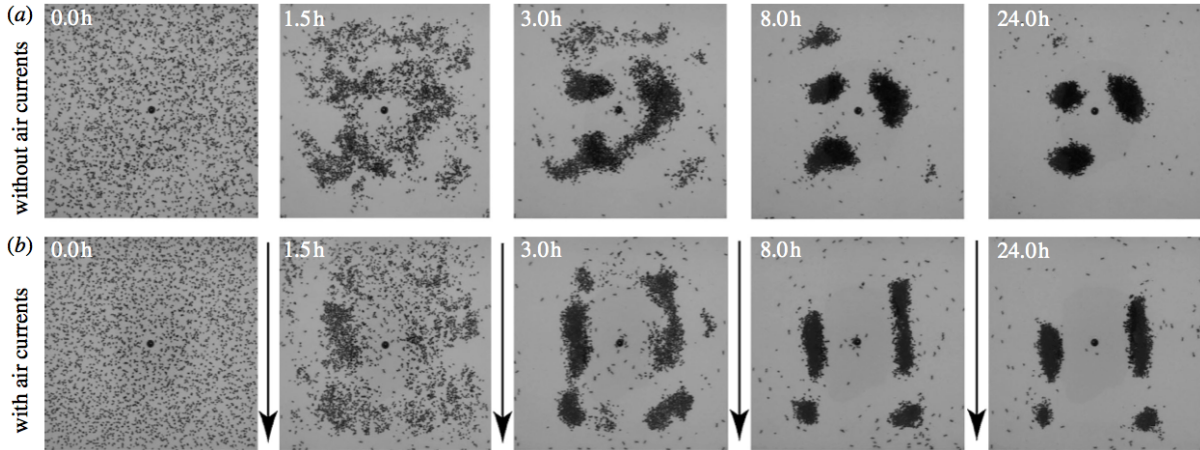


Figure 4.10 – Typical corpse clustering dynamics (seen from above in experimental setup Fig 4.5) without (a) or with (b) a laminar air flow of speed 1-5 cm/s at ant antenna height.

The overall clustering dynamics (surface of largest cluster, total surface of clusters, number of clusters) were very similar between the two experimental conditions (Fig 4.11(left)). However, differences appeared when looking at the form and the positions of the clusters. Fig 4.11(right) shows the dynamics of the ratio length (in direction of the laminar air flow) over width of the clusters. We see that in the condition with laminar air flows the clusters were elongated in direction of the air flow by factor 2, while without air flows or in the control experiment these ratios were close to 1. Fig 4.12 shows the clusters' barycentres: they moved at a speed of \approx 19 mm/day in direction of the laminar air flow, but no such movement was seen perpendicular to the air flow, without laminar air flow or in the control experiments.

4.3.2 Modulation of corpse picking-up and depositing by a laminar air flow

Since the air flow itself was too weak to move the corpses the observed elongation of the clusters and the movement of their barycentre had to be explained by the ant's clustering activity. A first clue was given by the modulation of corpse depositing and picking up probability on corpse clusters of size 1, 5, 10 and 50: we had arranged such clusters in the setup without air flows or in the grey zones in Fig 4.5(c), corresponding to wind speeds of 0 cm/s, 1 cm/s or 3-5 cm/s, and assessed the fraction of passing loaded ants that deposited their corpse or the fraction of passing free ants that picked up a corpse. Fig 4.13 shows the results: as in the 1D corpse clustering experiments (Theraulaz et al., 2002), depositing probability increased with cluster size and picking-up probability decreased with cluster size. This is again the positive feedback that leads to corpse clustering. Furthermore, the results in Fig 4.13 showed that this positive feedback is modulated by wind speed: it was highest when there was no air flow and lowest at the highest wind speeds.

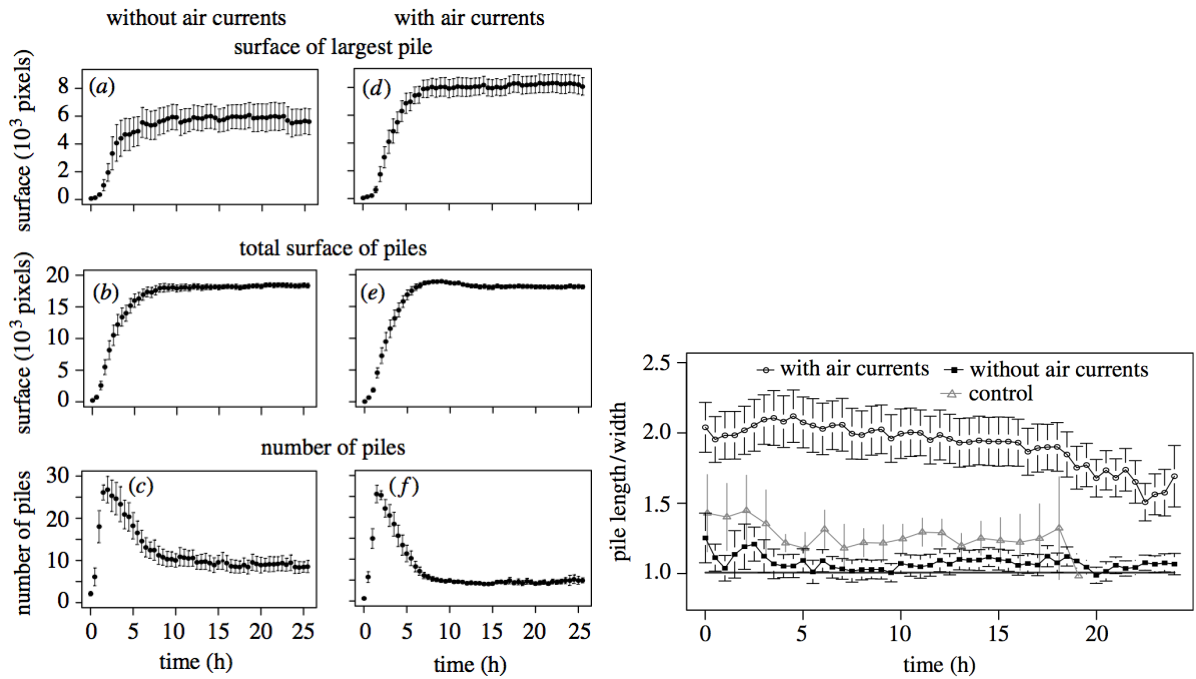


Figure 4.11 – (left) Characterization of the global corpse clustering dynamics (mean \pm se) by the surface of the largest cluster (a,d), the total surface of clusters (b,e) and the number of clusters (c,f) without air currents (a-c) or with air currents (d-f). (right) Dynamics of cluster length (in direction of the air flow) over width in the three experimental conditions. Figs 5 and 7 from [Jost et al. \(2007\)](#).

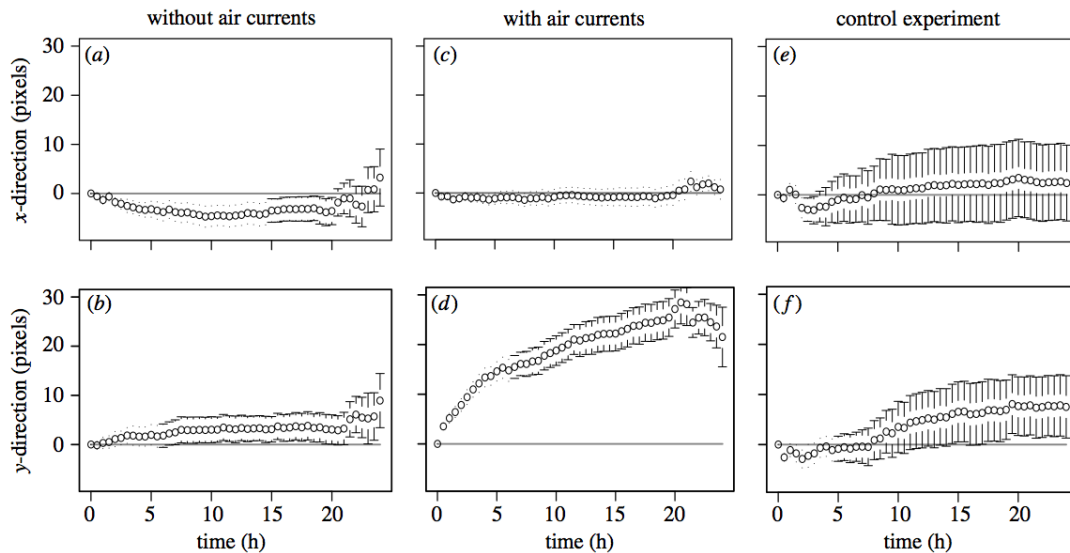


Figure 4.12 – Dynamics of the clusters' barycentres (x -axis perpendicular to air flow direction, y -axis with this direction) for the three experimental conditions (mean \pm se): no air flow (a,b), with a laminar air flow (c,d), control without laminar air flow (e,f). Fig 6 from [Jost et al. \(2007\)](#).

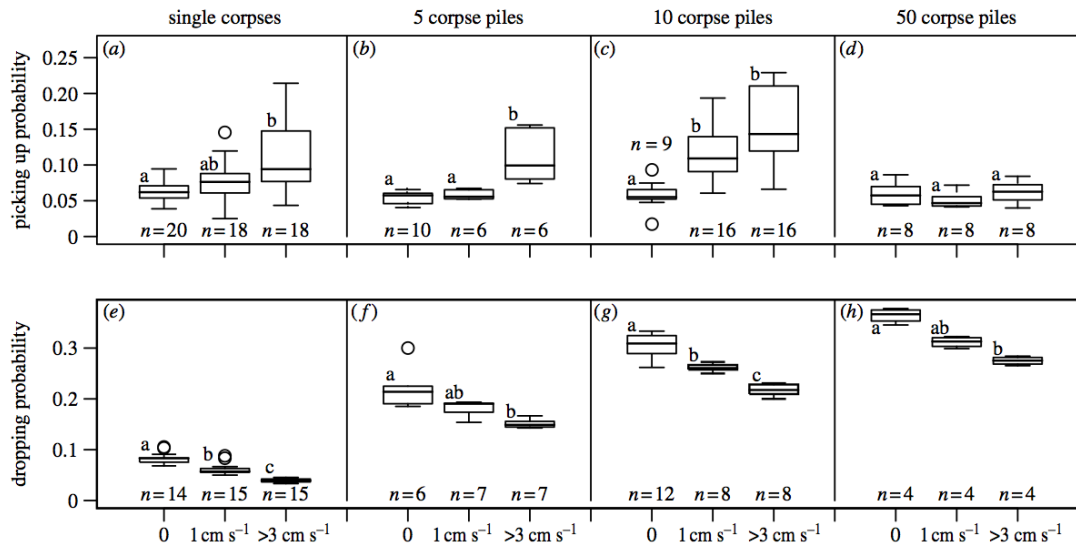


Figure 4.13 – Corpse depositing (top row) or picking-up (bottom row) probability as a function of pile size and wind speed. Fig 2 from [Jost et al. \(2007\)](#).

4.3.3 Clusters as a dynamic template that modulate positive feedback and thus their own growth

This modulation of positive feedback would by itself lead to a preferential clustering in the low wind speed zone in our setup (Fig 4.5), and could thus explain the movement of the cluster barycentres towards the low wind speed zone. However, where did the cluster elongation come from? To understand this phenomenon we did two more analyses. First, we simulated numerically how the laminar air flow was modulated around a corpse cluster. Actually, at ant antenna height there is a large low wind speed zone behind the cluster, a smaller such zone on the side facing the laminar flow, while on the other sides of the cluster the laminar flow is accelerated (Fig 4.14(a,b)). The probabilities of corpse depositing or picking-up were also modulated around the cluster: picking up was higher on the sides than in front or behind the clusters, while depositing was highest behind the cluster, lower in front of the cluster, and lowest on the sides of the cluster (Fig 4.14(c,d)). In terms of positive feedback, it was therefore highest behind the cluster, somewhat lower in front of the cluster and lowest on the lateral sides of the clusters. This observed positive feedback modulation is coherent with its modulation by wind-speed (Fig 4.13) and the modulation of wind speed by the cluster (Fig 4.14(a,b)). This positive feedback modulation also explains the elongation of the clusters and, since growth is fastest behind the cluster, the movement of the barycentre in direction of the laminar air flow. Overall, [Jost et al. \(2007\)](#) showed that the forming clusters act as dynamic templates that modulate the laminar air flow, which in turn modulates the positive feedback strength around the cluster and the subsequent growth of the clusters.

4.3.4 Modeling corpse clustering in 2D without a laminar air flow

When [Weitz \(2012\)](#) started to work on the modeling of corpse clustering in the case of a constant environment (constant temperature and no laminar air flows) there actually already existed individual based model (IBM) implementations of corpse clustering in 2D ([Theraulaz et al., 2003](#)) based qualitatively on the experiments done in [Challet \(2005\)](#) or [Casellas \(2005\)](#). These models did not include any thigmotactism, ants were moving around with standard correlated random walks. Sebastian's first task was to give such IBM's a solid experimental hold, that

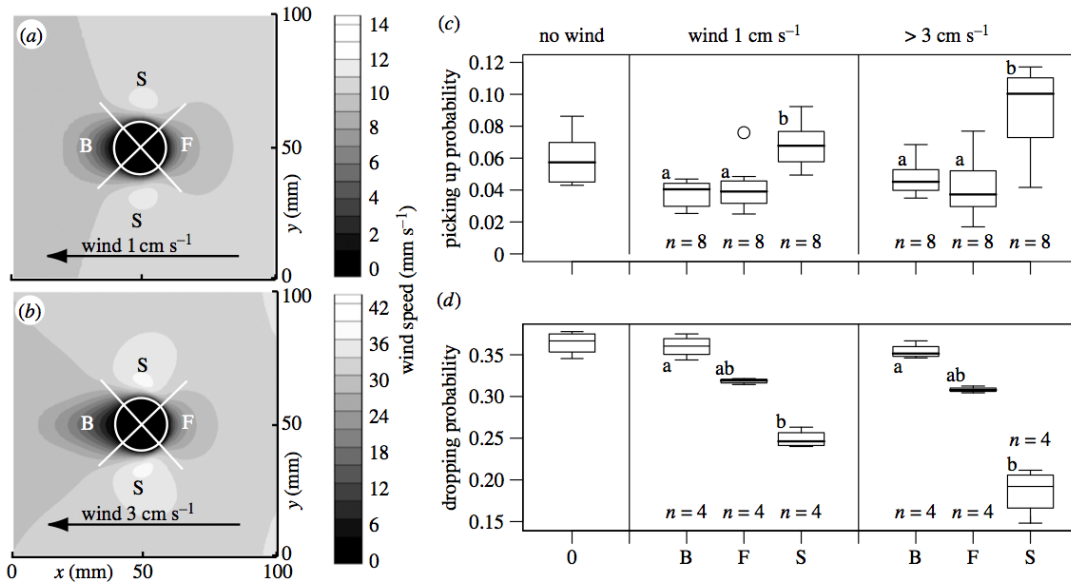


Figure 4.14 – Modulation of wind speed at ant antenna height around a corpse cluster in the zone with a laminar air flow of 1 cm/s (a) or 3-5 cm/s (b). Corpse depositing (c) or picking-up (d) probability as a function of position around the corpse cluster. Fig 3 from [Jost et al. \(2007\)](#).

is to enunciate the underlying behavioral models precisely and formally develop the associated inversion methods that permit parameter estimation from the experimental data (Fig 4.15, see [Weitz \(2012\)](#) for the associated equations). When he then predicted the emerging clusters with

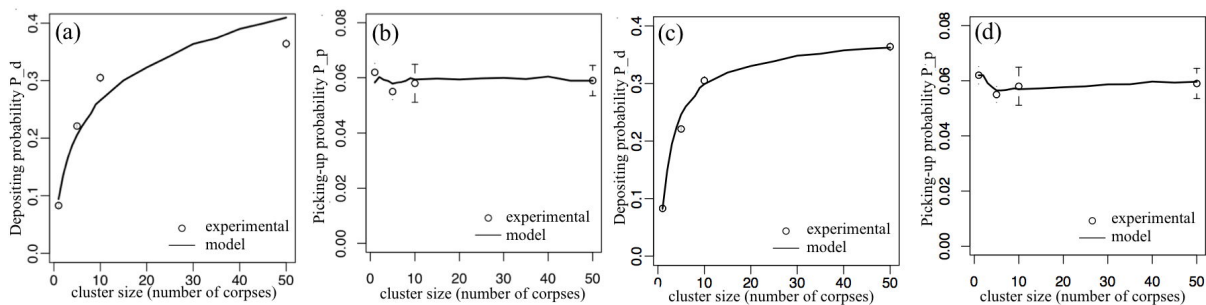


Figure 4.15 – Inversion of the depositing probability P_d and the picking-up probability P_p for ants moving with a correlated random walk (a,b) and for ants moving with the thigmotactic movement model (c,d). Modified after Figs 4.9 and 4.10 in [Weitz \(2012\)](#).

inversions for the rates to deposit or to pick up a corpse based on correlated random walk movement (Fig 4.15(a,b)) we knew for sure that thigmotactism had to be included: the clusters were far too numerous and too small (Fig 4.16(A-E,H)). Indeed, when using the inversions with the thigmotactic model (Fig 4.15(c,d)) the number of clusters were closer to the experimental observations (Fig 4.16(F,G,H)). However, the cumulated cluster surface was better predicted by the correlated random walks than by the thigmotactic movement (Fig 4.16(I)). We considered the first statistics, number of clusters, to be of higher importance and therefore continued the work with the thigmotactic movement model.

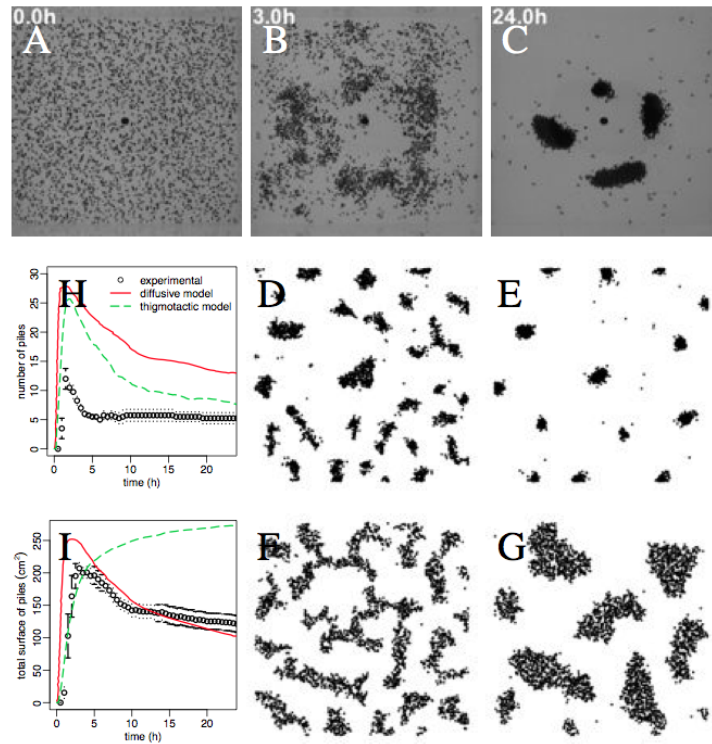


Figure 4.16 – (A-C) Example of a corpse clustering experiment at constant temperature (25°C) and without convective air currents (see Fig VI.14 in [Challet 2005](#)). (D-E) Simulated cluster formation with the model without thigmotactism (“diffusive” correlated random walks). (F-G) simulated cluster formation with the model with thigmotactism. (H) Dynamics of the number of clusters and (I) of the cumulated cluster surface (experimental and the two models with or without thigmotactism). Modified after Figs 4.11, and 4.14 in [Weitz \(2012\)](#).

4.3.5 Modeling corpse clustering in 2D with a laminar air flow

The coupling of the previous corpse clustering IBM with variable air flows required two steps. First, the corpse depositing and picking-up rates not only depended on local corpse density but also on local wind speed perceived at ant antenna height. Casellas (2005) had measured the corpse picking-up and depositing probabilities on clusters with 1, 5, 10 and 50 corpses at wind speeds 0 cm/s, 1 cm/s and >3 cm/s (see the gray zones in Fig 4.5(c)). Starting with the depositing and picking-up rates determined in the previous section (no air flow), Sebastian found that wind speed could be included by simply multiplying these rates with an exponential function of wind speed ($e^{-\epsilon_d \|u_{air}\|}$ in the case of depositing, $e^{\epsilon_p \|u_{air}\|}$ in the case of picking up, $\|u_{air}\|$ being wind speed at ant antenna height). Fig 4.17(C,D,E) shows the inversions of these functions on Casellas' experimental values. The second step was numerically more delicate: how

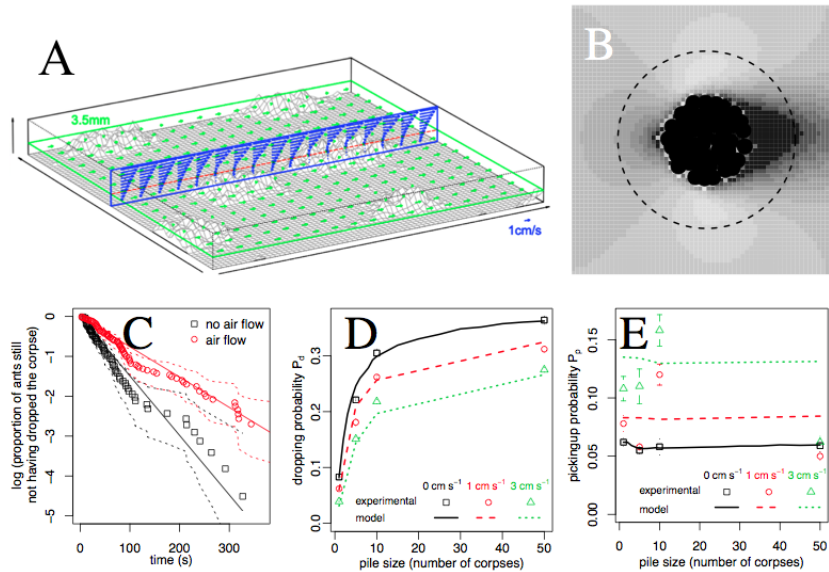


Figure 4.17 – (A) Numerical scheme to compute the air flows in the arena at ant antenna height (Lattice Boltzmann Method, LBM) and (B) the resulting air flow modulation around a typical corpse cluster (black no air flow, white highest air flows). (C) Inversion of spontaneous corpse depositing with or without an air flow of 1 cm/s. Inversion of corpse depositing probability (D) and picking-up probability (E) as a function of pile size. See Weitz (2012) for the associated equations. Modified after Figs 4.18, 4.19, 4.23, 4.24, 4.25 in Weitz (2012).

is the laminar air flow induced by the experimental setup modulated by the emerging corpse clusters? Sebastian solved this problem by a custom-tailored Lattice Boltzmann Method (LBM) which permits an efficient implementation of the boundary conditions around the corpse piles and can be easily parallelized (see section 4.6 in Weitz (2012) for the technical details and Fig 4.17(A,B) for the result).

The IBM was then coupled to the LBM by letting the latter recompute the air flow field every 5 minutes (this was sufficiently frequent to take into account the cluster modification by the IBM). The result is shown in Fig 4.18: (L,M) shows two snapshots of a single simulation, (N) shows the dynamics of corpse elongation and (O) the dynamics of cluster movement in the air flow direction. Both emerging statistics compare nicely to the experimentally observed dynamics (Jost et al., 2007).

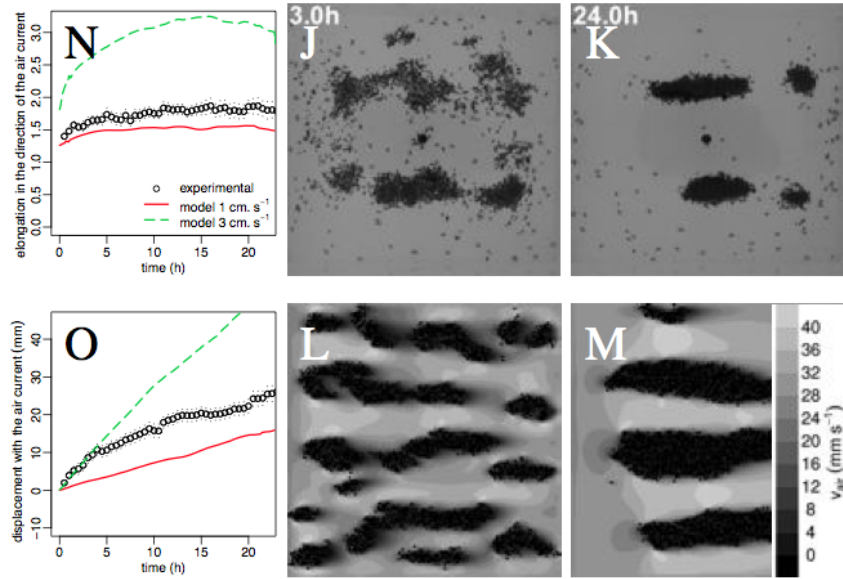


Figure 4.18 – (J-K) Example of a corpse clustering experiment with convective air currents (see Fig VI.18 in [Challet 2005](#)): the air flows from left to right. (L-M) Simulated corpse clustering with a laminar air flow (the emerging wind speeds at ant antenna height are coded in gray scale, white indicates highest wind speeds). (N) Corpse elongation at laminar air flows of 1 cm/s or 3 cm/s with the experimentally observed elongation in between them. (O) Corpse movement (mm/day) at laminar air flows of 1 cm/s or 3 cm/s with the experimentally observed movement. Modified after Figs 4.26, 4.27 and 4.29 in [Weitz \(2012\)](#).

4.3.6 Towards a macroscopic model of corpse clustering in 2D?

The previously mentioned models are based on a mesoscopic formulation of the animal’s clustering behavior and the numerical simulations are standard individual based models. The analysis of model sensitivity to behavioral or environmental parameters requires a lot of computing power, especially in the case with laminar air flows where the modulation of these air flows by the emerging structures has frequently to be updated. To simplify this type of analysis one might try to pass from the mesoscopic equations by integration to a macroscopic model in the form of a partial differential equations (PDE) system. Such macroscopic equations open the door to study the model’s properties analytically, thus in much more generality. Actually, [Challet \(2005\)](#) had already done this passage for a simple 2D version of the 1D model in [Theraulaz et al. \(2002\)](#) and she had obtained a set of three coupled PDEs (free ant density, loaded ant density and corpse density). In her case this model served for a preliminary assessment how the effect of temperature on individual movement and clustering behaviors influences the emerging cluster statistics (in particular how fast clustering occurs). However, her model did not include thigmotactic behavior, ants were freely diffusing independently of the current cluster organization.

When [Weitz \(2012\)](#) formulated his mesoscopic model of corpse clustering with thigmotactic behavior he carefully choose formulations that would not prohibit the integration to macroscopic equations. However, obtaining such a macroscopic model and its analysis were beyond the scope of his PhD. Another Master or PhD student could take up the work where he left it and do this analytical (and numerical) work. We haven’t gone in this direction not only because there was no such student at hand, but also because our interests have shifted from the corpse clustering paradigm to actual nest construction behavior (see next chapter). While corpse clustering was a perfect experimental system to study the underlying behaviors experimentally,

find adequate mathematical formulations and the inversion methods to estimate the associated parameters, the biological significance of corpse clustering is limited. As mentioned in the beginning of the chapter, corpses are treated by ants as any other waste, they are thrown out of the nest and in many species clustered in waste piles presumably for hygienic reasons. There are no “cemeteries” separated from the other waste. On the other side, nest construction is full of biological significance: protect the animals against environmental and predatory hazards, provide suitable habitats and microclimates to raise the next generation, let them survive in adverse climates (in particular dry savannas), We therefore chose to concentrate our efforts on the understanding of social insect nest construction.

Chapter 5

Nest construction in social insects: state of the art



Figure 5.1 – (from top to bottom) *Lasius* nests in Romania, *Cubitermes* nests in Guyana, *Cornitermes* nests in Brazil.

The clustering of objects (as the clustering of corpses in the previous chapter) is a first step towards the construction of some shelter or even a whole nest. Social insects show a huge variety of such nests, be it in wasps where the nest architecture was even used for phylogenetic studies (Wenzel, 1991), in ants who can build huge underground nests (Jonkman, 1980a,b; Moreira et al., 2004a,b) sometimes complemented by intricate above ground structures (Chauvin, 1959; van Damme, 1998; Kleineidam et al., 2001; Cosarinsky and Roces, 2011), or in the masters of

construction, termites (Noirot and Darlington, 2000; Turner, 2002; Korb, 2011). These animal's construction activity can become characteristic for whole landscapes (Fig 5.1) and their ecological role is sometimes of a major importance for nutrient (López-Hernández et al., 2006) and water management (Bonachela et al., 2015).

A nest is usually built by two activities, digging of tunnels/cavities and *de novo* construction. Both can be coupled since construction requires material often coming directly from the digging activity. In our work we concentrate on the actual construction activity where material is assembled and stuck together to build architectures of various complexity. Fig 5.2 shows some

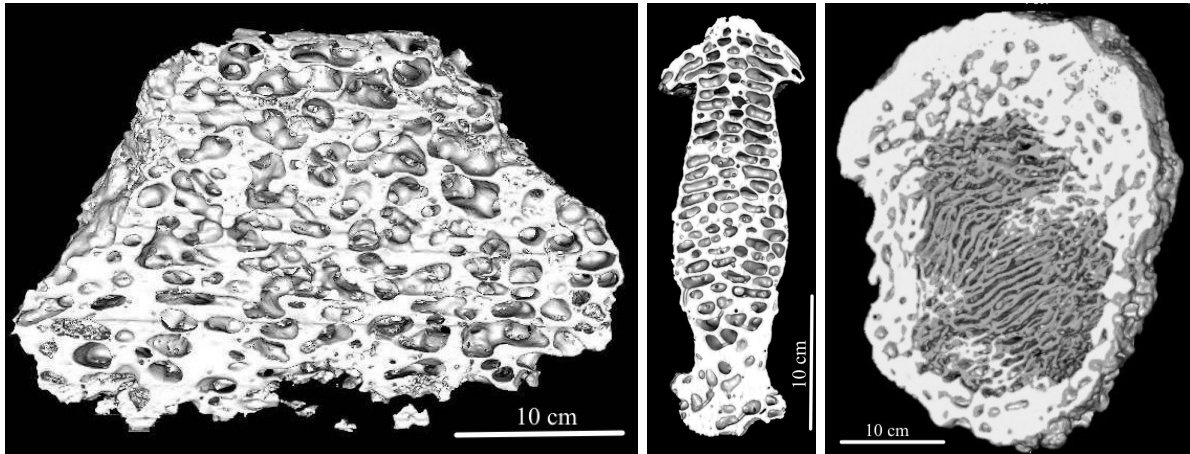


Figure 5.2 – (from left to right) Virtual cut through an above ground *Lasius* nest, an above ground *Cubitermes* nest and a *Cornitermes* nest partly below ground. These virtual cuts were obtained from X-ray tomographies of the excavated nests.

of the emerging architectures. In the case of the black garden ant *Lasius niger* these are simple interconnected cavities in the material that has been thrown out of the nest entrance during excavation of the underground part (note that we do not know whether they have dug in order to produce material for this construction, or if they primarily dig and the thrown out material has later been re-organized to provide additional living space, or if both go hand in hand). The above ground nests of West-African *Cubitermes* sp. termites resemble mushrooms and consist of many chambers interconnected by small diameter tunnels just large enough to let one termite pass. The Brazilian termite *Cornitermes cumulans* has a more complicated architecture with a solid outer shell that is partly immersed in the soil (and separated from it by a small air space) and a softer inner core with organic lamellae.

Our central question is how such architectures emerge from the individuals' construction activity. Templates may be involved (the aggregated brood cluster in the ant *Leptothorax tuberointerruptus*, Franks et al. 1992, or the physogastric queen in the termite *Macrotermes subhyalinus*, Bruinsma 1979). These templates are coupled with self-organization (see chapter 2). However, despite such conceptual simplicity, there is only one example where the full methodology (section 2.3) has been applied in order to validate the concepts: the blind bulldozing underlying the construction of the circular wall surrounding a *Leptothorax tuberointerruptus* colony in their naturally flat shelter under stones (Franks et al., 1992; Franks and Deneubourg, 1997). Even in *Macrotermes subhyalinus*, the best studied construction example in Termites (Bruinsma, 1979; Ladley and Bullock, 2005; Hill and Bullock, 2015), the full methodology cycle has not been closed and the existence and role of a central ingredient, cement pheromone, has recently been experimentally challenged (Petersen et al., 2015).

In order to work out such a full example we have started studying the construction behavior of *Lasius niger*. Several Master students (Julie Olivera, Victor Loisel, Marion Keromest) and two

PhD students (Anais Khuong, Chaker Sbai) were involved in this experimental and modeling work reported below (section 5.1). I co-supervised all these students except Anais who was supervised by Jacques Gautrais and a physics colleague, Jean-Jacques Beziau (my role was only that of an adviser on available experimental data from earlier students). Thanks to an ANR grant (MESOMORPH, ANR-06-BYOS-0008, 2007-2010) we also started assembling a database of Termite nest architectures through X-ray tomography. Only the Termitinae nests in this database could so far be characterized and analyzed (see section 5.2.1 below) in collaboration with a series of postdocs from biology (Andrea Perna) or physics (Matheus Viana, Young-Ho Eom). Since 2009 we also started to study construction behavior of termites in collaboration with our Brazilian colleague Ana-Maria Costa Leonardo from UNESP Rio Claro: due to the difficulty to raise such termites in a lab in France all experimental work has been done in Brazil, myself spending overall 6 months in the field and several of my Master students, Diane Fouquet and Christelle Péchabadens, spending half of their internship in Ana-Maria’s lab. Our efforts concentrate on two sympatric species, *Procornitermes araujoii* and *Cornitermes cumulans*, that are morphologically very similar but whose nest architectures are quite different (see section 5.2.4 below).¹

5.1 Ant nest construction: the case of the black garden ant *Lasius niger*

The work on *Lasius niger* construction was initiated by me in Toulouse in 2004 based on some preliminary results obtained during the PhDs of Dussutour (2004) and Buhl (2004). By 2010 the experimental data on the individual and the collective level were deemed sufficiently well advanced to link them through a spatially explicit simulation model during the PhD of Anaïs Khuong (which was also the occasion to centralize all the previous experimental work, Khuong 2013). The complete work, applying the full methodology from section 2.3, is currently submitted (Khuong et al., 2015) and contains the details of the work described below.

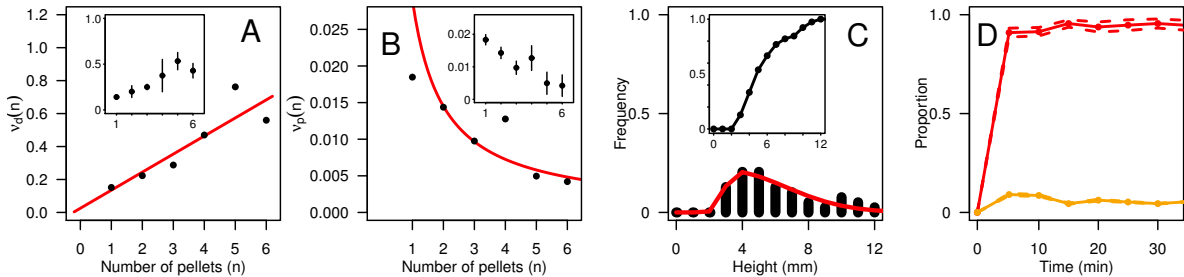


Figure 5.3 – Individual construction behavior: (A) rates and (inset) probabilities to deposit a pellet as a function of the number of perceived pellets (or, inset, the number of pellets in the pile encountered by a transporting ant) – the straight line is the model fit $\nu_d(n) = \nu_{d,0} + b_d n$; (B) rates and (inset) probabilities to pick up a pellet – the straight line is the model fit $\nu_p(n) = \frac{\nu_{p,1}}{n}$; (C) height distribution of pellets deposited along a vertical surface (the inset is the cumulated distribution $F(h)$) that can be well fit by a skew Normal distribution (red line), Frequency $f(h) = \frac{1}{\omega\pi} \exp(-\frac{(h-\xi)^2}{2\omega^2}) \int_{-\infty}^{\alpha(\frac{h-\xi}{\omega})} \exp(-\frac{t^2}{2}) dt$; (D) fraction of ants found around a pile made of freshly manipulated material (red line, \pm se) compared to the fraction of ants around a pile made of non-manipulated material (orange line) in a binary choice experiment containing the two types of pillars in the same Petri dish.

A first series of experiments (Olivera, 2006; Loisel, 2009) quantified the individual construc-

¹Note that this experimental and modeling work was also presented in a popular science paper, Theraulaz et al. (2012a, in french).

tion behavior of *L. niger*. Ants were led to choose shelter in a Petri Dish containing a humid plaster disk and under the cover of red plastic film. After removal of the red plastic film construction material (clay and sand in a 50:50 mixture) was made available directly in front of the nest entrance. Ants spontaneously started carrying this material pellet by pellet into the (now open) Petri dish and assembled a shelter (regularly spaced pillars finally covered by a roof). The full process could take a week, but we were only interested in the initial phase during which the gray pellets could be well distinguished against the white plaster background. We filmed this initial phase for 8 h and recorded for all transporting ants that entered the nest the sequence of encounters with previously deposited material until the final deposition of their pellet. These observations permitted to reconstruct the probabilities for a transporting ant to deposit their pellet on piles of sizes 1 to 6 (Fig 5.3A). From these probabilities we reconstructed by inversion the individual deposition rate $\nu_d(n)$ (n is the number of perceived previously deposited pellets, see legend Fig 5.3A). To study the picking up behavior of pellets we observed the evolution of some of the first emerging pillars (up to size $n = 6$), noting all contacts with either unloaded or loaded ants and whether these ants deposited or picked up a pellet. These observations permitted to model the picking up rate $\nu_p(n)$ as the inverse of the number of perceived pellets n (Fig 5.3B).

A next series of experiments was designed to observe at what height pellets are deposited on vertical surfaces. Ants were moving on a 2 mm thick humid sand-clay mixture (where ants started picking up pellets) which also contained vertical wood sticks. Most picked up pellets were deposited on these wood sticks. We noted the final distribution of pellets on these sticks and fitted it by a skew Normal distribution $f(h)$ (Fig 5.3C, h is the vertical distance between the ant's position and the nearest construction material pellet below the ant). To include this information in the model we simply multiplied the deposition rate by the cumulative distribution $F(h)$ of $f(h)$, $\nu_d(n, h) = \nu_d(n)F(h)$.

The experimental observations also suggested that recently modified piles changed their size more frequently than older piles. This observation suggests that deposited material is marked by some volatile chemical substance (“pheromone”) that influences the deposition and picking-up rates. We could not measure directly the influence of such a marking on these rates, but we showed that a pile made of freshly manipulated pellets is much more attractive to ants than a pile not manipulated by ants (Fig 5.3(D), Keromest 2008). Marking of pellets can therefore act on construction by increasing the ant density around piles (*i.e.*, modifying their movement pattern) or by manipulating the deposition and picking up rates (or act on both behaviors). We choose to include this marking effect by a modulation of the deposition rates, $\nu_d(n, \tau_m) = \nu_d(n) \exp(-\tau_m \nu_m)$ (where τ_m is the time since the latest size change of a pile and ν_m is the pheromone decay rate, thus assuming an exponential evaporation of the pheromone).² We were not able to estimate the pheromone decay rate ν_m directly, it was therefore a free parameter investigated in Khuong et al. (2015) by a sensitivity analysis and comparison between the model predicted and experimentally observed emerging structures (see below). Finally, given the choice that pellet marking modifies the pellet deposition rate but not the ant movement, we verified that ants move in an unmarked environment according to a (diffusive) correlated random walk (Khuong et al., 2013) and used this type of movement in the simulation model below (calibrated to reproduce the same net squared displacement as the real ants).

In order to observe the construction dynamics on the collective level we let the ants move

²However, this choice is quite arbitrary, one could also let the pheromone diffuse and ants climb the density gradient (as in Deneubourg 1977; Bonabeau et al. 1998b) in order to let them be more dense near recently manipulated piles, without changing the deposition rates. The currently available experimental data do not permit to decide which of these two mechanisms is at work.

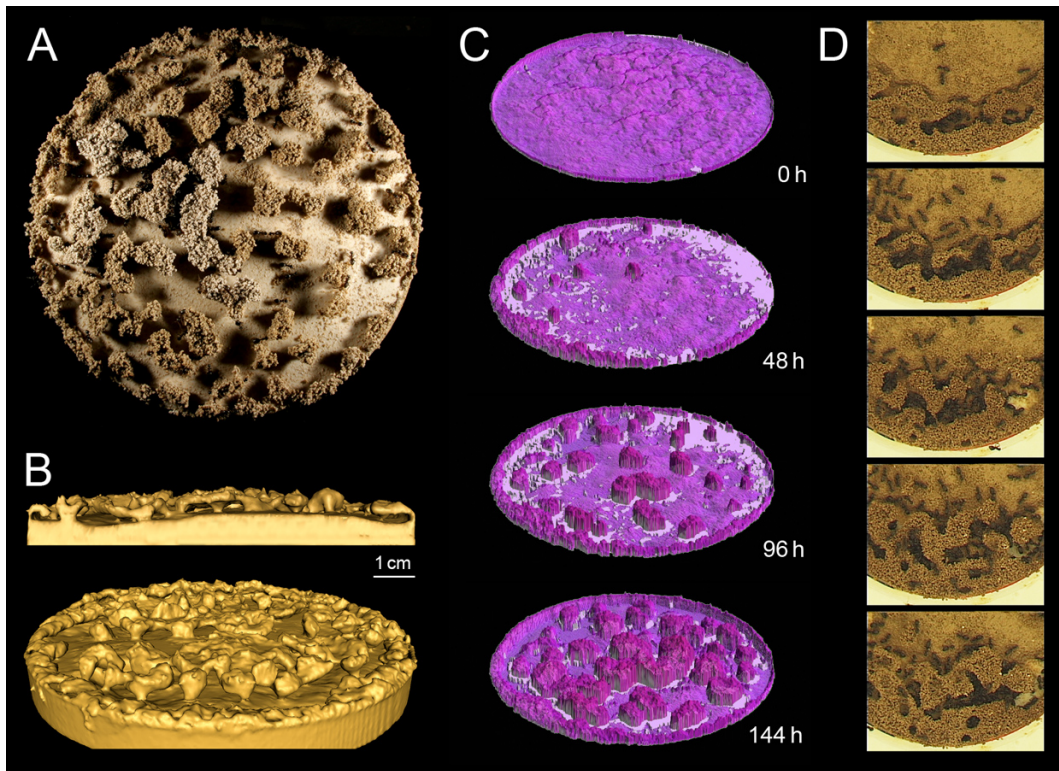


Figure 5.4 – Collective construction behavior: ants were moving freely in an arena containing a moistened circular disk ($\varnothing = 10$ cm, 2 mm high) of construction material (50% sand with 50% clay). They started building pillars to a certain height and then enlarged them on the sides (like mushrooms) that sometimes resulted in arches between pillars. The construction stopped because the amount of construction material was all used up for pillars and arches. (A) View from above on a construction after a one-week experiment. (B) Virtual cut through such a construction and view from the side (X-ray tomography at the end of the experiment). (C) Monitoring of the construction dynamics by a [NextEngine](#) surface scanner. (D) Construction never really stops, the built structures are continuously remodulated. Figure taken from [Khuong et al. \(2015\)](#).

freely in an arena containing a moistened circular disk of construction material. They started building pillars to a certain height (Fig 5.4A) and then enlarged them on the sides (like mushrooms) that sometimes resulted in arches between pillars (Fig 5.4(B)). The construction stopped because the amount of construction material was all used up for pillars and arches, but the ants continued to modify the structures (Fig 5.4D). The whole process was monitored by a surface scanner placed above the setup (Fig 5.4C), providing a matrix of heights every hour (the $x - y$ resolution was 0.3 mm). The whole experiment run one to two weeks (the construction speed was experimentally not controllable). The global statistics computed from these matrices are summarized in Fig 5.5 (time 0 was defined as the moment in an experiment when 3 pillars rose above 3 mm height, after which the dynamics were observed for 36 h). We monitored in

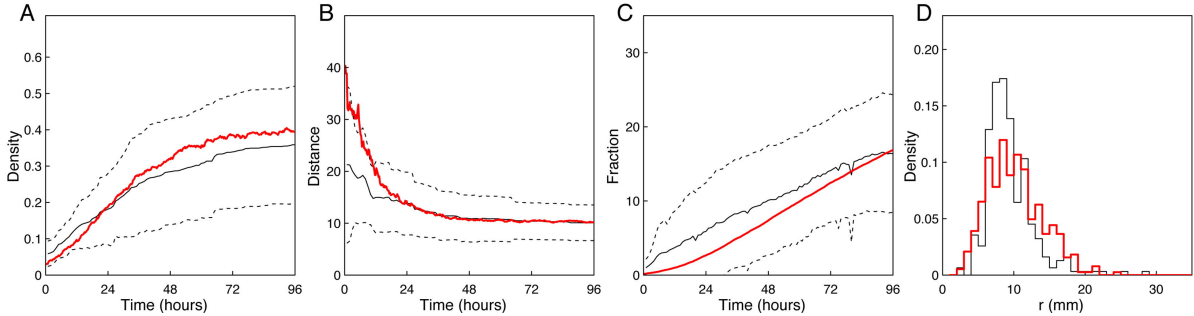


Figure 5.5 – Quantification of the construction dynamics (Fig 5.4). Black lines are the mean dynamics ($n=11$ experiments), black dashed lines the mean \pm standard deviation, and red lines the mean model predictions (average over 10 simulations). (A) Dynamics of pillar density (pillar cm^{-2}). (B) Dynamics of average nearest neighbor distance (mm). (C) Dynamics of the fraction of surface (in %) covered by structures exceeding 3 mm (0 mm corresponds to the average height of the initial disk of construction material). (D) Distribution of nearest neighbor distance between pillars after 96h. Figure taken from Khuong et al. (2015).

particular the density of pillars, where a pillar was any construction exceeding 3 mm in height and 14 mm^2 in surface (Fig 5.5A). This density monotonically increased to a plateau of ≈ 0.35 pillars/ cm^2 . We next computed the distance to the nearest neighbor at the moment the pillar emerged, a value that decreased monotonically until reaching 10 mm (Fig 5.5B). Another global statistics was the fraction of the setup’s surface covered by construction material exceeding 3 mm in height (Fig 5.5C). Finally, to get more detail on the nearest neighbor distance, we computed the distribution of the nearest neighbor distances at the end of the monitoring (96 h) (Fig 5.5D).

The link between individual behavior (Fig 5.3) and the emerging collective behavior (Fig 5.4) was established in Khuong et al. (2015) by a stochastic individual based model (IBM) on a 3D grid of size 200^3 (one cubic cell has volume 0.5^3 mm^3). A pellet has the size of a cell, they are picked up by moving ants and deposited according to the previously established rules, $\nu_p(n)$ and $\nu_d(n, \tau_m)$, where n is the number of pellets in the 26 neighboring cells in the 3D grid (subsequently called V_{26}), and τ_m is the time since the last picking up or deposit in V_{26} . Picking up occurs in the bottom layer of V_{26} , while the ant occupies one cell, deposits a pellet in this currently occupied cell and moves according to a constrained random walk on the built surface (that is, in an elementary move she chooses randomly one of the six orthogonal cells to its current position if it is free and shares a face with a cell occupied by a pellet; 1500 such elementary moves per $\Delta t = 1$ s were necessary to reproduce the same net squared displacement as observed for *L. niger* in Khuong et al. (2013)). Picking-up and deposition rates are calibrated to the observed behaviors (Fig 5.3). A body template effect is introduced when ants move along vertical surfaces: in that case the deposition rate is multiplied by the cumulative density function

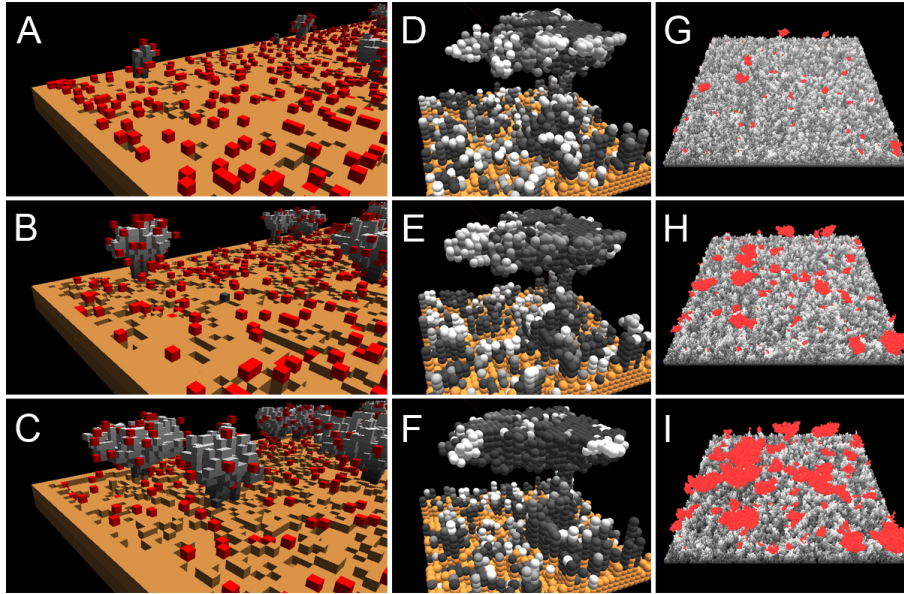


Figure 5.6 – A-C: sequence that shows the emergence of two pillars that are joined by an arch (ants are the red cells, brown cells are the initial construction material and grey cells are moved pellets/cells). D-F: a simulation run where the “age” of a moved pellet is visualized by a gray level, white referring to the most recently moved pellets (brown pellets have never been moved). G-I: the same representation (with pellet “age”) on a larger scale, emerging structures above height 3 mm colored in red (G: 24 h, H: 48 h, I: 96 h). All simulations were run with a pheromone mean life time of $1/\nu_m = 20$ min. Figure taken from [Khuong et al. \(2015\)](#).

in Fig 5.3C. The model is run with a discrete time step $\Delta t = 1$ s and 500 ants. In the beginning the five bottom layers (2.5 mm) of the grid were filled with construction material. Fig 5.6A-C is a typical simulation run showing the emergence of pillars and the formation of an arch. Figs 5.6 D-I visualize the complex topochemical landscape created by the evaporating pheromone.

Since the pheromone evaporation rate could not be determined experimentally we analyzed the sensitivity of the emerging structures to pheromone mean life time ν_m^{-1} ranging from 300 s to 7200 s (and ∞ simulated by a time of $3.6 \cdot 10^6$ s) or no pheromone at all (all pellets modulate picking up and dropping rates, even if they have never been moved). Fig 5.7 summarizes the results. If there was no pheromone at all no structures emerged, a volatile construction pheromone (whatever its precise effect) seems therefore to be necessary. With a non-volatile pheromone ($\nu_m^{-1} = 3.6 \cdot 10^6$ s) the pillar density became far too high. The experimental results were best reproduced by mean life times between 1000 s - 1200 s. The red curves in Fig 5.5 were made with $\nu_m^{-1} = 1200$ s (average over 10 simulations).

Overall, by calibrating a single free parameter (pheromone life time) our model correctly predicted all collective statistics in Fig 5.5. Though it would be more satisfactory to measure this pheromone life time also experimentally we consider this result to be strong evidence that such a construction pheromone exists (though whether it affects ant movement or ant deposition rates – as in our model – or ant picking up rates remains to be tested experimentally). Despite this free parameter we think that the modeling cycle postulated in section 2.3 has been satisfyingly applied to argue that construction in the ant *L. niger* is a self-organized process.

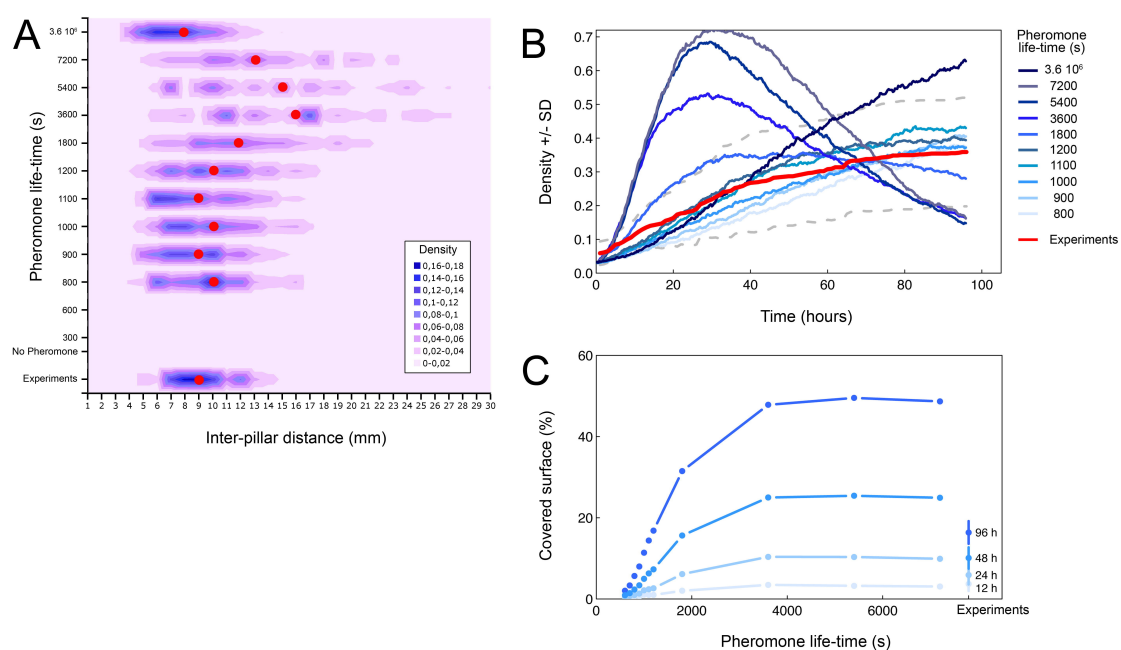


Figure 5.7 – Effect of pheromone life time ν_m^{-1} on the emerging structures. (A) Distribution of nearest neighbor pillar distance after 96 h. Red dots indicate the median value. (B) Evolution of pillar density from 0 to 96 h. The red line is the experimentally observed dynamics. (C) Fraction of surface (in %) covered by structures exceeding 3 mm at 12 h, 14 h, 48 h and 96 h. Fig taken from [Khuong et al. \(2015\)](#).

5.2 Termite nest construction: on architecture and underlying individual behaviors

The work on nest construction in the ant *Lasius niger* has shown that ants can build complex architectures based on rather simple individual construction behaviors. However, ants are slow constructors, the experiments run to obtain the emerging structures on the collective level took 500 ants one to two weeks. If you take the same setup but replace the 500 ants by 50 *Procornitermes araujoi* termites you get the same kind of architecture within a couple of hours. Furthermore, the solidity of an ant construction depends mostly on the clay content of the used building material, their structures quickly erode away under heavy rain fall. Termites, on the other side, have invented mortar (saliva and feces mixed with the construction material) that can render their structures as solid as air-dried brick buildings. Furthermore, termite architectures are fare more diverse than ant architectures (see for example the virtual visits in our online [virtual nest museum](http://www.mesomorph.org), <http://www.mesomorph.org>). Six years ago I started to collaborate with Ana Maria Costa Leonardo’s termite laboratory in Rio Claro, Brasilia, to work on nest construction behavior in termites. The already mentioned ANR grant (MESOMORPH, ANR-06-BYOS-0008, 2007-2010) also permitted to build a large data-base of 3D termite (and ant) nest architectures by X-ray tomography. The long term goal is to link the individual scale construction behavior research with the colony scale nest architecture research. Currently we are advancing on both fronts. Section 5.2.1 summarizes our network approach to understand the functioning (and growth) of Termitinae nests (based on the X-ray tomographies obtained in the MESOMORPH project, see Fig 5.8). This work was mostly performed by postdoc Andrea Perna ([Perna et al., 2008a,c,b, 2011](#)) which also served me to write the “Making Of” page in the [virtual nest museum](http://www.mesomorph.org): the text below is an extended version of this page. Section 5.2.4 concerns our results on individual construction behaviors and the involved stimuli in the Brazilian termite



Figure 5.8 – (left) Photo of the epigeal part of a *Cubitermes* sp. nest. (middle left) The X-ray tomography control room with a protected view on the scanner. On this photo a *Cubitermes* acquisition is under way. (middle right) Virtual mold of the *Cubitermes* nest, representing the habitable space of the termites by rendering the walls invisible. (right) Network representation of the *Cubitermes* nest. The color of the nodes indicates their degree. Figs taken from the [virtual nest museum](#).

5.2.1 The network approach to understand Termitinae nests

One of the most important nest functions is to allow the insects to move efficiently within these architectures. To describe this movement we have chosen to represent the nest as a communication graph. A graph has only two elements, nodes and edges, the latter connecting some of the nodes. In the case of a Termitinae nest (Fig 5.9) large diameter chambers are connected by small diameter tunnels, we can therefore represent each room as a node, and each tunnel connecting two rooms as an edge.

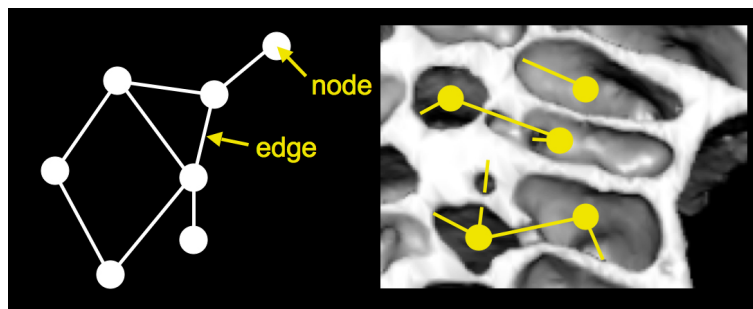


Figure 5.9 – Network with nodes (chambers) and edges (tunnels) connecting them, and how this network is projected inside a *Cubitermes* nest. Fig taken from the [virtual nest museum](#).

A graph is a much simpler object than the virtually reconstructed nest from X-ray tomography, and we can use the powerful toolbox provided by [graph theory](#). However, we must first identify all the chambers and passages between the chambers in a nest. What might seem like a relatively simple operation by observing a single cut from the X-ray tomography is actually a much more complex task when trying to automate it with a computer. Fig 5.10 explains the procedure to extract the connectivity graph of a *Cubitermes* nest from the slides obtained by X-ray tomography. In this species, the task is facilitated by the fact that the rooms have

a shape close to a sphere with a diameter much wider than the diameter of the tunnels that connect them.

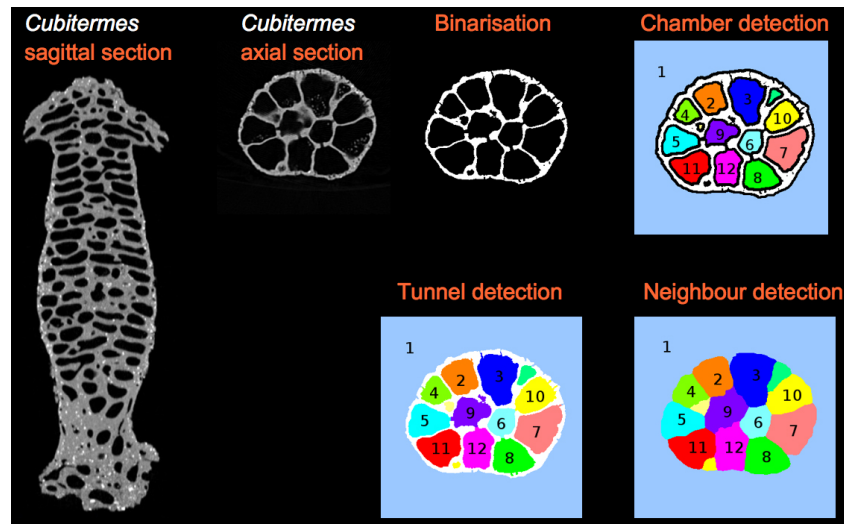


Figure 5.10 – Identification of chambers and tunnels from virtual slices of a CT scan. The first step, the binarization, applies thresholding to separate the walls from the empty space. In the second step, the walls grow a few pixels until all tunnels are closed. This identifies all rooms and permits to number them. Return now to the previous image and let the chambers grow without piercing walls. A tunnel is identified in this process by the meeting of two chambers. Finally we have to identify the neighboring chambers of a given chamber. For this we go back to the previous image and let the chambers grow this time through walls. When two chambers meet, we know they are neighbors. Obviously, all these analyzes must be done in 3D where the pixels are called voxels. Fig taken from the [virtual nest museum](#).

Each chamber is now representable by a node (virtually placed at the centroid of the chamber), tunnels by edges together with the information which chambers they connect. Fig 5.8 shows the result for a *Cubitermes* nest.

What do the graph representations teach us about nest functioning? Obviously, the representation of a termite nest in the form of a network is a rather crude approximation of their apparent complexity. However, the analysis of these networks revealed surprising properties. Let's start by examining some simple descriptors of a network: the degree of a node (that is to say the number of tunnels starting from a room, see Fig 5.11) and the shortest topological path between two nodes A and B (that is to say, the minimum number of edges that must be crossed to get from A to B, see Fig 5.11).

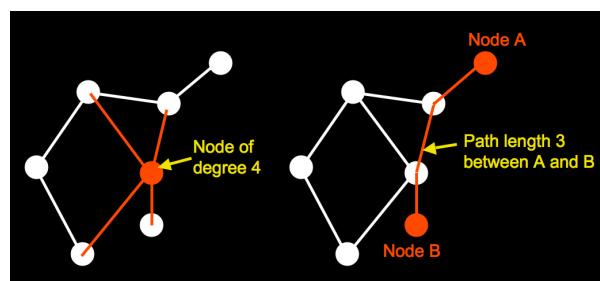


Figure 5.11 – Two basic statistics to describe a network. The degree of a node is the number of edges that depart from it. The shortest (topological) path between nodes A and B is the minimum number of edges through which one must pass to get from A to B. Fig taken from the [virtual nest museum](#).

Fig 5.12 shows the node degree distribution for the studied *Cubitermes* nests (white dots) and

also in the hypothetical case where the termites would connect each neighboring chambers. It is immediately apparent that the average node degrees in the studied nests are very low compared to the situation where each room were connected with all its neighboring nests: *Cubitermes* are very weakly connected.

It is also possible to "unfold" the connection network virtually on a plane (Fig 5.12); one can see that the network's structure resembles that of a tree with a very small number of main passages traversing the entire structure of the nest and on which are grafted groups of rooms organized in a bunch. This could be an adaptation to defend the nest: when a predator (like an army ant) managed to enter the nest, a single soldier can block the tunnel of the concerned branch to gain time for workers to close this communication channel.

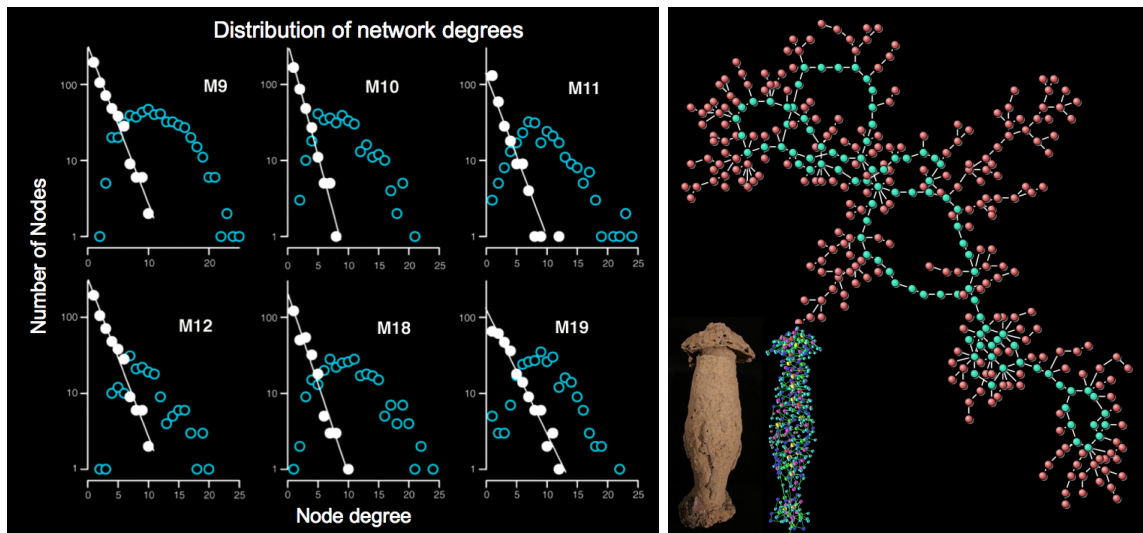


Figure 5.12 – (left) The degree distribution of the nodes for 6 different *Cubitermes* nests; in white those observed in the studied nests, and in blue those that would be obtained if all the neighboring chambers were connected by a tunnel. The nest M10 corresponds to that of Fig 5.8. (right) The virtually unfolded network of the nest in Fig 5.8: we see a structure that closely resembles that of a tree. Fig taken from the [virtual nest museum](#).

But the surprises continue. Look now at the distribution of the shortest topological paths. Fig 5.13 shows the distribution obtained in the studied nests, and that one would obtain if all the rooms were connected to their neighbors. The two distributions are very similar, as if the termites had carefully chosen the tunnels to minimize the distances between any two distant rooms.

Is it possible to obtain such a structure by choosing tunnels at random? This question is far from trivial. Indeed, what would be the structure of a network with the same number of nodes and edges as the original nests, but where the tunnels between the nodes were arranged at random? To build such a network, one must meet certain constraints. For example, each node must be connected to the network and tunnels may only connect adjacent chambers. Fig 5.14 describes an algorithm that creates random networks within these constraints.

By simulating a large number of random networks of this type, it is possible to calculate the average length of shortest paths and compare them to the original network. The result is shown in Fig 5.14. We can see that the average length is significantly shorter than for our random networks. This result indicates that termites do not choose edges randomly, but that they found a way to choose the most important tunnels in order to shorten the distances in the nest. The behavioral mechanisms that allow this ingenious choice are still completely unknown.

However, one may try to imagine such mechanisms that optimize the network in the sense

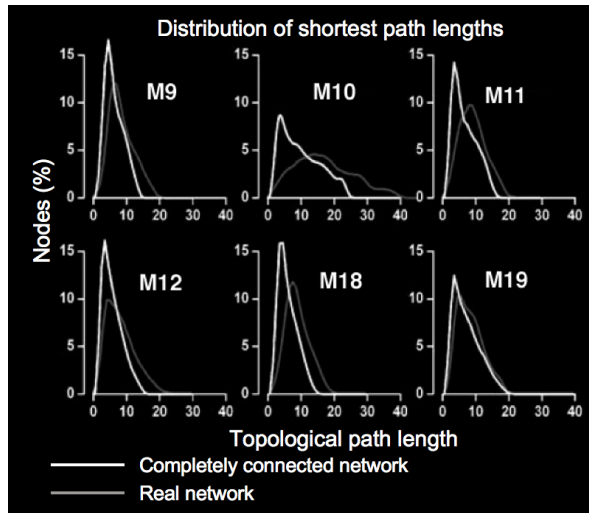


Figure 5.13 – The distribution of the shortest topological paths for 6 different Cubitermes nests; in gray the actually observed distribution and in white the one we would obtain if each chamber were connected to all its neighboring chambers. Fig taken from the [virtual nest museum](#).

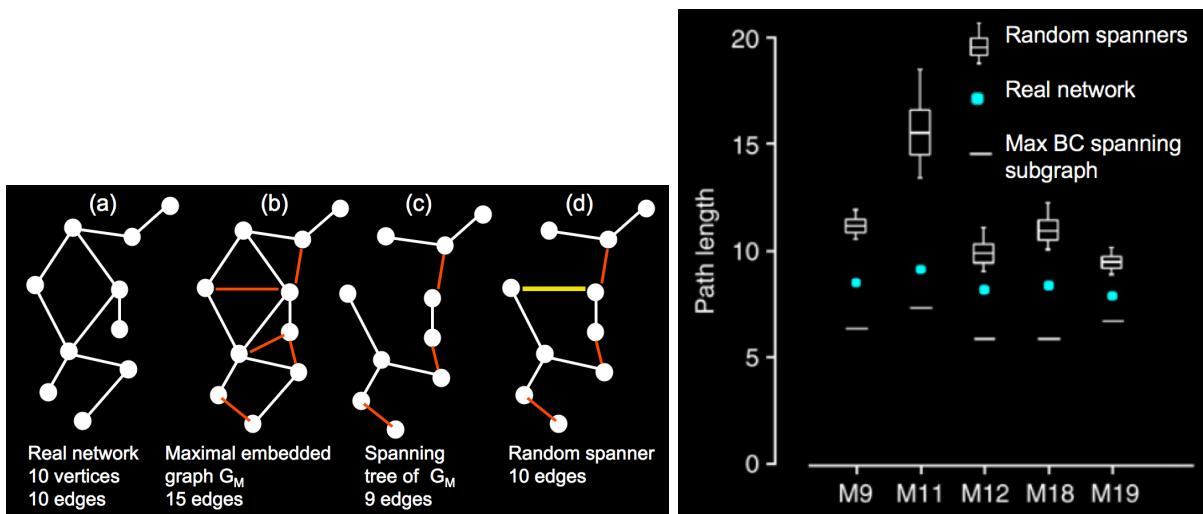


Figure 5.14 – (left) The construction of a random network while conserving the number of nodes and edges. (a) is the original network, (b) the complete network by connecting all the neighboring nodes, (c) the minimal tree that retains full connectivity, and (d) a random network by adding random edges to reach the number of edges in the original network. (right) The average length of the shortest topological paths for five Cubitermes nests, comparing the original network (green dots) to random networks (boxplots) and networks optimized to preserve the most important edges (horizontal line). Figs taken from the [virtual nest museum](#).

of providing short travel distances between distant chambers. While studying different models of network growth and dynamical change we were able to formulate such a hypothesis: the optimization procedure could rely on the termites' capacity to estimate in a non-centralized way another important edge characteristics, its centrality. For this estimation they could use the trail pheromone concentration that forms on every edge in the network from the termites passing through this edge (termites, just as ants, use chemical signals deposited on the ground to communicate indirectly, e.g. to guide termites to a new foraging site). Centrality is a measure of an edge's importance for the traffic within a network and its value corresponds to the total number of shortest paths between any two nodes that pass through this edge. The pheromone used by the termites will tend to accumulate on the edges with the most passages, that is to say on the "most central" edges. In the scenario that we simulated in our model, we start with the maximally connected network and remove progressively the edges with the smallest centralities until we have the same number of edges as in the original *Cubitermes* network (the mean path lengths represented by a horizontal line in Fig 5.14 were computed with this algorithm). The resulting network only contains the most important edges. The results show that networks built by this algorithm share many characteristics with the networks built by termites (Fig 5.15). Or, field observations show that *Cubitermes* termites indeed rework sometimes the structure of the communication network between the chambers by blocking certain passages. This simple mechanism of path conservation according to traffic intensity could allow termites to collectively optimize the network structure within their nest, in a totally decentralized manner and without any insect needing information on the global network.

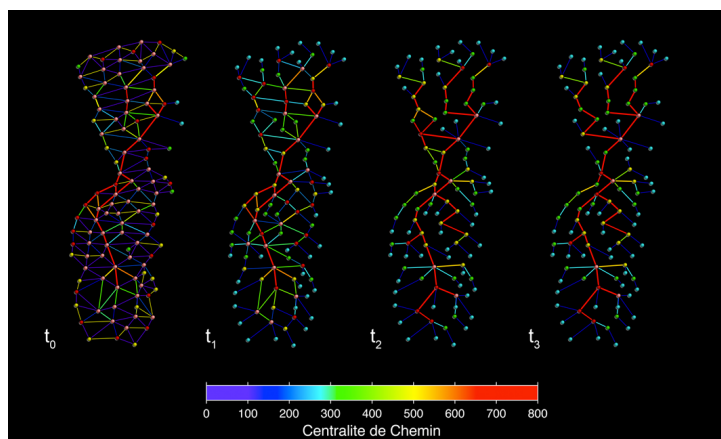


Figure 5.15 – Simulation of the network evolution when the edges (galleries) having a low centrality value are gradually eliminated, while ensuring that the network remains connected. In networks produced by this model, the distances between nodes are relatively short, although a large number of edges have been removed. Fig taken from the [virtual nest museum](#).

We continued this work on the network structure in *Cubitermes* termite nests with a new approach provided by the research group of Luciano da F. Costa in Sao Carlos (Brazil). With his student Matheus Viana he had developed a network measure that characterizes dynamics on a network: accessibility (Viana et al., 2012; da F. Costa, 2008). For a given number of k steps from node to node on a network, accessibility quantifies the mean number of nodes that can be reached in k steps (out-accessibility) or the mean number of nodes from which a focus node can be accessed in k steps (in-accessibility). This accessibility has biological meaning when it comes to transportation/movement inside the nest or defense of the nest against invading ant predators. The application (Viana et al., 2013) on the 6 *Cubitermes* nest networks of Perna et al. (2008a,c) revealed that in- and out-accessibility are mostly symmetrical

(Fig 5.16c). Furthermore, dividing the nest in three parts (cells on the nest surface, S; central cells with now contact with the surface, C; cells in the bottleneck zone between the nest and the underground tunneling network, B; see Fig 5.16a) surprisingly showed that accessibility was lowest in the B zone. This result can be interpreted in the context of nest defense against ant predators who have to pass through this bottleneck zone when accessing the epigeous nest after entering through the underground tunneling network (or vice versa). Termites themselves can bypass the restrictions of accessibility by circulating on pheromone trail networks, but further work will be needed to assess how the termites actually move around in their nests.

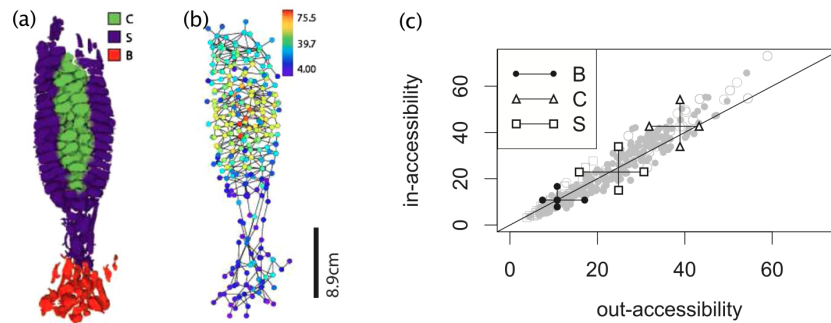


Figure 5.16 – Accessibility analysis of *Cubitermes* nest communication networks (each chamber is a node, a tunnel between adjacent chambers is an edge). (a) separation of the nest in three parts: chambers along the nest surface (S), internal chambers without surface contact (C) and chambers in the bottleneck zone between the nest and the underground tunnel network. (b) Network representation of the same nest. Node colors code for out-accessibility. (c) comparison between in- and out-accessibility for the three nest parts (the crosses represent the median \pm quartiles). Figs modified after [Viana et al. \(2013\)](#).

All previously presented work analyzed the properties of the networks extracted from the real nests. [Perna et al. \(2008c\)](#) had compared these networks to random graphs. However, his random graphs were still based on the node coordinates and edge statistics of the original networks, they were not based on a network generation algorithm starting from an initial chamber as in termite nest construction. [Valverde et al. \(2009\)](#) went a step further by generating networks with random node coordinates: based on the observation that *Cubitermes* nests were layered with different connection probabilities between horizontal layers and within them he formulated a network growth model that started with a fully connected regular cubic lattice of the same dimensions as the real nest, then removed edges randomly until obtaining the same connection probabilities as in the original network, and finally added stochastic noise to the node coordinates that may result in the fusion of nodes that had become too close. The analysis of these random graphs showed that the connectivity probabilities in the real nest networks brought them close to the percolation threshold (fewer edges would lead to network disconnection), confirming the earlier results by [Perna et al. \(2008a\)](#) that these networks are sparsely connected and rather resemble trees than networks. However, the model of [Valverde et al. \(2009\)](#) was not an actual network growth model since it started with an existing grid of the right size.

In [Eom et al. \(2015\)](#) we therefore tried to develop a network growth algorithm that started from a single initial node and whose growth rules were only based on locally available information. In this work we added to the six *Cubitermes* nests six other Termitinae nests: four *Proculitermes* nests and two *Thoracotermes* nests. An edge connecting two nodes is characterized by its length, its angle on the horizontal plane and its angle on a vertical plane (see Fig 5.17(left)). [Eom et al. \(2015\)](#) showed that in all 12 nests edge length and the angle on a vertical plane had Gaussian distributions while the angles on the horizontal plane had isotropic

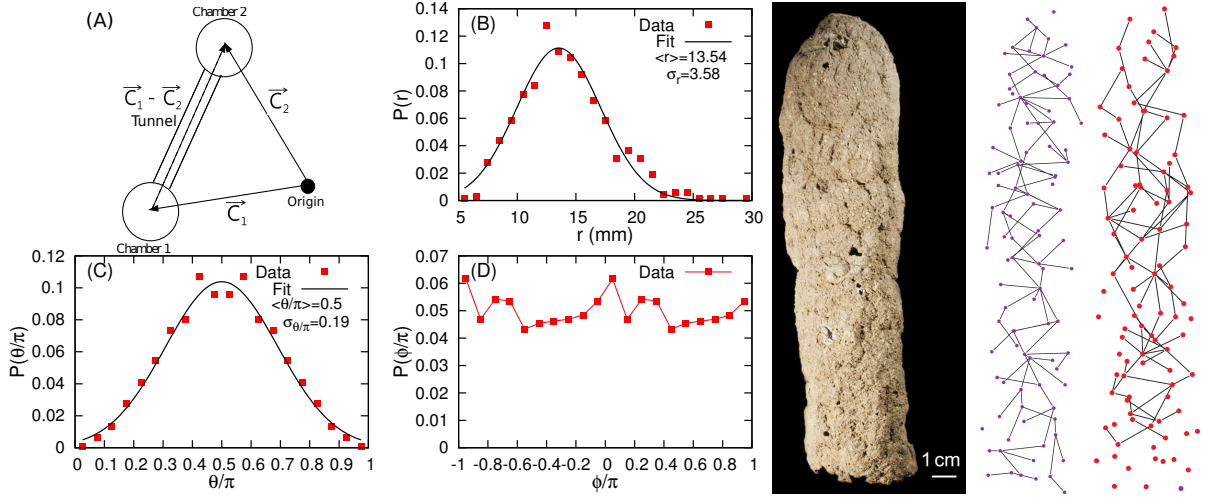


Figure 5.17 – (left) Empirical network description in the case of nest C9 (*Cubitermes* sp., Central African Republic, see Fig 1B in [Perna et al. \(2008a\)](#)). (a) Each tunnel or edge is represented as a vector in spherical coordinates, (b) tunnel lengths (r) distribution, (c) distribution of the vertical component (θ , 0 points upwards and π points downwards), (d) distribution of the horizontal component (ϕ). (c) and (d) are symmetric and periodic respectively because both $\vec{c}_1 - \vec{c}_2$ and $\vec{c}_2 - \vec{c}_1$ are used. (right) The analyzed *Thoracotermes* nest T29 with its network representation (middle) and a simulated network (right). The pink node (lower right) indicates the initial node of the simulated network. Note that while there are isolated chambers in the original network, isolated chambers are more prevalent in the simulated nests. Figs taken from [Eom et al. \(2015\)](#).

distributions. This led him to a network growth algorithm starting from a single initial node, adding then iteratively new edges to randomly chosen nodes with length and angles drawn from the empirically characterized distributions. When a new edge came too close to an existing node it connected to it without generating a new node. Edges were also constrained to remain within a vertical cylinder (with elliptic base) of the same size as the original nests. The node from where to start a new edge was not chosen randomly but preferring the most recently added nodes with an exponential decay of their attractiveness (as if there was a volatile pheromone incorporated into the construction material, with decay rate η). Furthermore, at each iteration step (adding an edge) the edge with the lowest betweenness centrality was pruned with a fixed probability p . These steps were repeated until the random network had the same number of nodes as the original one. The two parameters, η and p , were calibrated to each nest in order to reproduce the same number of edges and the same nest height. Fig 5.17(right) shows an example random network for a *Thoracotermes* nest.

This calibrated model correctly predicted in all 12 nests several emerging characteristics: node degree distribution, average topological distance between any two nodes and backbone link ratio (the latter is the fraction of edges whose removal leads to a disconnection of the network). The growth rules therefore seem plausible, and in a next step one could investigate experimentally how termites actually initiate new edges according to the postulated rules.

5.2.2 The virtual nest museum

An important part in the mentioned ANR project MESOMORPH was the visualisation of the nest architectures acquired through X-ray tomography. Modern tomographs have a resolution of 0.3 mm in all three dimensions, scanning a nest with a typical height of 30-50 cm therefore results in several hundred slides that have to be processed. Software to visualize these tomo-

graphics target medical applications. Though some of them are free or competitively priced for science (we used initially the free [Osirix](#) viewer based on 32 bit technology, though the size of the files quickly obliged us to buy the commercial 64 bit version), these viewers are not particularly adapted to investigate nest architectures. The [Laboratoire Informatique de Nantes \(LINA\)](#), one of the four partners in the project, developed therefore an application for handling the rather large digital files. This software has been designed to allow interactive navigation within the visualized structures. This mode of interaction allows to study the internal physical characteristics of a nest or confirm working hypotheses without having to physically destroy it. But to move freely in a three dimensional space one has to simultaneously handle six degrees of freedom: 3 translations along the x, y and z axes and 3 rotations around these same axes. To facilitate this interaction, the software supports devices specifically designed for that purpose: 3D mouse and inertial sensors (Fig 5.18).

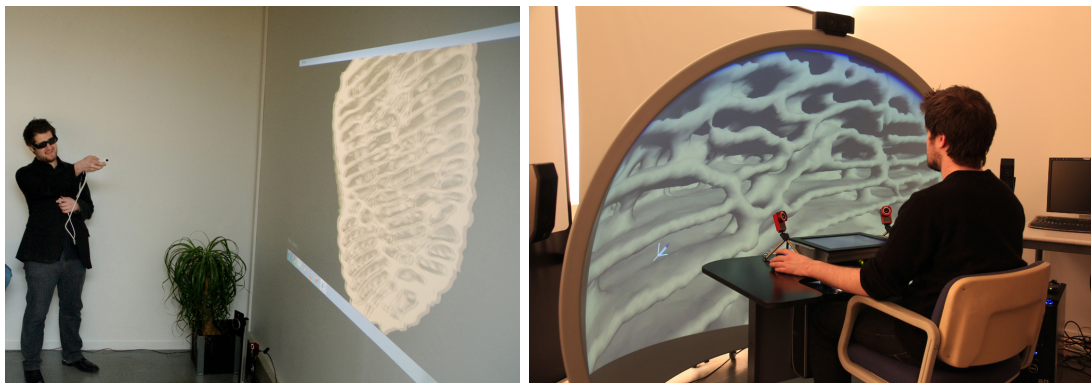


Figure 5.18 – (left) 3D navigation in an *Apicotermes* nest with "Wii" type technology. (right) Navigation with a 3D mouse in an *Apicotermes* nest projected on the interior of a dome to give a 3D feeling.

However, this software was only used amongst the MESOMORPH partners, its complexity and specificity made it difficult to provide a stable version to a larger community. All the beautiful visualisations of the complex nest architectures acquired through this project therefore remained mostly hidden from a larger public. We found this disappointing and therefore sought ways to render these architectures available to a large public. A first part was to write a public science portfolio in the Journal "Pour la Science" ([Theraulaz et al., 2012b](#)) that was distributed together with anaglyph 3D glasses in order to visualize some of the nest architectures in 3D. A second part was to design and develop a [Virtual Nest Museum](#)³ that presented for each studied species general scientific information, photos of the nests and the termites, 2D and 3D visualizations made from the X-ray tomographies, and movies showing the virtual navigation through these nests (Fig 5.19). This website was designed with an open architecture, that is a backoffice interface allows to add new nests (with their visualizations) as soon as we have them. This Virtual Nest Museum contains currently information for six genera: *Cubitermes*, *Procupitermes*, *Apicotermes*, *Thoracotermes*, *Sphaerotermes* and *Trinervitermes*.

5.2.3 Tunnel networks in termites

Many termites search their food (dead organic material such as wood or grass) by digging an extensive underground tunnel network. Tunneling provides also the raw material for construction activity. The mechanisms underlying tunneling activity therefore provides supplementary information to the understanding of construction activity. We studied such foraging tunnel

³<http://www.mesomorph.org>

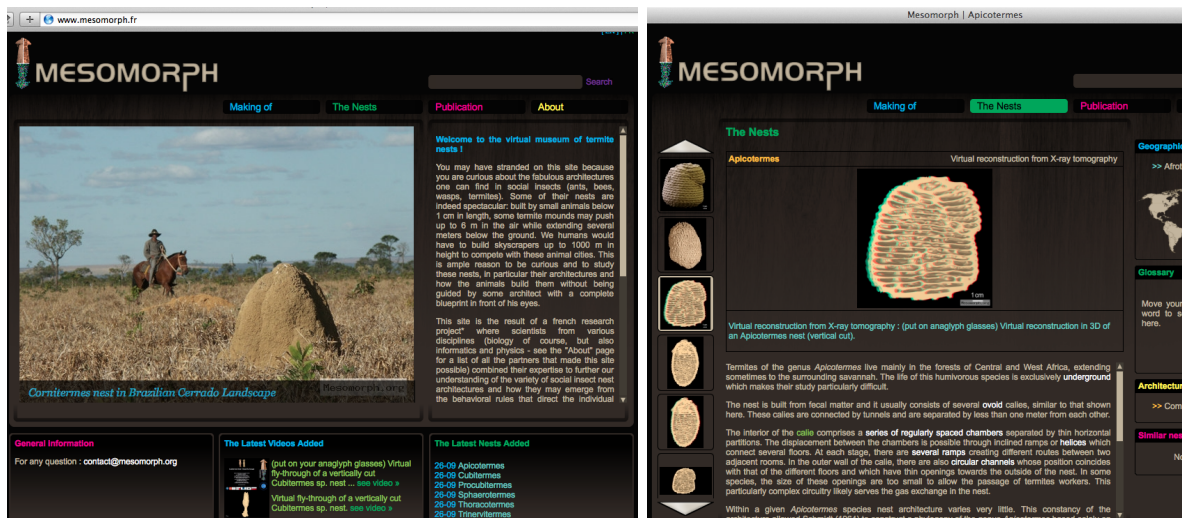


Figure 5.19 – (left) Welcome page of the [Virtual Nest Museum](#). The “Making of” part describes how termite nests can be analyzed with X-ray tomography, while the “Nests” part gives access to a data base where we can provide for each species or nest type a general text providing some biological information and as many visualizations (photos, virtual reconstructions, virtual fly throughs) as available. (right) A typical page for a genus/species (here *Apicotermes*) with the general biological information below and the available visualizations on the left. Clicking on one of these icons loads the image or movie in the main window above the text, and a further click on this object opens it in a large popup window for better visualization.

networks in three Brazilian termite species: *Velocitermes heteropterus*, *Procornitermes araujo* and *Cornitermes cumulans*. We made them dig under laboratory conditions during 3-5 days in horizontally placed sand disks where tunnel progression can be monitored by taking photographs at regular time intervals. The sand disks were accessed at a single location and tunnels radiated away from this entry point (Fig 5.20). In all three species several tunnels were dug in parallel and branched frequently. Digging occurs at a constant speed but slows down towards the end of the experiments. The analysis of the inter branching tunnel lengths showed that they have exponential distributions (Fig 5.20a+b top), suggesting that branching occurs at a constant rate (Haifig et al., 2011; Jost et al., 2012). In *V. heteropterus* two castes participated in this digging activity, majors and minors. Single caste experiments showed that they have caste specific branching rates, but in mixed caste experiments the one of the major caste dominated (Haifig et al., 2011).

P. araujo and *C. cumulans* are two sympatric species of near identical morphology and living on the same resources. Experimental encounters between the two species show that they quickly engage in aggressive behaviors with ferocious fights where soldiers and workers participate equally. We studied how competition affects their tunnel networks by letting them access the same sand disk from two different entry points (Fig 5.20b, Jost et al. 2012)⁴. When the two tunnel networks met the usual reaction was to wall off the breach immediately, thus avoiding direct fights. There is even evidence that *P. araujo* can detect *C. cumulans* tunnels some distance before actually encountering them. However, both species do not hesitate to invade part of the other species’ tunnel network and incorporate it into their own network. Nevertheless, in natural 3-dimensional soil environments encounters between the tunnel networks are supposedly rare, the competition between these two species is therefore rather of the “exploitation competition” type, not of

⁴see additional material on my homepage <http://cognition.ups-tlse.fr/~christian/TermiteNetworks-InsSoc-012/CornitermesProcornitermes.html>

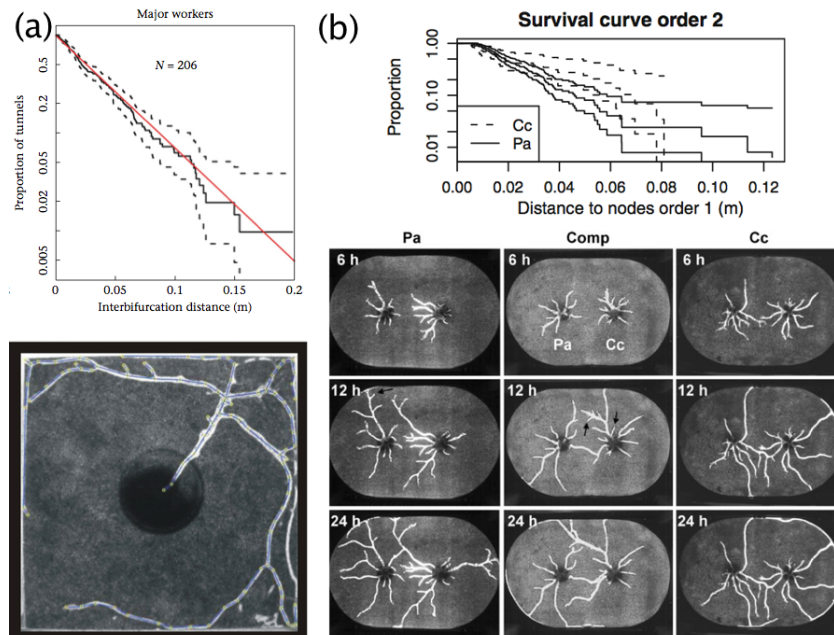


Figure 5.20 – Tunnel networks in (a) *Velocitermes heteropterus* or (b) *Procornitermes araujoii* (Pa) and *Cornitermes cumulans* (Cc). The survival curves on top show the exponential distribution of the inter-bifurcation distances. In (b) the ‘Comp’ column shows what happens when the tunnel networks of the two species encounter each other (interference, walling off). Figures modified after [Haifig et al. \(2011\)](#) and [Jost et al. \(2012\)](#).

the “interference competition” type. However, we noted that, at least for *C. cumulans*, the foraging tunnels progress at a constant depth below the surface, with frequent branchings that mount to the surface to let termites locate food (unpublished). The 2D topological nature of the tunnel networks found in our artificially 2D experimental setups (constant branching rates) may therefore also apply in field conditions.

5.2.4 Comparative study of *Procornitermes araujoii* and *Cornitermes cumulans* nests

Preliminary construction experiments also showed that *P. araujoii* as well as *C. cumulans* are good experimental models to study their construction behavior: 20-50 workers placed in a 5 cm \varnothing Petri dish with soil rebuild a complete shelter within a couple of hours (as in the ant *Lasius niger* construction starts with pillars that are then covered by a roof). Both species live in the same area (sympatry), sometimes in the same field. They are taxonomically close, of nearly identical morphology (*C. cumulans* is on average slightly larger, [Jost et al. 2012](#)) and can only be distinguished by a line of microscopic hairs on the hind leg of *C. cumulans* ([Constantino, 1998](#)). However, their nest architectures are quite different, with *P. araujoii* building a homogeneous sponge like network of interconnected chambers that resembles the nest of *L. niger* in Fig 5.2 (in particular, one cannot distinguish distinct tunnels as in the Termitinae nests), while *C. cumulans* builds very solid and compact nests with a distinct paraecy (empty space) separating it from the surrounding soil and an internal organisation composed of a massive outer shell made of clay and a softer inner part made of organic material and organized in lamellae (Figs 5.2(right) and 5.21).

Given these observations we decided to concentrate on the construction behavior and their coordination mechanisms in both species, first to test whether the similar architectures in *L.*



Figure 5.21 – (left) Sagittal cut of a *Procornitermes araujoii* nest in Rio Claro, Brazil, with the epigeous constructed part and the hypogeous dug out part. A yellow square is of size 5 cm × 5 cm. (middle) Excavated nest of a *Cornitermes cumulans* nest in Brasilia, Brazil, showing the below ground paraecy that separates the nest from the surrounding soil (with foraging tunnels extending from the paraecy towards the foraging grounds and the ground water level). The epigeous part is ≈ 40 cm high. (right) Sagittal cut through a small *C. cumulans* nest from Rio Claro, Brazil. Only 5 cm of the nest are epigeous. One can clearly distinguish the massive outer shell (made of clay) and the soft inner part (made of organic material).

niger and *P. araujoii* are based on similar construction behaviors, and second to identify the behavioral differences at the base of the architectural differences between *P. araujoii* and *C. cumulans*. We hypothesize that the basic construction behaviors are the same, but that their modulation by environmental stimuli (such as humidity, CO₂, temperature) or colony specific stimuli (colony odor, trail pheromones) can explain these architectural differences.

Construction behavior in *P. araujoii* was studied in Fouquet et al. (2014)⁵. Fig 5.22 shows the termites during construction, a close-up of the typical epigeous nest architecture, and the result of a 1 h construction experiment where 10 or 25 termite workers are placed in a 4 cm ∅ plastic beaker on a 4 mm deep soil disk: they quickly start digging tunnels, but are stopped by the beaker bottom before finding shelter. With the excavated material they build pillars and start extending them laterally (exactly as in *L. niger*), stopped finally by the scarcity of available construction material. The experiment was filmed from the top. When a termite deposits an excavated pellet it makes a characteristic **screwing motion of the head**. This screwing motion can be detected by eye and backward playing of the movie permits to identify where the pellet has been dug out. By this procedure the first ≈150 (in the experiments with 10 workers) or ≈400 (in the experiments with 25 workers) pellet transports were identified with their excavation coordinates, transport path and deposition coordinates. From these data we could reconstruct how many previously deposited pellets a transporting termite could detect at each moment (with their antenna, therefore a circular perception area with radius = antenna length). Assuming that termite behavior is Markovian (an assumption that has frequently been found to be sufficiently accurate for social insect behavior, Camazine et al. 2001) we could then reconstruct the survival curves of pellet transports for a fixed number of detected pellets. Fig 5.23 shows the results of this analysis. First, the survival curves all resembled exponential

⁵see also additional material on my homepage http://cognition.ups-tlse.fr/_christian/FouquetEtal-014-webPage/FouquetEtal-InsSoc-2014.html

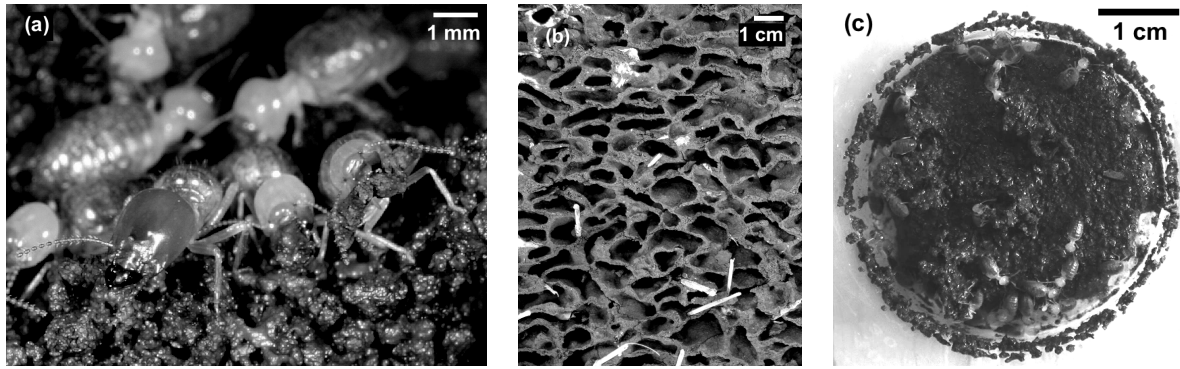


Figure 5.22 – Construction activity in the termite *Procornitermes araujoii*. (a) two workers fixing a breach in the nest wall while being guarded by a soldier, (b) typical architecture of their nest with densely packed chambers separated by thin walls, (c) experimental *de novo* construction with 25 workers + 3 soldiers in the laboratory (3 h after beginning the experiment). Fig 1 from Fouquet et al. (2014).

distributions, pellet deposition behavior can therefore be modeled by a constant deposition rate (estimated as the inverse of mean transport time or as the slope of the survival curve on log-linear scale). Second, the deposition rates increased with the number of detected pellets. There

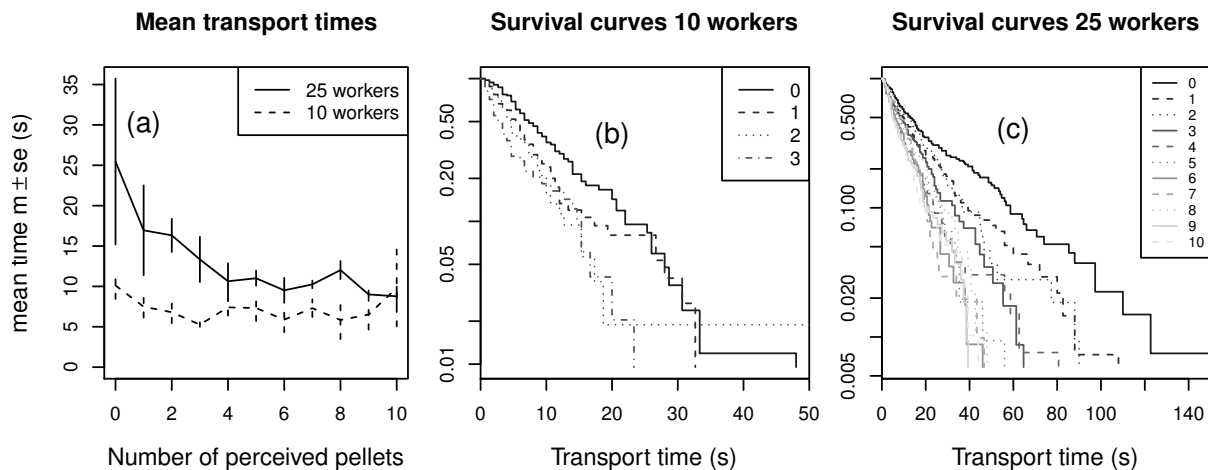


Figure 5.23 – Transport times as a function of termite density and the local density of previously dropped pellets. (a) The mean transport times, (b) survival curves of the transport times in experiments with 10 workers for 0 to 3 perceived pellets, (c) survival curves of transport times in experiments with 25 workers, separately for each number or perceived dropped pellets (0 to 10). Fig 4 from Fouquet et al. (2014).

is therefore a double positive feedback: digging stimulates further digging (tunnel formation) and deposits stimulate further deposits (pillar formation). Third, the deposition rates were also influenced by termite density, being smaller at higher densities. This predicts a larger spacing between pillars at higher densities, a prediction not yet experimentally tested.

The literature on termite construction behavior (Bruinsma, 1979; Grassé, 1984) also suggests that pellets are marked with some construction pheromone which stimulates deposition behavior. In order to identify whether the detected positive feedback in pellet deposition behavior relies on such a marking we run a second series of experiments (Fig 5.24). Based on the strong positive feedback on digging we provided two small holes to initiate digging in them.

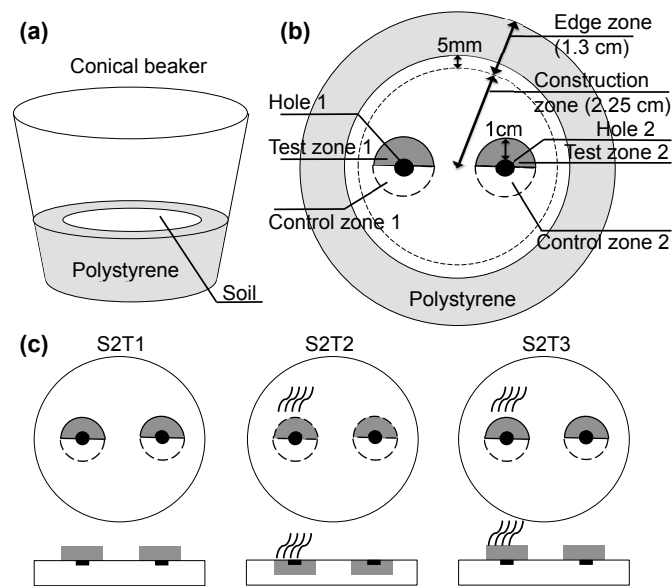


Figure 5.24 – The experimental setup for the binary choice experiments. Termites move in a conical beaker on a 6.3 cm wide soil disk that is surrounded by a polystyrene ring that is level with the soil. Inside the disk two stimuli were placed (see c) asymmetrically around two small holes in the soil that stimulate digging activity close to the stimuli. Termites that exit from the hole with a soil pellet have therefore the choice between the stimulus (test zone) and standard soil (control zone). (a) shows the complete setup, and (b) shows the zones on the termite moving ground where picking up and dropping events were counted. (c) The three types of experiments used: (S2T1) two unmarked soil heaps, (S2T2) marked and unmarked soil embedded in the sand disk (the curly lines indicate marking), and (S2T3) marked versus unmarked soil heaps. The distance between the two stimuli (4 cm) is larger than the average distance between two constructed piles observed in the construction experiments. Fig 2 from [Fouquet et al. \(2014\)](#).

Termites were therefore in a binary choice situation (would they concentrate digging effort only on one hole or on both? See [Detrain and Deneubourg \(2008\)](#) for an extensive discussion on collective decision making and the underlying individual mechanisms). We added a second binary choice situation by providing different stimuli on two sides of the holes: (I) an artificial unmarked pillar vs. level unmarked soil, (II) level marked soil vs. level unmarked soil, and (III) a repeat of setup (I) but with one of the pillars made with marked material (marked material was always taken from another ongoing construction experiment with termites from the same colony). Case (I) tests whether elevated structure stimulate deposition on them, case (II) tests

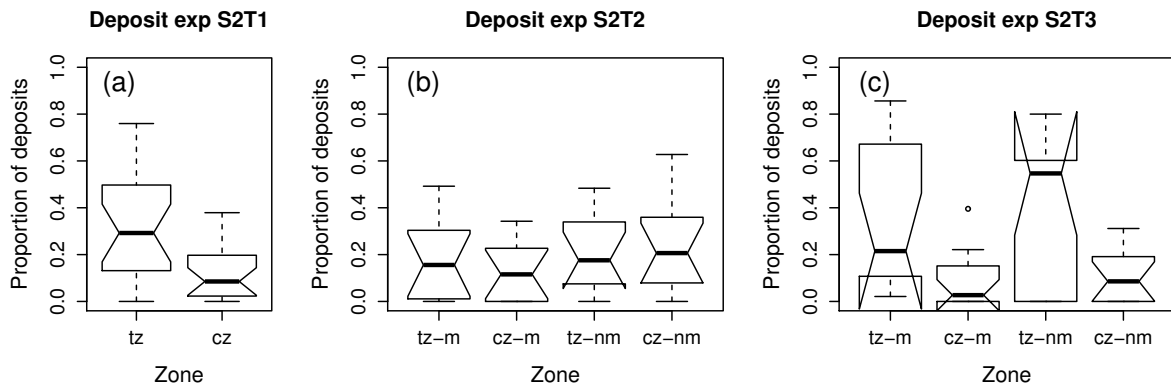


Figure 5.25 – RWP’s (Renormalized Weighted Proportions) of deposits in the binary choice experiments: (a) comparison between test (structure, tz) and control zone (cz) for experiments of type I, and (b,c) comparison between these two zones and whether the test zone contained marked (m) material or not (nm) for experiments of type II and III. Fig 7 from [Fouquet et al. \(2014\)](#).

whether marked soil stimulates deposition, and case (III) tests whether there is an interaction between the two stimuli (structure and marking). In all cases an experiment started with the introduction of 30 worker termites in the arena and their construction activity was filmed for 30 min. We identified in each replication the positions of the first 50 digging and deposition events and attributed them to 8 zones: hole 1 or 2, test zone (pillar or soil insets) 1 or 2, control zone (opposite pillar or soil inset) 1 or 2, construction zone (rest of setup where soil is present) or edge zone. To test for structure or marking effects we weighted these counts by the surface of each zone and renormalized the new values to sum to one in a given experiment. We will refer to these Renormalized Weighted Proportions as RWP. 90% of digging events occurred in the holes, while 90% of the pellet depositions occurred in the control or test zones. Fig 5.25 summarizes the depositions in control and test zones. In case (I) there is a clear effect of structure, pillars attract further deposits even if not marked. In case (II) no effect of marking can be detected, termites deposit as often on marked as on unmarked soil. In case (III) we find around both holes the same result as in case (I), termites deposit preferentially on pillars but without making a distinction between marked and unmarked pillars. On first sight marking of soil seems therefore to be of no importance. However, when testing for collective choices between activity around holes 1 and 2 we could detect such collective choices only in case (III): if there were no marking effect we should have detected these collective choices also in case (I). On the other hand, it is known that asymmetries in binary choices can accentuate the collective decision making ([Beckers et al., 1992a](#)). There is therefore nevertheless some indirect evidence that marking plays a role, though it is not clear which one.

We rerun the experiments of case (II) with a higher replication number and in a simplified version with only one initial hole and a single binary choice between depositing on the side of an inset with marked material or on the side with an inset of unmarked material ([Pechabadens,](#)

2014). But still no effect of marking on pellet deposition could be detected. Actually, the simple stigmergic mechanism “termites preferentially deposit on recently manipulated material” that is suggested in the literature (Bruinsma, 1979; Grassé, 1984) and that can produce the observed emergent constructions (Courtois and Heymans, 1991; Bonabeau et al., 1998a; Ladley and Bullock, 2005; Hill and Bullock, 2015) seems to be more complex: Petersen et al. (2015) performed the same kind of experiment with a different species, *Macrotermes michaelseni*, and they found that recently manipulated material had the effect that termites simply spent more time near marked material. Higher deposition rates on marked material might therefore simply be a side effect of this “arrestant” (sensu Petersen et al. (2015)) property. This reminds us of a first model leading to pillar construction where marking actually did not modulate the deposition rates but the movement of individuals that followed the gradient of the volatile marking (Deneubourg, 1977). In sum, volatile marking of construction material seems to be necessary in the formation of pillars (Khuong et al., 2015), but the actual role of marking on animal behavior remains to be determined.

I will finish this section with two preliminary experimental results (Fig 5.26). First, *P. araujoii* also seems to use its body as a template when depositing pellets on a vertical surface: the highest deposition frequency occurs at a height of 6-7 mm that just corresponds to these termites’ length (Fig 5.26(left)). These experimental data will allow us to start implementing *P. araujoii* construction behavior in 3D just as we did in the case of *L. niger* (see next chapter). However, contrary to *L. niger*, *P. araujoii* heavily relies on pheromone trails already

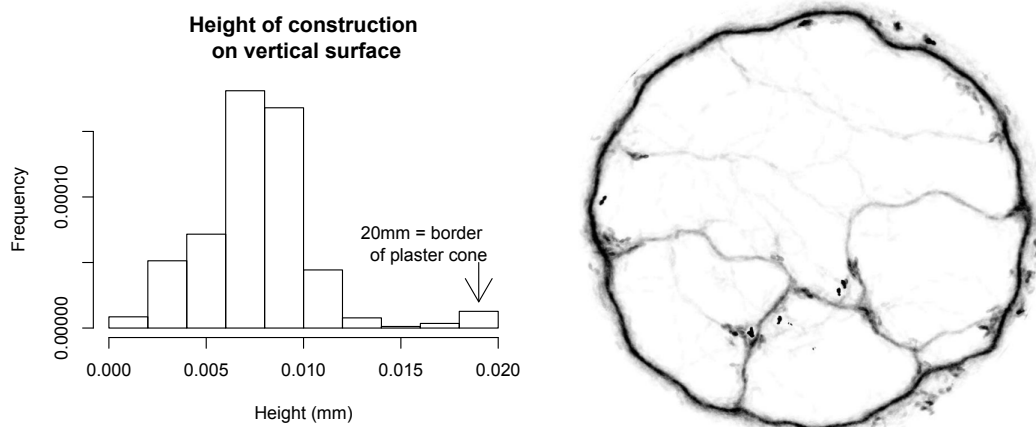


Figure 5.26 – (left) distribution of construction material along a vertical surface. (right) average termite density (averaged over 5 min, black indicates high density) of 100 termites moving in a 24 cm \varnothing arena on white paper at the end of a 1 h experiment.

during exploration behavior (Fig 5.26(right)). A recent simulation study of termite construction (Hill and Bullock, 2015) had shown that such pheromone trails strongly influence the emerging structures. Bruinsma (1979) had also run nuptial chamber construction experiments where the worker’s bellies were varnished, they were therefore unable to lay a pheromone trail: no nuptial chamber was constructed in these experiments, the pillars remained very flat. These pheromone trails play therefore an important role in termite construction, but their exact effect in the case of *P. araujoii* remains to be explored by applying the full methodology of section 2.3 (see next chapter).

Chapter 6

Where to go now?

In the last chapter we announced that we want to concentrate on construction behavior in *Procornitermes araujo* and *Cornitermes cumulans*, first to test whether the similar architectures in *L. niger* and *P. araujo* are based on similar construction behaviors, and second to identify the behavioral differences at the base of the architectural differences between *P. araujo* and *C. cumulans*. The reported research shows that we are just at the beginning of the first goal. Within the next four years I plan to advance on several fronts.

6.1 The role of individual movement in the emergence of the nest architecture in *Procornitermes araujo*

The experimental data that are available on *P. araujo* individual construction behavior are comparable to what was available in [Khuong et al. \(2015\)](#). From my 2009 stay in Brazil we also have three collective construction experiments that had been monitored by a microtomograph (provided by Carlos Vaz from [EMBRAPA Instrumentação](#)). We are therefore ready to start closing the methodological cycle from section 2.3. During the last two years this project was offered as a PhD project in the [International PhD Office of the University of Toulouse](#), and we were lucky that a Chinese physics student obtained a 4-year Chinese Scientific Council (CSC) grant to work in our group on this project (starting in October 2015). Beyond simply redoing the work of [Khuong et al. \(2015\)](#) for a different species we want to take in this PhD a closer look at the role of individual movement on the emerging nest structures. *P. araujo* relies much more on pheromone trails than *L. niger* (Fig 5.26), and the simulation work by [Hill and Bullock \(2015\)](#) had shown that pheromone trails modify the morphospace of the emerging structures. Furthermore, a recent paper ([Perna et al., 2012](#)) provides a methodology how to analyze and to model such emerging trail networks. A first task will therefore be to develop a trail formation algorithm for *P. araujo* and incorporate this algorithm in a simulation platform for construction¹. This will permit to assess whether the incorporation of this movement type improves the predictive power on the collective level. Note also that the individuals move around on a surface in 3D. [Khuong et al. \(2013\)](#) had shown that the correlated random walk of *L. niger* is modulated by this third dimension. Preliminary data on *P. araujo*² indicate that this is also the case in our study species. Another task will therefore be to assess whether this modulation is important to correctly predict the emerging constructions on the collective level. All-together, this is an ambitious program and we will see how far we get in the framework of

¹Experimental data to apply this methodology to *P. araujo* had been collected during my two months invited professorship in Rio Claro in 2012

²Also gathered during 2012 in Rio Claro

this CSC PhD. This PhD is for me also the occasion to reinforce our workgroup's collaboration with two physicists from the [LAPLACE laboratory in Toulouse](#), Richard Fournier and Stéphane Blanco. I also hope to develop during this time collaborations with external partners that can help us advance on how to characterize the complex architectures found in *P. araujoii* and in *C. cumulans*.

6.2 The interplay between nest architecture, environmental parameters and individual behavior

The architectural differences between *P. araujoii* and *C. cumulans* are probably linked to their ecological function, that is the way the architecture helps the colony to survive and to produce sexual individuals that can themselves found new colonies. The architecture can in particular help control environmental variables such as temperature and humidity, and it plays also a role in the gaseous exchange with the environment (export CO₂ produced in the nest by metabolic activity and renew the consumed O₂). We therefore hypothesize that the environmental variables best controlled by some architecture are stimuli involved in the modulation of construction behavior in order to obtain this particular architecture. This idea is at the base of another PhD who already started in fall 2014. His first task will be to monitor in the field temperature and humidity both outside and inside the mounds of *P. araujoii* and *C. cumulans* in order to assess whether the more complex architecture of *C. cumulans* better controls these factors³. If this turns out to be true he will assess in an experimental approach how these factors modulate construction behaviors and how this modulation modifies the emerging architectures. He will also test whether the individuals of the species with better controlled environmental variables are more sensitive to changes in these variables. We hope to gain from this PhD not only a better understanding of the ecological role of these species' architectures but also to become able to formulate clear hypotheses how environmental variables affect individual construction behavior in these species in order to let certain architectures emerge. The field and experimental work during this PhD will again be executed in the termite laboratory of A-M Costa Leonardo in Rio Claro, and this PhD will also be the occasion to add some neotropical termite nests to the virtual nest museum. While the PhD will focus on temperature and humidity we will also start to acquire the necessary technology to study the effect of CO₂ concentration on construction behavior (as done in [Römer \(2014\)](#) in the case of nest construction in leaf-cutting ants). CO₂ is a candidate how termites estimate their position in the nest with respect to the nest paraecy, and thus a potential stimulus to explain the transition from the soft inner core to the hard outer shell in *C. cumulans* (Fig 5.21).

6.3 Are there alternatives to our methodology to study self-organization?

Our methodology to analyze collective animal behavior (introduced in section 2.3) is, as already mentioned, simply a variant of the well known in-sample and out-of-sample methodology - estimate the parameters by fitting the model to some data, then use different data to test the predictive power of the fitted model. If the model predicts the (out-of-sample) observed phenomenon satisfyingly one concludes that the underlying behavioral model is likely to cause this phenomenon. Several candidate models can be subjected to this methodology, and the one

³The termite literature often mentions that the temperature and humidity inside the fungus cultures of Savannah termites are kept at nearly constant levels throughout the year. However, there is no direct experimental evidence for this claim, rather the contrary ([Turner and Soar, 2008](#)).

that best predicts the observed phenomenon can be selected as the most likely explanation. We are now in the context of model selection, a very challenging field in the statistical literature (Linhard and Zucchini, 1986; Burnham and Anderson, 2002; Claeskens and Hjort, 2008). The question is what criterion should be chosen to decide whether one model is better than another. The mentioned in-sample and out-of-sample methodology combined with a simple comparison statistic such as the squared differences between observed and predicted values can do fine. However, the models linking individual to collective behavior are all of the non-linear type. The predictions of non-linear models can be very sensitive to slight changes in parameter values (chaotic dynamics) or slight changes in the used functional descriptions (Wood and Thomas, 1999). Since these parameters are estimated on the individual level with some limited precision, one may ask the question whether some slight tweaking of these values to improve the fit on the collective level is legitimate - but how much tweaking is legitimate without compromising the fitting done on the individual level? This question made us reconsider the in-sample and out-of-sample framework and come back to fitting the complete model to all available data (Sbai et al., 2015).

The literature suggests two main methods for model selection when several alternative models are fit to the same data set. The first is the likelihood ratio test to compare between nested models. The second is the information criterion (IC) approach promoted by Burnham and Anderson (2002). It has recently been given quite some attention in the behavioral sciences (special issue of Behavioural Ecology and Sociobiology 2011, V 65, Nr 1). Both methods are based on the formulation of a likelihood function that quantifies the likelihood of a model M given the data D , $L(M; D)$. A model M is fitted to the data D by maximizing this likelihood. In practice this means to find the numerical values of the model parameters θ that maximize the likelihood. If there are two models M_1 and M_2 with K_1 and K_2 parameters respectively we can compute the maximum likelihood fits of both models, $L_{M_1}(\hat{\theta}_1; D)$ and $L_{M_2}(\hat{\theta}_2; D)$.

If M_1 is nested in M_2 (that is, M_1 can be obtained from M_2 by fixing some of M_2 's parameters to specific values) we can compute the log likelihood ratio statistic

$$\mathcal{D} = -2 \log \left(\frac{L_{M_1}(\hat{\theta}_1; D)}{L_{M_2}(\hat{\theta}_2; D)} \right) = -2 \left[\log L_{M_1}(\hat{\theta}_1; D) - \log L_{M_2}(\hat{\theta}_2; D) \right] \quad (6.1)$$

(since M_1 is nested in M_2 the latter will have a less negative maximum log likelihood, we therefore have the relation $\log L_{M_1}(\hat{\theta}_1; D) < \log L_{M_2}(\hat{\theta}_2; D)$ and $\mathcal{D} > 0$). According to Wilks theorem, \mathcal{D} will be asymptotically χ^2 distributed with $K_2 - K_1$ degrees of freedom. One can therefore test whether model M_2 fits significantly better than model M_1 .

In the information criterion approach model selection is not based on a statistical test but by comparing the likelihoods after penalising them in some way by the number of model parameters. The best known information criterion is Akaike's Information Criterion AIC (Akaike, 1973), defined as

$$AIC = -2 \log(L_M(\hat{\theta}; D)) + 2K. \quad (6.2)$$

One selects the model with the smallest AIC . Information criteria are also valid for non-nested model selection. Furthermore, if the goal is to estimate a parameter common to several models the IC approach also allows to do multi-model parameter estimation, thus avoiding the question of model selection (Burnham and Anderson, 2002). However, in the present case we consider the case where one is looking for a single best-fitting model.

Can these model selection schemes also be used when trying to identify the underlying behaviors of a collective phenomenon? Recall that the key issue outlined above was to estimate parameters with data on the individual level, but to validate the model with data on the collective level without actually fitting it to these data. However, the likelihood function computed

with the data on the collective level will not be at its maximum with the parameter values fitted on the individual level - on the other hand, all the statistical theory behind the likelihood and information criterion approach assumes to be at this maximum. In the outlined in-sample and out-of-sample approach we therefore cannot use these two model selection methods.

Nevertheless, we think that this approach can be applied to find the model that explains the observed data with the least complex functional relationships (parsimony). The key issue is to develop a likelihood function that correctly combines model fit on the individual and the collective level. Since likelihoods are based on probabilities we suggest that one can simply develop a likelihood function on each of these levels, and maximize the global likelihood that is the product of these two likelihoods. Let D_I and D_C be the (independent) data on the individual and on the collective level respectively, M_I and M_C the statistical models on the two levels and θ_I and θ_C their associated parameter sets. On the collective level this can be as simple as modeling a statistic from replicate experiments by its mean and standard deviation. Let $L_I(\theta_I; D_I)$ be the likelihood function on the individual level and $L_C(\theta_C; D_C)$ the one on the collective level. θ_I and θ_C can be estimated independently from the data on the individual and the collective level respectively. But if the collective behavior emerges from the individual behaviors in M_I then some of the parameters in M_C will be predicted by the individual parameters θ_I (for example the mean value of some collective statistic), though not necessarily all of them. We can write in this case $\theta_C = (\theta_\iota, \theta_\kappa)$, with $\theta_\iota = \theta_\iota(\theta_I)$ being the parameters emerging from the parameters on the individual level and θ_κ the parameters exclusive to collective behaviour.

If individual and collective behaviors are consistent with each other, they should bring consistent estimates of the linked parameters θ_ι , that is, the estimates derived independently from individual and collective behaviors should be estimates of the same parameters. This is tested by comparing the joint log likelihood L_{CI} evaluated with $\theta_\iota = \theta_\iota(\theta_I)$ (the joint maximum likelihood estimate $\hat{\theta}_{\iota, CI}$) to the log likelihood $L_{C/I}$ obtained by separately fitting each type of observations. That is, we compare

$$L_{CI} = L_I(\hat{\theta}_{I, CI}; D_I) \cdot L_C(\hat{\theta}_{C, CI}; D_C), \quad (6.3)$$

where $\hat{\theta}_{C, CI} = (\hat{\theta}_{\iota, CI}, \hat{\theta}_{\kappa, CI}) = (\hat{\theta}_{\iota, CI}(\hat{\theta}_{I, CI}), \hat{\theta}_{\kappa, CI})$, to

$$L_{C/I} = L_I(\hat{\theta}_{I, C/I}; D_I) \cdot L_C(\hat{\theta}_{C, C/I}; D_C), \quad (6.4)$$

where $\hat{\theta}_{I, C/I}$ maximizes $L(\hat{\theta}_{I, C/I}; D_I)$ and $\hat{\theta}_{C, C/I} = (\hat{\theta}_{\iota, C/I}, \hat{\theta}_{\kappa, C/I})$ maximizes $L_C(\hat{\theta}_{C, C/I}; D_C)$ independently.

Both likelihoods are based on the same data set (D_C, D_I) , we can therefore use both model selection schemes explained above. This idea is applied in [Sbai et al. \(2015\)](#) to the thigmotactic data of [Casellas et al. \(2008\)](#). Since I am not a professional statistician I want to work on such a theme with competent people. At the moment the project is on hold mostly by open questions how to apply the scheme in detail to our data and a lack of time to dive into these questions, but since model selection has been on my interest list since my PhD I plan to follow up on these ideas.

Bibliography

- Akaike H., 1973. Information theory and an extension of the maximum likelihood principle. In B.N. Petran and F. Csaki (eds.) *International Symposium on Information Theory*, pp. 267–281. Akademia Kiado, Budapest, Hungary, 2nd edition
- Amé J.M., Halloy J., Rivault C., Detrain C. and Deneubourg J.L., 2006. Collegial decision making based on social amplification leads to optimal group formation. *Proc Natl Acad Sci U S A* **103**: 5835–40. doi:10.1073/pnas.0507877103
- Amé J.M., Rivault C. and Deneubourg J.L., 2005. Cockroach aggregation based on strain odour recognition. *Animal Behaviour* **68**: 793–801. doi:10.1016/j.anbehav.2004.01.009
- Beckers R., Deneubourg J.L. and Goss S., 1992a. Trail laying behaviour during food recruitment in the ant *Lasius niger* (L.). *Insectes Sociaux* **39**: 59–72
- Beckers R., Deneubourg J.L. and Goss S., 1992b. Trails and U-turns in the Selection of a Path by the ant *Lasius niger*. *Journal of Theoretical Biology* **159**: 397–415
- Beckers R., Deneubourg J.L., Goss S. and Pasteels J.M., 1990. Collective decision making through food recruitment. *Insectes Sociaux* **37**: 258–267
- Blanco S. and Fournier R., 2003. An invariance property of diffusive random walks. *Europhysics Letters* **61**: 168–173
- Blanco S. and Fournier R., 2006. Short-Path Statistics and the Diffusion Approximation. *Physical Review Letters* **97**: 230604. doi:10.1103/PhysRevLett.97.230604
- Bollazzi M. and Roces F., 2003. Thermal preference for fungus culturing and brood location by workers of the thatching grass-cutting ant *Acromyrmex heyeri*. *Insectes Sociaux* **49**: 153–157
- Bonabeau E., Theraulaz G. and Deneubourg J.L., 1998a. The synchronization of recruitment-based activities in ants. *BioSystems* **45**: 195–211
- Bonabeau E., Theraulaz G., Deneubourg J.L., Aron S. and Camazine S., 1997. Self-organizing in social insects. *Trends in Ecology and Evolution* **12**: 188–192
- Bonabeau E., Theraulaz G., Deneubourg J.L., Franks N.R., Rafelsberger O., Joly J.L. and Blanco S., 1998b. A model for the emergence of pillars, walls and royal chambers in termite nests. *Philosophical Transactions of the Royal Society of London, B* **353**: 1561–1576
- Bonachela J.A., Pringle R.M., Sheffer E., Coverdale T.C., Guyton J.A., Caylor K.K., Levin S.A. and Tarnita C.E., 2015. Termite mounds can increase the robustness of dryland ecosystems to climatic change. *Science* **347**: 651–655. doi:10.1126/science.1261487

- Bourjade M., Thierry B., Hausberger M. and Petit O., 2015. Is leadership a reliable concept in animals? An empirical study in the horse. *PLoS One* **10**: e0126344. doi:10.1371/journal.pone.0126344
- Box G.E.P., 1976. Science and statistics. *Journal of the American Statistical Association* **71**: 791–799
- Brian M.V., 1983. *Social insects: ecology and behavioural biology*. Chapman and Hall
- Bruinsma O.H., 1979. An analysis of building behaviour of the termite *Macrotermes subhyalinus*. Ph.D. thesis, Lanbouwhoogeschool te Wageningen, Belgium
- Buhl J., 2004. Étude expérimentale et modélisation de la morphogenèse des réseaux de galeries chez la fourmi *Messor sancta*. Ph.D. thesis, University of Toulouse III - Paul Sabatier
- Burnham K.P. and Anderson D.R., 2002. *Model selection and multimodel inference: a practical information-theoretic approach*. Springer, 2nd edition
- Camazine S., Deneubourg J.L., Franks N.R., Sneyd J., Theraulaz G. and Bonabeau E., 2001. *Self-organization in biological systems*. Princeton University Press, Princeton, 538 pp.
- Camhi J.M. and Johnson E.N., 1999. High-frequency steering maneuvers mediated by tactile cues: antennal wall-following in the cockroach. *Journal of Experimental Biology* **202**: 631–643
- Canonge S., Sempo G., Jeanson R., Detrain C. and Deneubourg J.L., 2009. Self-amplification as a source of interindividual variability: shelter selection in cockroaches. *J Insect Physiol* **55**: 976–82. doi:10.1016/j.jinsphys.2009.06.011
- Case K. and Zweifel P., 1967. *Linear transport theory*. Addison-Wesley, New York, USA
- Casellas E., 2005. Influence d'un courant de convection naturelle sur les comportements individuels impliqués dans l'agrégation de cadavres chez la fourmi *Messor sancta*. Master's thesis, Université Paul Sabatier, Toulouse, France
- Casellas E., Gautrais J., Fournier R., Blanco S., Combe M., Fourcassié V., Theraulaz G. and Jost C., 2008. From individual to collective displacements in heterogenous environments. *Journal of Theoretical Biology* **250**: 424–434
- Challet M., 2002. Influence de la température sur les comportements individuels et sur la dynamique d'agrégation collective de cadavres chez la fourmi *Messor sancta*. Master's thesis, Université François Rabelais, Tours
- Challet M., 2005. Influence de la température et des courants d'air sur la morphogenèse des cimetières chez la fourmi *Messor sancta*. Ph.D. thesis, Université Paul Sabatier, Toulouse, France
- Challet M., Fourcassié V., Blanco S., Fournier R., Theraulaz G. and Jost C., 2005a. A new test of random walks in heterogeneous environments. *Naturwissenschaften* **92**: 367–370
- Challet M., Jost C., Grimal A., Lluc J. and Theraulaz G., 2005b. How temperature influences displacements and corpses aggregation behaviors in the ant *Messor sancta*. *Insectes Sociaux* **52**: 305–315
- Chauvin R., 1959. La construction du dôme chez *Formica rufa*. *Insectes Sociaux* **6**: 307–311

- Chrétien L., 1996. Organisation spatiale du matériel provenant de l'excavation du nid chez *Messor barbarus* et des cadavres d'ouvrières chez *Lasius niger* (Hymenoptera: Formicidae). Ph.D. thesis, Université Libre de Bruxelles, Belgium
- Claeskens G. and Hjort N.L., 2008. *Model Selection and Model Averaging*. Statistical and Probabilistic Mathematics. Cambridge University Press
- Codling E.A., Plank M.J. and Benhamou S., 2008. Random walk models in Biology. *Journal of the Royal Society Interface* p. in press
- Conradt L. and Roper T.J., 2010. Deciding group movements: where and when to go. *Behav Processes* **84**: 675–7. doi:10.1016/j.beproc.2010.03.005
- Constantino R., 1998. Catalog of the living termites of the New World (Insecta: Isoptera). *Arquivos de Zoologia* **35**: 135–231
- Cosarinsky M.I. and Roces F., 2011. The Construction of Turrets for Nest Ventilation in the Grass-Cutting Ant *Atta vollenweideri*: Import and Assembly of Building Materials. *Journal of Insect Behavior* **25**: 222–241. doi:10.1007/s10905-011-9290-8
- Courtois P.J. and Heymans F., 1991. A simulation of the construction process of a termite nest. *Journal of Theoretical Biology* **153**: 469–475
- Cowan N.J., Lee J. and Full R.J., 2006. Task-level control of rapid wall following in the American cockroach. *Journal of Experimental Biology* **209**: 1617–1629
- Creed Jr R.P. and Miller J.R., 1990. Interpreting animal wall-following behavior. *Experientia* **46**: 758–761. doi:10.1007/BF01939959
- da F. Costa L., 2008. Inward and Outward Node Accessibility in Complex Networks as Revealed by Non-Linear Dynamics. *arXiv* p. arXiv:0801.1982v1. URL <http://arxiv.org/abs/0801.1982>
- Dambach M. and Goehlen B., 1999. Aggregation density and longevity correlate with humidity in first instar nymphs of the cockroach (*Blattella germanica* L., Dictyoptera). *Journal of Insect Physiology* **45**: 423–429
- Dawkins R., 1982. *The extended phenotype*. Oxford University Press
- Deneubourg J.L., 1977. Application de l'ordre par fluctuations à la description de certaines étapes de la construction du nid chez les termites. *Insectes Sociaux* **24**: 117–130
- Detrain C. and Deneubourg J.L., 2008. Collective Decision-Making and Foraging Patterns in Ants and Honeybees. *Advances in Insect Physiology* **35**: 123–173. doi:10.1016/S0065-2806(08)00002-7
- Downing H.A. and Jeanne R.L., 1988. Nest construction by the paper wasp, *Polistes*: a test of stigmergy theory. *Animal Behaviour* **1729-1739**: 1729–1739
- Dussutour A., 2004. Organisation spatio-temporelle des déplacements collectifs chez les fourmis. Ph.D. thesis, University of Toulouse III - Paul Sabatier
- Dussutour A., Deneubourg J.L. and Fourcassié V., 2005. Amplification of individual preferences in a social context: the case of wall-following in ants. *Proceedings of the Royal Society of London, B* **272**: 705–714

- Dussutour A., Fourcassié V., Helbing D. and Deneubourg J.L., 2004. Optimal traffic organization in ants under crowded conditions. *Nature* **428**: 70–73
- Einstein A., 1905. Über die von der molekularkinetischen Theorie der Wärme geforderte Bewegung von in ruhenden Flüssigkeiten suspendierten Teilchen. *Annalen der Physik* **17**: 549–560
- Eom Y.H., Perna A., Fortunato S., Darrouzet E., Theraulaz G. and Jost C., 2015. Network-based model of the growth of termite nests. *Physical Review E* **92**: 62810. doi:10.1103/PhysRevE.00.002800. In press
- Erban R. and Othmer H.G., 2004. From individual to collective behavior in bacterial chemotaxis. *SIAM Journal of Applied Mathematics* **54**: 847. doi:10.1137/S0036139903433232
- Erban R. and Othmer H.G., 2007. Taxis equations for amoeboid cells. *Journal of Mathematical Biology* **54**: 847–885. doi:10.1007/s00285-007-0070-1
- Fagan W.F., Cantrell R.S. and Cosner C., 1999. How habitat edges change species interactions. *The American Naturalist* **153**: 165–182
- Fouquet D., Costa-Leonardo A.M., Fournier R., Blanco S. and Jost C., 2014. Coordination of construction behavior in the termite *Procornitermes araujoii*: structure is a stronger stimulus than volatile marking. *Insectes Sociaux* **61**: 253–264. doi:10.1007/s00040-014-0350-x
- Fraenkel G.S. and Gunn D.L., 1961. *The orientation of animals: kineses, taxes and compass reactions*. Dover publications, Inc, New York, 376 pp.
- Franks N.R. and Deneubourg J.L., 1997. Self-organizing nest construction in ants: individual worker behaviour and the nest's dynamics. *Animal Behaviour* **54**: 779–796
- Franks N.R., Wilby A., Silverman B.W. and Tofts C., 1992. Self-organizing nest construction in ants: sophisticated building by blind bulldozing. *Animal Behaviour* **44**: 357–375
- Garnier S., 2004. Modélisation d'un comportement d'agrégation à l'aide de micro-robots. Master NCC, University of Toulouse III - Paul Sabatier, Toulouse, France
- Garnier S., 2011. From Ants to Robots and Back: How Robotics Can Contribute to the Study of Collective Animal Behavior. In Y. Meng and Y. Jin (eds.) *Bio-inspired self-organizing robotic systems*, volume SCI355, pp. 105–120. Springer-Verlag
- Garnier S., Combe M., Jost C. and Theraulaz G., 2013. Do ants need to estimate the geometrical properties of trail bifurcations to find an efficient route? A swarm robotics test bed. *PLoS Comput Biol* **9**: e1002903. doi:10.1371/journal.pcbi.1002903
- Garnier S., Gautrais J., Asadpour M., Jost C. and Theraulaz G., 2009a. Self-Organized Aggregation Triggers Collective Decision Making in a Group of Cockroach-Like Robots. *Adaptive Behavior* **17**: 109–133. doi:10.1177/1059712309103430
- Garnier S., Guérécheau A., Combe M., Fourcassié V. and Theraulaz G., 2009b. Path selection and foraging efficiency in Argentine ant transport networks. *Behavioral Ecology and Sociobiology* **63**: 1167–1179. doi:10.1007/s00265-009-0741-6
- Garnier S., Jost C., Gautrais J., Asadpour M., Caprari G., Jeanson R., Grimal A. and Theraulaz G., 2008. The embodiment of cockroach aggregation behavior in a group of micro-robots. *Artif Life* **14**: 387–408. doi:10.1162/artl.2008.14.4.14400

- Garnier S., Jost C., Jeanson R., Gautrais J., Asadpour M., Caprari G. and Theraulaz G., 2005. Collective decision-making by a group of cockroach-like robots. In *Proceedings of the 2nd IEEE Swarm Intelligence Symposium*. IEEE Computer Society Press, Los Alamitos, CA
- Garnier S., Tâche F., Combe M., Grimal A. and Theraulaz G., 2007. Alice in Pheromone Land: An Experimental Setup for the Study of Ant-like Robots. In *Swarm Intelligence Symposium (SIS)*, pp. 37–44. IEEE. doi:10.1109/SIS.2007.368024
- Gautrais J., 2010. The hidden variables of leadership. *Behav Processes* **84**: 664–7. doi:10.1016/j.beproc.2010.03.002
- Gautrais J., 2015. Dynamiques auto-organisées et morphogénèse: des sociétés animales aux tissus cellulaires. Habilitation thesis, University of Toulouse. doi:10.13140/RG.2.1.2285.5203
- Gautrais J., Ginelli F., Fournier R., Blanco S., Soria M., Chaté H. and Theraulaz G., 2012. Deciphering interactions in moving animal groups. *PLoS Comput Biol* **8**: e1002678. doi:10.1371/journal.pcbi.1002678
- Gordon D.M., 1983. Dependence of necrophoric response to oleic acid on social context in the ant, *Pogonomyrmex badius*. *Journal of Chemical Ecology* **9**: 105–111
- Grassé P.P., 1959. La reconstruction du nid et les coordinations interindividuelles chez *Belligositermes natalensis* et *Cubitermes* sp. La théorie de la stigmergie: essai d'interprétation du comportement des termites constructeurs. *Insectes Sociaux* **6**: 41–83. doi:10.1007/BF02223791
- Grassé P.P., 1967. Nouvelles expériences sur le termite de Müller (*Macrotermes mulleri*) et considérations sur la théorie de la stigmergie. *Insectes Sociaux* **14**: 73–102. doi:10.1007/BF02222755
- Grassé P.P., 1984. *Termitologia, tome 2: Fondation des sociétés, construction*. Masson, Paris, 613 pp.
- Haifig I., Jost C., Janei V. and Costa-Leonardo A.M., 2011. The size of excavators within a polymorphic termite species governs tunnel topology. *Animal Behaviour* **82**: 1409–1414. doi:10.1016/j.anbehav.2011.09.025
- Halloy J., Sempo G., Caprari G., Rivault C., Asadpour M., Tâche F., Saïd I., Durier V., Canonge S., Amé J.M., Detrain C., Correll N., Martinoli A., Mondada F., Siegward R. and Deneubourg J.L., 2007. Social Integration of Robots into Groups of Cockroaches to Control Self-Organized Choices. *Science* **318**: 1155–1158
- Haskins C.P. and Haskins E.F., 1974. Notes on necrophoric behavior in the archaic ant *Myrmecia vindex* (Formicidae: Myrmeciinae). *Psyche* **81**: 258–267
- Hill N. and Bullock S., 2015. Modelling the Role of Trail Pheromone in the Collective Construction of Termite Royal Chambers. In *Advances in Artificial Life*, p. 376660. ECAL. URL <http://eprints.soton.ac.uk/id/eprint/376660>
- Howard D.F. and Tschinkel W.R., 1976. Aspects of necrophoric behavior in the red imported fire ant, *Solenopsis invicta*. *Behaviour* **56**: 157–180
- Jackson D.E., Holcombe M. and Ratnieks F.L.W., 2004. Trail geometry gives polarity to ant foraging networks. *Nature* **432**: 907–909

- Jeanson R., Blanco S., Fournier R., Deneubourg J.L., Fourcassié V. and Theraulaz G., 2003. A model of animal movements in a bounded space. *Journal of Theoretical Biology* **225**: 443–451
- Jeanson R., Rivault C., Deneubourg J.L., Blanco S., Fournier R., Jost C. and Theraulaz G., 2005. Self-organized aggregation in cockroaches. *Animal Behaviour* **69**: 169–180. doi:10.1016/j.anbehav.2004.02.009
- Jeanson R. and Weidenmüller A., 2014. Interindividual variability in social insects - proximate causes and ultimate consequences. *Biol Rev Camb Philos Soc* **89**: 671–87. doi:10.1111/brv.12074
- Jones J.C., Myerscough M.R., Graham S. and Oldroyd B.P., 2004. Honey bee nest thermoregulation: diversity promotes stability. *Science* **305**: 402–4. doi:10.1126/science.1096340
- Jonkman J.C.M., 1980a. The external and internal structure and growth of nests of the leaf-cutting ant *Atta vollenweideri* Forel, 1893 (Hym.: Formicidae) - Part I. *Zeitschrift für angewandte Entomologie* **89**: 158–173
- Jonkman J.C.M., 1980b. The external and internal structure and growth of nests of the leaf-cutting ant *Atta vollenweideri* Forel, 1893 (Hym.: Formicidae) - Part II. *Zeitschrift für angewandte Entomologie* **89**: 217–246
- Jost C., 1993. Ein Mehrgitterverfahren für eine Petrov-Galerkin Diskretisierung der Stokes Gleichung. Master's thesis, University of Zürich, Institut für angewandte Mathematik, Universität Zürich, Switzerland
- Jost C., 1998. Comparing Predator-Prey Models Qualitatively and Quantitatively with Ecological Time-Series Data. Ph.D. thesis, Institut national agronomique, Paris-Grignon. URL <http://tel.archives-ouvertes.fr/tel-00005771>
- Jost C., Garnier S., Jeanson R., Asadpour M., Gautrais J. and Theraulaz G., 2004. The embodiment of cockroach behaviour in a micro-robot. In *Conference Proceedings of ISR (International Symposium on Robotics)*, BIOROB-CONF-2004-008. Paris, France
- Jost C., Haifig I., de Camargo-Dietrich C.R.R. and Costa-Leonardo A.M., 2012. A comparative tunnelling network approach to assess interspecific competition effects in termites. *Insectes Sociaux* **59**: 369–379. doi:10.1007/s00040-012-0229-7
- Jost C., Jeanson R., Theraulaz G., Deneubourg J.L. and Rivault C., 2002. Self-organized aggregation in cockroaches: sensitivity to model structure. In C. Hemelrijk (ed.) *Conference Proceedings of the International workshop on self-organization and evolution of social behaviour, Monte Verità, Switzerland*, pp. 237–246
- Jost C., Verret J., Casellas E., Gautrais J., Challet M., Lluc J., Blanco S., Clifton M. and Theraulaz G., 2007. The interplay between a self-organized process and an environmental template: corpse clustering under the influence of air currents in ants. *Journal of the Royal Society Interface* **4**: 107–116
- Kazama T., Sugawara K. and Watanabe T., 2004. Collecting behavior of interacting robots with virtual pheromone. In *Proceedings 7th International Symposium on Distributed Autonomous Robotic Systems*, pp. 331–340
- Keromest M., 2008. Mécanismes de construction de structures épigées chez la fourmi *Lasius niger*. Master's thesis, University of Toulouse III - Paul Sabatier, Toulouse, France

- Khuong A., 2013. Modèle comportemental de la dynamique de construction de la structure épigée du nid chez la fourmi *Lasius niger*. Approches expérimentales et théoriques. Ph.D. thesis, University of Toulouse III - Paul Sabatier
- Khuong A., Gautrais J., Perna A., Sbai C., Combe M., Moreau M., Kuntz P., Jost C. and Theraulaz G., 2015. Stigmergic construction and topochemical information shape ant nest architecture. *Proc Natl Acad Sci U S A* In press
- Khuong A., Lecheval V., Fournier R., Blanco S., Weitz S., Bezian J.J. and Gautrais J., 2013. How Do Ants Make Sense of Gravity? A Boltzmann Walker Analysis of *Lasius niger* Trajectories on Various Inclines. *PLoS One* **8**: e76531. doi:10.1371/journal.pone.0076531
- King A.J., 2010. Follow me! I'm a leader if you do; I'm a failed initiator if you don't? *Behav Processes* **84**: 671–4. doi:10.1016/j.beproc.2010.03.006
- Kleineidam C., Ernst R. and Roces F., 2001. Wind-induced ventilation of the giant nests of the leaf-cutting ant *Atta vollenweideri*. *Naturwissenschaften* **88**: 301–305
- Korb J., 2011. Termite Mound Architecture, from Function to Construction. In D.E. Bignell, Y. Roisin and N. Lo (eds.) *Biology of Termites: A modern synthesis*, chapter 13, pp. 349–374. Springer. doi:10.1007/978-90-481-3977-4
- Krause J. and Ruxton G.D., 2002. *Living in Groups*. Oxford University Press
- Ladley D. and Bullock S., 2005. The role of logistic constraints in termite construction of chambers and tunnels. *Journal of Theoretical Biology* **234**: 551–564
- Linhard H. and Zucchini W., 1986. *Model Selection*. John Wiley & Sons, New York
- Loisel V., 2009. Identification des mécanismes de la construction du nid chez *Lasius niger*. Master's thesis, University of Toulouse III - Paul Sabatier, Toulouse, France
- López-Hernández D., Brossard M., Fardeau J. and Lepage M., 2006. Effect of different termite feeding groups on P sorption and P availability in African and South American savannas. *Biol. Fertil. Soils* **42**: 207–214
- Moreira A.A., Forti L.C., Andrade A.P.P., Boaretto M.A.C. and Lopes J.F.S., 2004a. Nest architecture of *Atta laevigata* (F. Smith, 1858) (Hymenoptera: Formicidae). *Studies on Neotropical Fauna and Environment* **39**: 109–116
- Moreira A.A., Forti L.C., Boaretto M.A.C., Andrade A.P.P., Lopes J.F.S. and Ramos V.M., 2004b. External and internal structure of *Atta bisphaerica* Forel (Hymenoptera: Formicidae) nests. *Journal of Applied Entomology* **128**: 204–211
- Noirot C. and Darlington J., 2000. Termite nests: architecture, regulation and defence. In T. Abe, D.E. Bignell and M. Higashi (eds.) *Termites: evolution, sociality, symbioses, ecology*, pp. 121–139. Kluwer Academic Publishers Dordrecht
- Olivera J., 2006. Etude des mécanismes de coordination chez la fourmi *Lasius niger* lors de la construction de structures épigées. Master's thesis, University of Toulouse III - Paul Sabatier, Toulouse, France
- Ovaskainen O. and Cornell S.J., 2003. Biased movement at a boundary and conditional occupancy times for diffusion processes. *Journal of applied probability* **40**: 557–580

- Pechabadens C., 2014. Role of pheromones in termite construction behavior and estimation of their evaporation rate. Master's thesis, University of Toulouse III - Paul Sabatier, Toulouse, France
- Perna A., Granovskiy B., Garnier S., Nicolis S.C., Labédan M., Theraulaz G., Fourcassié V. and Sumpter D.J.T., 2012. Individual rules for trail pattern formation in Argentine ants (*Linepithema humile*). *PLoS Computational Biology* **8**: e1002592. doi:10.1371/journal.pcbi.1002592
- Perna A., Jost C., Couturier E., Valverde S., Douady S. and Theraulaz G., 2008a. The structure of gallery networks in the nests of termite *Cubitermes* spp. revealed by X-ray tomography. *Naturwissenschaften* **95**: 877–884. doi:10.1007/s00114-008-0388-6
- Perna A., Jost C., Valverde S., Gautrais J., Theraulaz G. and Kuntz P., 2008b. The Topological Fortress of Termites. *Lecture Notes in Computer Science* **5151**: 165–173
- Perna A., Kuntz P., Theraulaz G. and Jost C., 2011. From local growth to global optimization in insect built networks. In P. Lio and D. Verma (eds.) *Biologically inspired networking and sensing: algorithms and architectures*, chapter 7, pp. 132–144. IGI Global, Hershey PA 17033. doi:10.4018/978-1-61350-092-7
- Perna A., Valverde S., Gautrais J., Jost C., Solé R.V., Kuntz P. and Theraulaz G., 2008c. Topological efficiency in three-dimensional gallery networks of termite nests. *Physica A* **387**: 6235–6244. doi:10.1016/j.physa.2008.07/019
- Petersen K., Bardunias P., Napp N., Werfel J., Nagpal R. and Turner J.S., 2015. Arrestant property of recently manipulated soil on *Macrotermes michaelseni* as determined through visual tracking and automatic labeling of individual termite behaviors. *Behavioural Processes* **116**: 8–11. doi:10.1016/j.beproc.2015.04.004
- Petit O. and Bon R., 2010. Decision-making processes: the case of collective movements. *Behav Processes* **84**: 635–47. doi:10.1016/j.beproc.2010.04.009
- Prokopy R.J. and Roitberg B.D., 2001. Joining and avoidance behavior in nonsocial insects. *Annu Rev Entomol* **46**: 631–65. doi:10.1146/annurev.ento.46.1.631
- Roces F. and Kleineidam C., 2000. Humidity preference for fungus culturing by workers of the leaf-cutting ant *Atta serdens rubropilosa*. *Insectes Sociaux* **47**: 348–350
- Römer D., 2014. Where and how to build? Influence of social and environmental cues on nest building behavior in leaf-cutting ants. Ph.D. thesis, University of Würzburg. URL http://opus.bibliothek.uni-wuerzburg.de/frontdoor/deliver/index/docId/10940/file/Dissertation_Roemer_Daniela.pdf
- Saïd I., Costagliola G., Leoncini I. and Rivault C., 2005. Cuticular hydrocarbon profiles and aggregation in four *Periplaneta* species (Insecta: Dictyoptera). *J Insect Physiol* **51**: 995–1003. doi:10.1016/j.jinsphys.2005.04.017
- Sbai C., Rousset F., David P. and Jost C., 2015. Model selection in the context of collective animal behaviours. In preparation
- Scholes S.R., Sendova-Franks A.B., Swift S.T. and Melhuish C., 2006. Ants can sort their brood without a gaseous template. *Behavioral Ecology and Sociobiology* **59**: 531 – 540

- Seeley T.D., Visscher P.K., Schlegel T., Hogan P.M., Franks N.R. and Marshall J.A.R., 2012. Stop signals provide cross inhibition in collective decision-making by honeybee swarms. *Science* **335**: 108–11. doi:10.1126/science.1210361
- Sempo G., Depickère S., Amé J.M., Detrain C., Halloy J. and Deneubourg J.L., 2006. Integration of an Autonomous Artificial Agent in an Insect Society: Experimental Validation. In S. Nolfi, G. Baldassarre, R. Calabretta, J.C.T. Hallam, D. Marocco, J.A. Meyer, O. Miglino and D. Parisi (eds.) *From Animals to Animats 9*, 4095, pp. 703–712. Springer-Verlag. doi: 10.1007/11840541_58
- Smith A.P., 1978. An investigation of the mechanisms underlying nest construction in the mud wasp *Paralastor* sp.(Hymenoptera: Eumenidae). *Animal Behaviour* **26**: 232–240. doi: 10.1016/0003-3472(78)90023-4
- Sugawara K., 2005. Development of Virtual Dynamic Environment for Autonomous Robots. In *International Symposium on Nonlinear Theory and its Applications (NOLTA2005)*, volume 3, pp. 3074–3079. Bruges, Belgium
- Sumpter D.J.T., 2010. *Collective animal behavior*. Princeton University Press
- Theraulaz G. and Bonabeau E., 1999. A brief history of stigmergy. *Artificial Life* **5**: 97–116
- Theraulaz G., Bonabeau E., Nicolis S.C., Solé R.V., Fourcassié V., Blanco S., Fournier R., Joly J.L., Fernández P., Grimal A., Dalle P. and Deneubourg J.L., 2002. Spatial patterns in ant colonies. *Proceedings of the National Academy of Sciences of the USA* **99**: 9645–9649
- Theraulaz G., Gautrais J., Camazine S. and Deneubourg J.L., 2003. The formation of spatial patterns in social insects: from simple behaviours to complex structures. *Philosophical Transactions: Mathematical, Physical & Engineering Sciences* **361**: 1263–1282
- Theraulaz G., Perna A. and Kuntz P., 2012a. L’art de la construction chez les insectes sociaux. *Pour la science* **420**: 28–35. URL http://www.pourlascience.fr/ewb_pages/a/article-1-art-de-la-construction-chez-les-insectes-sociaux-30411.php
- Theraulaz G., Picarougne F. and Jost C., 2012b. Voyage au centre des termitières. *Pour la science* **420**: 36–43. URL http://www.pourlascience.fr/ewb_pages/a/article-voyage-au-centre-des-termitieres-et-des-fourmilieres-30407.php
- Thomé G., 1972. Le nid et le comportement de construction de la fourmi *Messor ebenius*, Forel (Hymenoptera, Formicoïdea). *Insectes Sociaux* **19**: 95–103
- Turner J.S., 2002. *The extended organism: the physiology of animal-built structures*. Harvard University Press
- Turner J.S. and Soar R., 2008. Beyond Biomimicry: What Termites Can Tell Us about Realizing the Living Building. In *The 1st International Conference On Industrialised, Integrated, Intelligent Construction*, pp. 215–231. URL <http://citeseerx.ist.psu.edu/viewdoc/download?doi=10.1.1.379.2791&rep=rep1&type=pdf#page=224>
- Valverde S., Corominas-Murtra B., Perna A., Kuntz P., Theraulaz G. and Solé R.V., 2009. Percolation in insect nest networks: Evidence for optimal wiring. *Physical Review E* **79**: 066106. doi:10.1103/PhysRevE.79.066106
- van Damme T., 1998. Modélisation et étude expérimentale de la construction et du transport chez les fourmis. Ph.D. thesis, Université Libre de Bruxelles, Brussels, Belgium

- Verret J., 2004. Impact d'un écoulement de convection naturelle sur les processus de morphogénèse de cimetière chez la fourmi *Messor sancta*. Desups, University of Toulouse
- Viana M., Batista J.L.B. and Costa L.d.F., 2012. Effective number of accessed nodes in complex networks. *Physical Review E* **85**: 036105. doi:http://dx.doi.org/10.1103/PhysRevE.85.036105
- Viana M., Fourcassié V., Perna A., da F. Costa L. and Jost C., 2013. Accessibility in networks: a useful measure for understanding social insect nest architecture. *Chaos, Solitons and Fractals* p. in press
- Weitz S., 2012. Modélisation de marches aléatoires diffuses et thigmotactiques en milieu hétérogène à partir d'observations individuelles : Application à l'agrégation et à la construction dans les sociétés d'insectes. Ph.D. thesis, University of Toulouse III - Paul Sabatier
- Weitz S., Blanco S., Fournier R., Gautrais J., Jost C. and Theraulaz G., 2012. Modeling collective animal behavior with a cognitive perspective: a methodological framework. *PLoS ONE* **7**: e38588. doi:10.1371/journal.pone.0038588
- Weitz S., Blanco S., Fournier R., Gautrais J., Jost C. and Theraulaz G., 2014. Residence times and boundary-following behavior in animals. *Phys Rev E Stat Nonlin Soft Matter Phys* **89**: 052715. doi:10.1103/PhysRevE.89.052715
- Wenzel J.W., 1991. Evolution of Nest Architecture. In K.G. Ross and R. Matthews (eds.) *The social biology of wasps*, chapter 14, pp. 480–519. Cornell University Press, Ithaca, New York
- Wilson E.O., Durlach N.I. and Roth L.M., 1958. Chemical relasers of necrophoric behavior in ants. *Psyche* **65**: 154–161
- Wood S.N. and Thomas M.B., 1999. Super-sensitivity to structure in biological models. *Proceedings of the Royal Society of London, B* **266**: 565–570